



National Library
of Canada

Bibliothèque nationale
du Canada

Canadian Theses Service

Services des thèses canadiennes

Ottawa, Canada
K1A 0N4

CANADIAN THESES

THÈSES CANADIENNES

NOTICE

AVIS

The quality of this microfiche is heavily dependent upon the quality of the original thesis submitted for microfilming. Every effort has been made to ensure the highest quality of reproduction possible.

La qualité de cette microfiche dépend grandement de la qualité de la thèse soumise au microfilmage. Nous avons tout fait pour assurer une qualité supérieure de reproduction.

If pages are missing, contact the university which granted the degree.

S'il manque des pages, veuillez communiquer avec l'université qui a conféré le grade.

Some pages may have indistinct print especially if the original pages were typed with a poor typewriter ribbon or if the university sent us an inferior photocopy.

La qualité d'impression de certaines pages peut laisser à désirer, surtout si les pages originales ont été dactylographiées à l'aide d'un ruban use ou si l'université nous a fait parvenir une photocopie de qualité inférieure.

Previously copyrighted materials (journal articles, published tests, etc.) are not filmed.

Les documents qui font déjà l'objet d'un droit d'auteur (articles de revue, examens publiés, etc.) ne sont pas microfilmés.

Reproduction in full or in part of this film is governed by the Canadian Copyright Act, R.S.C. 1970, c. C-30. Please read the authorization forms which accompany this thesis.

La reproduction, même partielle, de ce microfilm est soumise à la Loi canadienne sur le droit d'auteur, SRC 1970, c. C-30. Veuillez prendre connaissance des formules d'autorisation qui accompagnent cette thèse.

THIS DISSERTATION
HAS BEEN MICROFILMED
EXACTLY AS RECEIVED

LA THÈSE A ÉTÉ
MICROFILMÉE TELLE QUE
NOUS L'AVONS REÇUE



National Library of Canada

Bibliothèque nationale du Canada

Ottawa, Canada
K1A 0N4

TC -

0-315-23315-X

CANADIAN THESES ON MICROFICHE SERVICE - SERVICE DES THÈSES CANADIENNES SUR MICROFICHE

PERMISSION TO MICROFILM - AUTORISATION DE MICROFILMER

• Please print or type - Ecrire en lettres moulées ou dactylographier

AUTHOR - AUTEUR

Full Name of Author - Nom complet de l'auteur

Date of Birth - Date de naissance

Canadian Citizen - Citoyen canadien

Yes Oui

No Non

Country of Birth - Lieu de naissance

Permanent Address - Residence fixe

THESIS - THÈSE

Title of Thesis - Titre de la thèse

Degree for which thesis was presented
Grade pour lequel cette thèse fut présentée

Year this degree conferred
Année d'obtention de ce grade

University - Université

Name of Supervisor - Nom du directeur de thèse

AUTHORIZATION - AUTORISATION

Permission is hereby granted to the NATIONAL LIBRARY OF CANADA to **microfilm** this thesis and to **lend** or **sell copies of the film**.

L'autorisation est, par la présente, accordée à la BIBLIOTHÈQUE NATIONALE DU CANADA de **microfilmer** cette thèse et de **prêter** ou de **vendre des exemplaires du film**.

The author reserves other publication rights, and neither the thesis nor extensive extracts from it may be printed or otherwise reproduced without the author's written permission

L'auteur se réserve les autres droits de publication, ni la thèse ni de longs extraits de celle-ci ne doivent être imprimés ou autrement reproduits sans l'autorisation écrite de l'auteur

ATTACH FORM TO THESIS - VEUILLEZ JOINDRE CE FORMULAIRE À LA THÈSE

Signature

Date

THE UNIVERSITY OF ALBERTA

Sedimentary Heat Flow in the $\Delta Q=0$ Region of Alberta

by

Robert Beach

A THESIS

SUBMITTED TO THE FACULTY OF GRADUATE STUDIES AND RESEARCH
IN PARTIAL FULFILMENT OF THE REQUIREMENTS FOR THE DEGREE

OF Master of Science

IN

Geophysics

Physics

EDMONTON, ALBERTA

FALL 1985

• COLOURED PAPER
PAPIER DE COULEUR

THE UNIVERSITY OF ALBERTA

RELEASE FORM

NAME OF AUTHOR Robert Beach
TITLE OF THESIS Sedimentary Heat Flow in the $\Delta Q=0$ Region
of Alberta
DEGREE FOR WHICH THESIS WAS PRESENTED Master of Science
YEAR THIS DEGREE GRANTED 1985

Permission is hereby granted to THE UNIVERSITY OF ALBERTA LIBRARY to reproduce single copies of this thesis and to lend or sell such copies for private, scholarly or scientific research purposes only.

The author reserves other publication rights, and neither the thesis nor extensive extracts from it may be printed or otherwise reproduced without the author's written permission.

(SIGNED) *Robert Beach*

PERMANENT ADDRESS:

802-1 Evergreen Pl
Winnipeg, Manitoba
R3L 0E9

DATED Oct 7 1985

THE UNIVERSITY OF ALBERTA
FACULTY OF GRADUATE STUDIES AND RESEARCH

The undersigned certify that they have read, and recommend to the Faculty of Graduate Studies and Research, for acceptance, a thesis entitled Sedimentary Heat Flow in the $\Delta Q=0$ Region of Alberta submitted by Robert Beach in partial fulfilment of the requirements for the degree of Master of Science in Geophysics.

.....
.....

Supervisor

.....
.....
.....

Date... Oct 7 '85

Abstract

The heat flows and temperatures at the base of the sediments are calculated at twenty-four well locations in Alberta. The average of the heat flows calculated is 71 mW/m^2 , with a standard deviation of 12 mW/m^2 . The average uncertainty in the twenty-four heat flow calculations is 18 mW/m^2 , and the average uncertainty in the temperatures at the base of the sediments is $11 \text{ }^\circ\text{C}$.

The twenty-four wells are chosen in a region of Alberta where it is reasonable to assume that vertical groundwater motion is negligible. In this region the heat flows are interpreted to be the heat flows at the surface of the Precambrian basement. No definite relationship is found between heat flow and heat generation at the surface of the Precambrian basement.

Acknowledgement

I would like to acknowledge the assistance of Dr. J. A. Majorowicz throughout the course of this work. Additional assistance was provided by A. Linville, D. Jones, and J. P. Pascal. Special thanks to S. Pitts for proofreading the manuscript and for his valuable questions and comments. Finally, I would like to thank my supervisor, Dr. F. W. Jones, for his support and assistance.

I would also like to acknowledge the financial assistance of a teaching assistantship at the University of Alberta during the past two years.

Table of Contents

Page

1. Introduction	1
Geothermal Heat Flow: Basic Formulae	2
Heat Flow from the Crystalline Basement	3
2. Thermal Conductivity of Sedimentary Rocks in Alberta	4
Introduction	4
Net Rock Analysis Data File	5
Factors Affecting the Thermal Conductivity of Sedimentary Rocks	6
Experimental Results from Alberta: Limestone, Dolomite, Shale, Siltstone, and Sandstone	10
Temperature Dependence: The Thermal Conductivity of Shale	11
Thermal Conductivities of Remaining Rock Types	12
Summary of Thermal Conductivity Results	13
Effective Conductivity of Sediments	14
3. Temperature Gradients	15
Cases 1, 2, and 3	16
Cases 4 and 5: Regional Corrections	17
Periodic Perturbations of the Surface Temperature	18
4. Heat Flow, Temperature at the Base of the Sediments, and Heat Generation	20
Heat Flow and Temperature at the Base of the Sediments	20
Summary	21
Heat Generation in Sediments	22

Heat Generation at the Surface of the Precambrian Basement	7
Groundwater Motion	11
Conclusions	12
References	13
Appendix I. Location of Net Rock Analysis Wells	14
Appendix II. Regional Temperature Gradients	15
Appendix III. Local Uncorrected Gradients for Case 4 and Case 5 Wells	16
Appendix IV. Final Temperature Gradient Plots	17
Appendix V. Heat Generation at the Surface of the Precambrian Basement in Western Canada	18

LIST OF TABLES

Table	Description	Page
2.1	Anisotropy and vertical conductivity of limestone, dolomite, shale, sandstone, and siltstone	26
2.2	Summary of thermal conductivity results for sedimentary rock types	36
2.3	Sedimentary thicknesses and effective conductivities of sedimentary layers for net rock analysis wells	40
3.1	Regional percentage corrections to temperature gradients	51
3.2	Regional corrections to local gradients for the case 4 and case 5 wells	54
4.1	Heat flows above and below the split depth for the case 3 and case 5 wells	62
4.2	Heat flows and temperatures at the base of the sediments	64
4.3	Heat production of sedimentary rocks	68
4.4	Contribution of heat generation in sediments to surface heat flow	70

LIST OF FIGURES

Figure	Description	Page
1.1	ΔQ heat flow map for Alberta	6
1.2	Groundwater motion in the Alberta basin and its influence on temperature gradients and heat flow	8
1.3	Locations of net rock analysis wells	11
2.1	Number of kilometers of the thirteen sedimentary rock types for all twenty-four wells	15
2.2	Locations of the wells from which measurements of thermal conductivities were made	21
2.3	Lateral thermal conductivity histograms for limestone, dolomite, shale, sandstone, and siltstone	23
2.4	Porosity histograms corresponding to thermal conductivity histograms in Figure 2.3	25
2.5	The thermal conductivity of shale as a function of temperature	29
2.6	Porosity considered as a function of depth in the Alberta basin	31
3.1	An example of case 1. Temperature as a function of depth for well number 1	44
3.2	An example of case 2. Temperature as a function of depth for well number 19	47
3.3	An example of case 3. Temperature as a function of depth for well number 9	49
3.4	An example of case 4. The uncorrected local temperature gradient for well number 10	53
3.5	Case 5. The uncorrected local temperature gradient for well number 21	56
4.1	Heat flows at the net rock analysis well locations	66

4.2	Heat generation at the surface of the Precambrian basement	73
4.3	Heat flow versus heat generation in the $\Delta Q=0$ region of Alberta	76

CHAPTER 1

Introduction

It is well known that temperature increases from the surface of the earth toward its center. A consequence of this temperature gradient is an outward flow of heat through the surface of the earth. This geothermal heat flow is a basic property of the earth and is related to processes within the earth, such as radioactive decay and convection. In the crust of the earth, groundwater motion influences the surface heat flow. This study is concerned with the flow of heat through the crust of the earth in Alberta which consists of about 35 to 40 Km of crystalline basement rock, and 0 to 6 Km of overlying sediments. The steady state heat flow densities at twenty-four well locations in Alberta are calculated, as well as the temperatures at the base of the sediments at these well locations. In addition, the contribution of heat generation in the sediments to surface heat flow is estimated at the well locations, and a relationship is sought between heat flow through the sediments and heat generation at the surface of the crystalline basement in the $\Delta Q=0$ region of Alberta.

Geothermal Heat Flow: Basic Formulae

The basic equations of geothermal heat flow are found in Lachenbruch and Sass (1977). The vertical component of heat flow through a rock is defined by

$$q = k \frac{\partial T}{\partial z} \quad (1.1)$$

where k is the thermal conductivity of the rock, and $\partial T/\partial z$ is the temperature gradient. The quantity q is actually heat flow density, but it will be referred to throughout as simply heat flow. In equation (1.1), z is taken as positive downward, so that a positive heat flow is an upward heat flow. If the heat flow is constant in each layer of a sedimentary sequence and the average gradient for the column is known, then the heat flow in terms of the average gradient $\langle \nabla T \rangle$ is

$$q = k_{\text{eff}} \langle \nabla T \rangle \quad (1.2)$$

in which k_{eff} is the effective conductivity given by

$$k_{\text{eff}} = \frac{\sum_i \Delta z_i}{\sum_i \left(\frac{\Delta z_i}{k_i} \right)} \quad (1.3)$$

where i represents the depth intervals.

The general one-dimensional heat flow equation is

$$\frac{\partial q}{\partial z} = -A - \rho'c'v \frac{\partial T}{\partial z} + \rho c \frac{\partial T}{\partial t} \quad (1.4)$$

where A is the heat generation in the rock due to

radioactive decay, $\rho'c'$ is the volumetric heat capacity of the fluid in the rock, v is the upward volume flux of fluid, and ρc is the volumetric heat capacity of the solid rock. The first term on the right represents the increase in heat flow toward the surface due to heat generation in the rock. The second term represents the change in heat flow with depth due to fluid motion in the rock. If the fluid motion is upward, heat flow will increase toward the surface, and if the fluid motion is downward, heat flow will decrease toward the surface. The last term in equation (1.4) represents the change in heat flow with depth due to a non-steady-state condition. A steady-state condition is assumed here, so that the last term in equation (1.4) is zero.

Heat Flow from the Crystalline Basement

In this study the geothermal heat flow is calculated from temperature data taken from the sediments. If the heat flow is assumed to be constant from the surface to the base of the sediments, then the heat flow values calculated here represent the heat flux through the surface of the crystalline basement.

The sedimentary rock in Alberta may be separated into two main sections. The top section consists of the Cenozoic and Mesozoic strata, and the bottom section consists of the Paleozoic strata. The boundary between the two intervals is known as the Paleozoic erosional surface. Majorowicz et al.

(1985a,b) calculated the heat flow above and below the Paleozoic erosional surface throughout the Alberta Basin. The differences

$$\Delta Q_i = Q_i(\text{top}) - Q_i(\text{bot.}) \quad (1.5)$$

were also calculated, where the index $i=1, \dots, 379$ corresponds to the 3 X 3 township-range area for which ΔQ was calculated. The resulting ΔQ map is reproduced in Figure 1.1.

From the map, it is seen that the ΔQ values increase regionally from about -40 mW/m^2 in the southwest part of Alberta to roughly 60 mW/m^2 in the north central part of the province. This regional variation was explained in terms of the effect of groundwater motion, and the model is shown in Figure 1.2. The foothills area of Alberta is a regional recharge area, with a downward component of groundwater motion. North central Alberta, on the other hand, is a regional discharge area, with an upward component of groundwater motion. The intermediate area is a region of lateral flow. The effect of groundwater motion will be discussed in more detail in Chapter 4. This regional groundwater motion is a possible explanation for the regional ΔQ variation shown in Figure 1.1.

Majorowicz et al. (1985b) estimated the uncertainty in their ΔQ values to be about 20 mW/m^2 . Hence, the unshaded region in Figure 1.1 between the -20 mW/m^2 and 20 mW/m^2 contours will be called the ' $\Delta Q=0$ ' region. For this study,

Figure 1.1: Heat flow above the Paleozoic erosional surface minus heat flow below the Paleozoic erosional surface (from Majorowicz et al., 1985b).

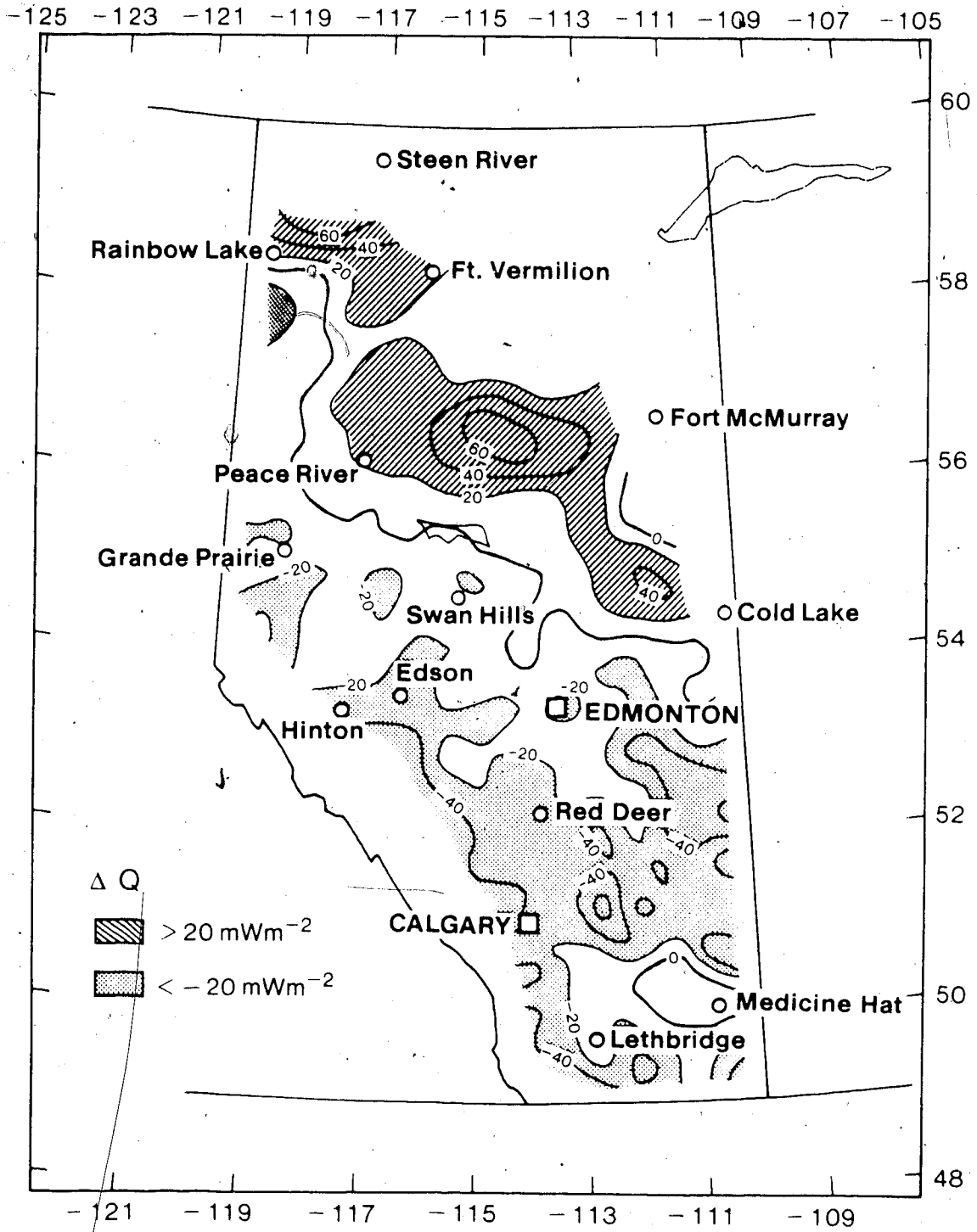
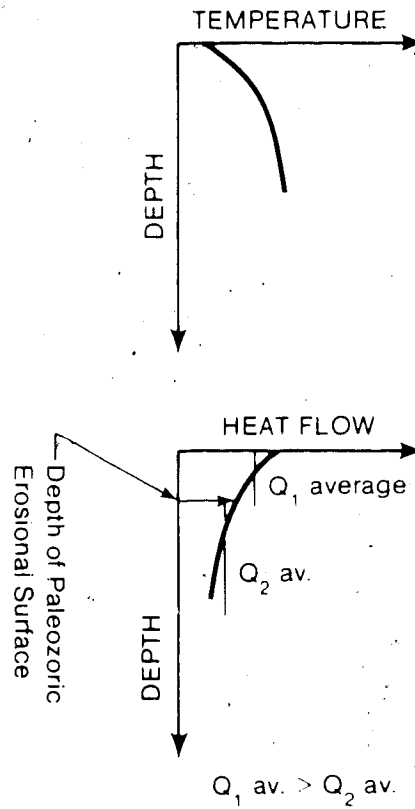
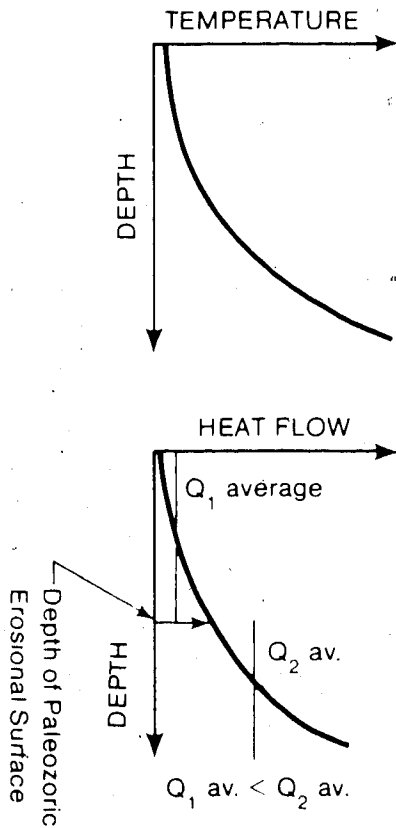
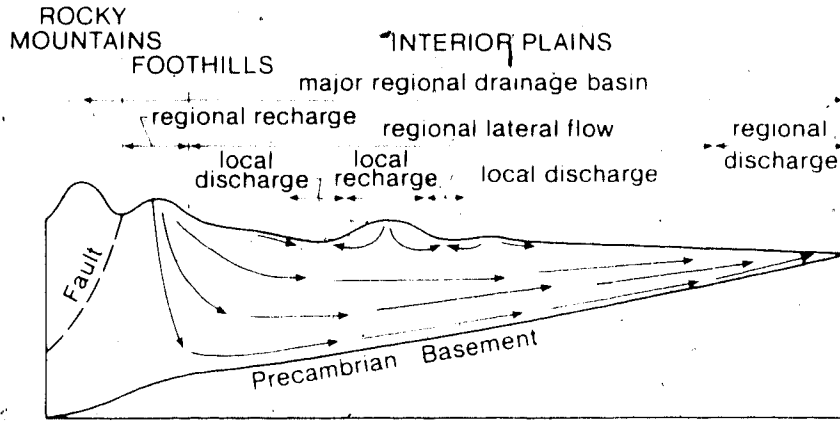


Figure 1.2: Groundwater motion in the Alberta basin and its effect on temperature and heat flow as a function of depth (from Majorowicz et al, 1985b). The hydrodynamic model is from Hitchon (1984).

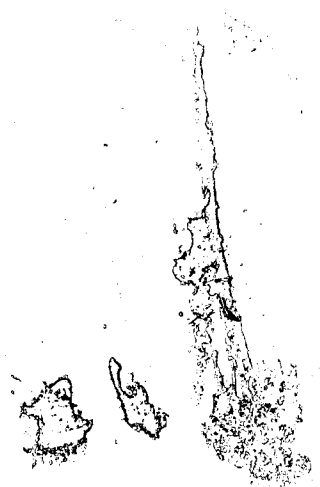
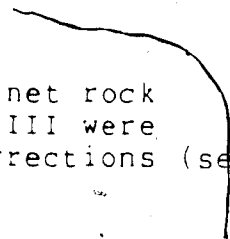


twenty-four locations distributed throughout the $\Delta Q=0$ region were selected for detailed heat flow calculations. These locations are shown in Figure 1.3. The locations of the wells in the township-range-meridian system are given in Appendix I. At each of these locations, a net rock analysis was available for the whole section from the earth's surface to the base of the sediments.

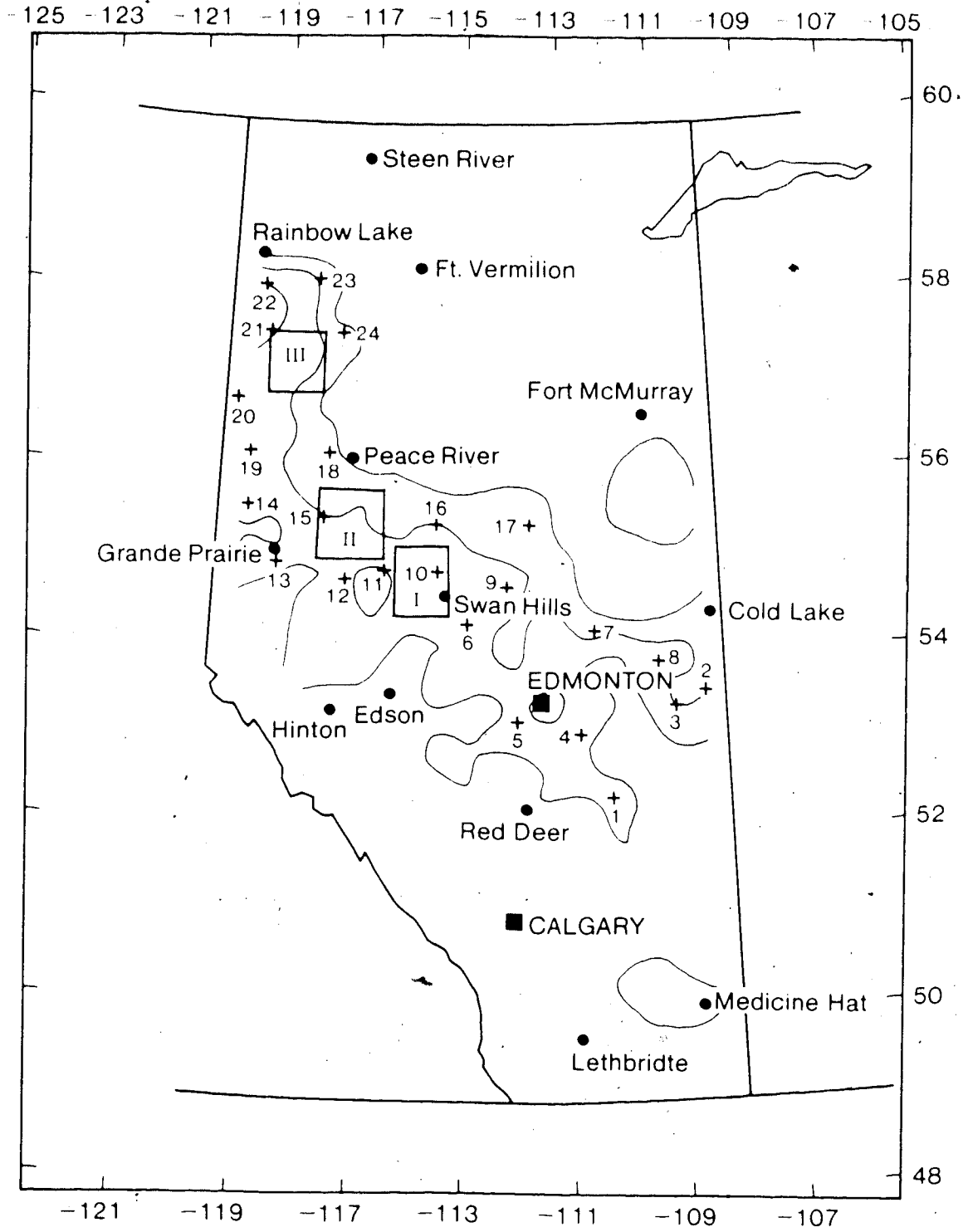
On the basis of the work of Majorowicz et al. (1985b), it will be assumed that $\frac{d^2 T}{dz^2} = 0$ in the $\Delta Q=0$ region. In other words, each of the terms in equation (1.4) are assumed to be zero within the sediments. Under this assumption, the heat flow results will represent the heat flux at the surface of the Precambrian basement. This is important because a relationship will be sought between heat flow and heat generation at the surface of the Precambrian basement. Also, for some locations where the temperature data are only available down to some intermediate depth, it will be assumed that heat flow is constant from the surface to the base of the sediments when the temperature at the base of the sediments is calculated. Outside the $\Delta Q=0$ region, this latter calculation could not be done without taking into account the groundwater motion.

To calculate ΔQ values for the Alberta basin, Majorowicz et al. (1985a) estimated effective thermal conductivities above and below the Paleozoic erosional surface at eighty equally spaced net rock analysis well locations. The results were then contoured to enable

Figure 1.3: Well locations of the twenty four net rock analysis wells. The areas labelled I, II, and III were selected for regional temperature gradient corrections (see Chapter 3).



Net Rock Analysis Wells



interpolation between the data points. The same net rock analysis data are used in this study for the wells in the $\Delta Q=0$ region.

The objective of this study is to calculate, as accurately as possible with the temperature and thermal conductivity data available, the heat flows and temperatures at the base of the sediments at the twenty-four well locations in the $\Delta Q=0$ region. This thesis uses the same temperature data that were available to Majorowicz et al. (1985a,b). However, different thermal conductivities are assigned to the sedimentary rock types and a proper uncertainty analysis is given. Another difference is that a temperature dependence function is assumed for the thermal conductivities of some rock types. Finally, the heat generation at the surface of the Precambrian basement is calculated for 182 samples from western Canada, and a relationship is sought between heat flow through the sediments and heat generation at the surface of the Precambrian basement in the $\Delta Q=0$ region.

CHAPTER 2

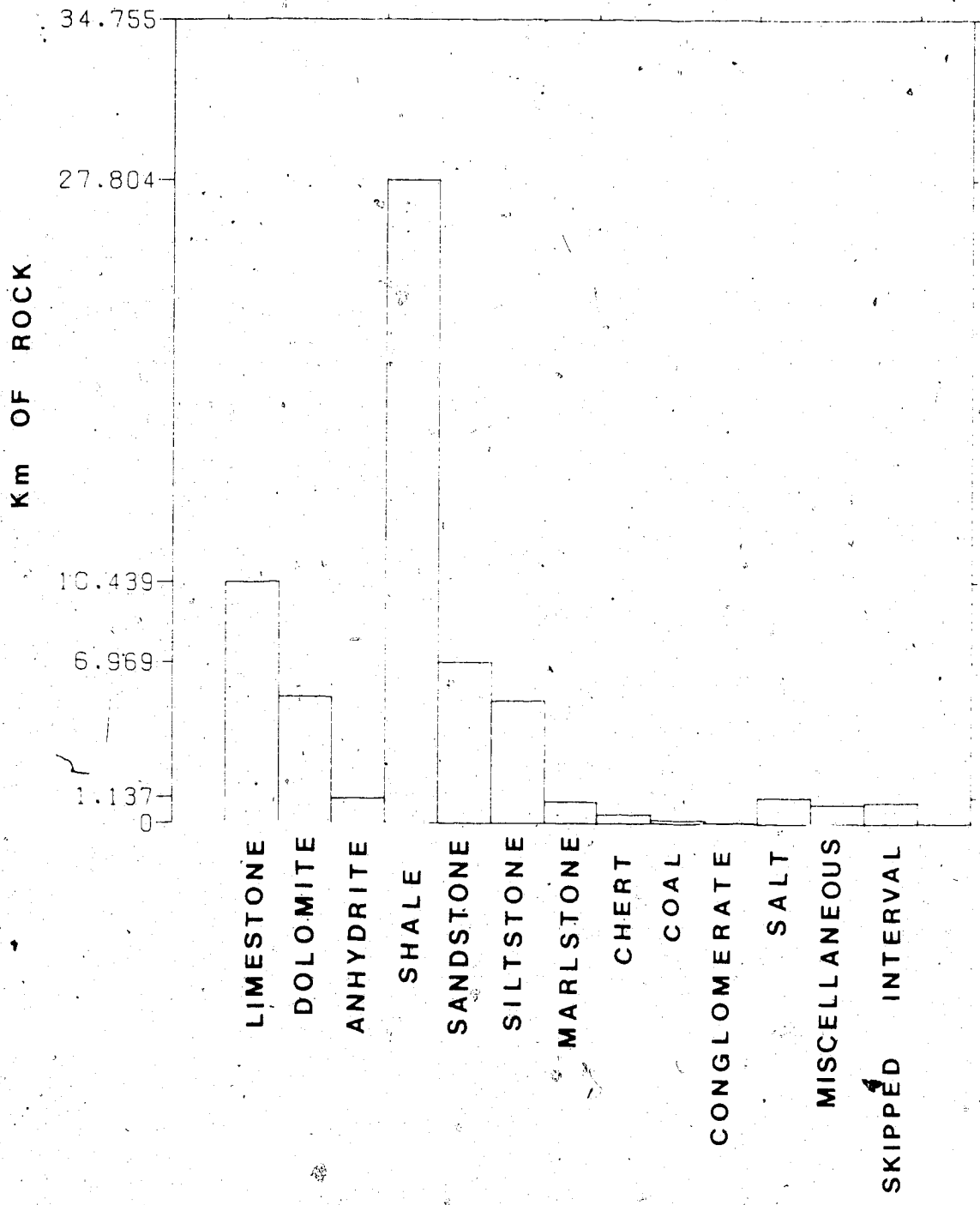
Thermal Conductivity of Sedimentary Rocks in Alberta

Introduction

Thermal conductivity was not measured as a function of depth for the twenty-four well locations of this study. However, the rock type sequences were known from the surface to the base of the sediments for each well location. Therefore, it was necessary to calculate the effective conductivity of the sediments on the basis of rock types.

The composition of the sedimentary strata is known in terms of thirteen basic rock types. The total number of kilometers of each rock type for all twenty four wells is shown in the bar graph of Figure 2.1. From the graph, shale is by far the most abundant sedimentary rock, accounting for 45% of the total number of kilometers of rock. It is also noteworthy that shale, limestone, sandstone, dolomite, and siltstone account for 91% of the total number of kilometers of rock. The remaining rock types, namely anhydrite, marlstone, chert, coal, conglomerate, salt, glacial till, and skipped intervals account for less than 10% of the total volume of rock. Skipped intervals are intervals in the net rock analyses that have not been assigned rock types.

Figure 2.1: Number of kilometers of the thirteen sedimentary rock types for all twenty-four wells.



Net Rock Analysis Data File

A net rock analysis of the sedimentary sequence for each of the twenty-four wells was done under contract from Energy, Mines and Resources, Ottawa by Sproule Associates Ltd. of Calgary in 1981 and the results were provided for use in this work by the Earth Physics Branch, EMR. The data file gives the compositions of consecutive depth intervals for each of the wells, and the number of depth intervals for a given well is roughly twenty-five. The thicknesses of the depth intervals are highly variable, and range from tens of meters to hundreds of meters.

Factors Affecting the Thermal Conductivity of Sedimentary Rocks

There are many factors which affect the thermal conductivities of sedimentary rocks, such as rock type, porosity, temperature, and pressure. Measured values also depend on the sample location and direction in which the thermal conductivity measurement is made.

A brief discussion of the pressure dependence of the thermal conductivity of rocks can be found in Kappelmeyer and Haenel (1974). The effect of pressure on the thermal conductivity of rocks is generally small, and for this work is assumed to be negligible for all types of rocks.

However, temperature dependence of thermal conductivity is taken into account in this study. In general, the thermal conductivity of a rock decreases with increasing

temperature. Various temperature functions have been used to describe the thermal conductivity of sedimentary rock types. Moss and Haseman (1981) investigated the thermal conductivity of polyhalite and anhydrite as a function of temperature. Other studies were conducted by Skvarla et al. (1981), and Birch and Clark (1940). In their study of heat flow in the Uinta Basin of northeastern Utah, Chapman et al. (1984) assumed that the solid rock conductivity was inversely proportional to the absolute temperature of the rock. An inverse temperature dependence of thermal conductivity is also assumed in this study (formula 2.7).

Porosity is also an important consideration in the thermal conductivity of a rock (Chapman et al., 1984). The thermal conductivity k_r of a saturated porous rock can be expressed as

$$k_r = k_w^\phi k_s^{1-\phi} \quad (2.1)$$

where ϕ is the porosity, k_w is the thermal conductivity of the fluid which is assumed to be water, and k_s is the thermal conductivity of the solid rock.

Finally, it must be mentioned that sedimentary rocks are anisotropic. The thermal conductivity measured in the lateral direction is generally different from the thermal conductivity measured in the vertical direction. This is not surprising if one remembers how sedimentary rocks are formed. The anisotropy in thermal conductivity of a rock is defined by

$$A = \frac{k_{||}}{k_{\perp}} \quad (2.2)$$

where k_{\parallel} is the thermal conductivity parallel to the bedding plane, and k_{\perp} is the conductivity perpendicular to the bedding plane.

Experimental Results from Alberta:
Limestone, Dolomite, Shale, Siltstone,
and Sandstone

The experimental determination of the thermal conductivity of rocks is not the subject of this study. However, the results of measurements made at the geothermal laboratory of the Department of Physics, University of Alberta, are analysed to estimate the thermal conductivities of limestone, dolomite, shale, sandstone, and siltstone. The measurements were made under contract from Energy, Mines and Resources, Ottawa.

The samples for these measurements were discs 38 mm in diameter and about one centimeter in thickness. They were from core plugs cut laterally across core sections obtained from the wells for petroleum exploration purposes. The water saturated samples were measured in a divided-bar apparatus at room temperature and under a confining pressure sufficient to maintain good thermal contact. Some of these thermal conductivity results were reported by Jones et al. (1985). The samples originate from 84 wells in the province of Alberta, and the locations of these wells are shown in Figure 2.2. Figure 2.3 shows thermal conductivity histograms for the five rock types, and gives the mean conductivities and standard deviations from the means. The corresponding

porosity histograms are shown in Figure 2.4.

A simple calculation shows that variations in porosity alone are not enough to explain the spread in the thermal conductivity values. For instance, consider limestone which has a measured lateral conductivity equal to 3.22 ± 1.16 W/m^{°K} and a mean porosity of 3.22%. The thermal conductivity of water at 22°C is 0.599 W/m^{°K}. Substituting into equation 2.1 gives the solid conductivity of limestone in the lateral direction equal to 3.40 W/m^{°K}. A decrease in the lateral thermal conductivity of limestone by one standard deviation, from 3.22 to 2.05 W/m^{°K} corresponds to an increase in porosity from 3% to 29%. But Figure 2.4 shows that there are no samples of limestone with a porosity of 29%. Consequently, the spread in the lateral thermal conductivity values must be due to other factors besides porosity variations, such as variations in chemical composition.

The thermal conductivities given in Figure 2.3 are lateral thermal conductivity values and are not used in the heat flow calculations unless the rock is isotropic. This is the case for siltstone. Table 2.1 lists the anisotropy factors used for the five rock types as well as the vertical conductivities calculated with these anisotropy factors. The anisotropy factors given in Table 2.1 are based on Table 6.6 of Kappelmeyer and Haenel (1974).

Figure 2.2: Locations of the wells from which measurements of thermal conductivities were made.

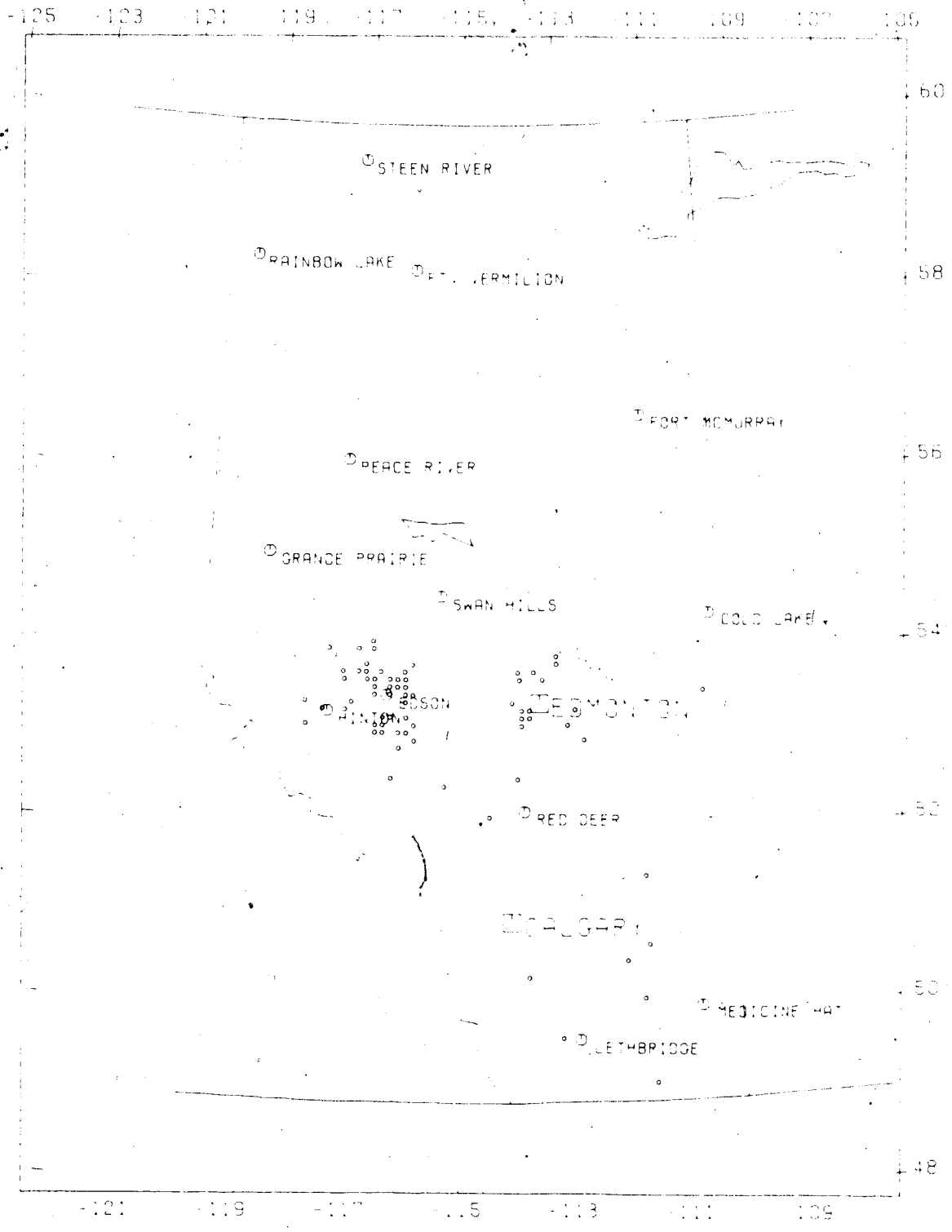


Figure 2.3: Lateral thermal conductivity histograms for limestone, dolomite, shale, sandstone, and siltstone.

LIMESTONE

MEAN = 3.22 W/m⁰K
STANDARD DEVIATION = 1.18 W/m⁰K

THERMAL CONDUCTIVITY W/m⁰K

DOLOMITE

MEAN = 3.19 W/m⁰K
STANDARD DEVIATION = 1.42 W/m⁰K

THERMAL CONDUCTIVITY W/m⁰K

SHALE

MEAN = 2.71 W/m⁰K
STANDARD DEVIATION = 0.83 W/m⁰K

THERMAL CONDUCTIVITY W/m⁰K

SANDSTONE

MEAN = 3.44 W/m⁰K
STANDARD DEVIATION = 1.44 W/m⁰K

THERMAL CONDUCTIVITY W/m⁰K

SILTSTONE

MEAN = 3.16 W/m⁰K
STANDARD DEVIATION = 1.27 W/m⁰K

THERMAL CONDUCTIVITY W/m⁰K

Figure 2.4: Porosity histograms corresponding to the thermal conductivity histograms in figure 2.3.

LIMESTONE

MEAN = 1.22 %

POROSITY %

DOLOMITE

MEAN = 2.16 %

SHALE

MEAN = 4.48 %

POROSITY %

POROSITY %

SANDSTONE

MEAN = 7.31 %

SILTSTONE

MEAN = 4.01 %

POROSITY %

POROSITY %

Table 2.1: Anisotropy and Vertical Conductivity of Limestone, Dolomite, Shale, Sandstone, and Siltstone

Rock Type	k(par.) (W/m ² K)	Anisotropy	k(perp.) (W/m ² K)
Limestone	3.2 ± 1.2	1.33	2.42 ± 0.88
Dolomite	3.2 ± 1.4	1.02	3.1 ± 1.4
Shale	2.71 ± 0.83	1.96	1.38 ± 0.42
Sandstone	3.4 ± 1.4	1.12	3.1 ± 1.3
Siltstone	3.2 ± 1.3	1.00	3.2 ± 1.3

According to Table 2.1, shale is the most anisotropic rock type, with an anisotropy of 1.96. The vertical thermal conductivity of shale, equal to 1.38 ± 0.42 W/m²K, is in agreement with the value of 1.05 to 1.25 W/m²K reported by Blackwell et al. (1981) for the thermal conductivity of shale in midcontinental regions of North America.

Temperature Dependence: The Thermal Conductivity of Shale

In order to determine the thermal conductivity of water-saturated shale as a function of temperature, it is necessary to know the thermal conductivity of water as a function of temperature. The following functions were used:

$$k_w = 0.563 + 0.00166T \quad 0 \leq T \leq 50^\circ\text{C} \quad (2.3)$$

$$k_w = 0.417 + 0.0575 \ln T \quad 50 \leq T \leq 100^\circ\text{C} \quad (2.4)$$

These functions are best fit curves to the data given in Table 6.8.2 of Kappelmeyer and Haenel (1974).

Figure 2.5 shows three thermal conductivity curves for shale. The three functions are

$$k_s(T) = [k_s(22)] \left(\frac{295}{T+273} \right) \quad (2.5)$$

$$k_r(T) = [k_s(T)]^{1-\phi(T)} \cdot [k_w(T)]^{\phi(T)} \quad (2.6)$$

$$k_r(T) = [k_r(22)] \left(\frac{295}{T+273} \right) \quad (2.7)$$

where T is the temperature in degrees Celsius. Each formula assumes that the thermal conductivity k of water-saturated shale with porosity 4.5% is 1.38 ± 0.42 W/m°K at 22°C (Table 2.1). Curve 2.5 represents the solid rock conductivity as a function of temperature. $k_s(22)$ is the solid conductivity at 22°C, calculated from equation 2.1 to be 1.43 W/m°K. Curve 2.6 in Figure 2.5 is the thermal conductivity of water saturated porous shale. The expression for $\phi(T)$ was obtained by calculating the best fit exponential decay for all of the porosity measurements considered as a function of depth. In total there were 1588 porosity measurements for rocks from various depths. The porosity-depth function and the data are shown in Figure 2.6. Porosity as a function of temperature was then calculated assuming a temperature gradient of 30°C/Km. Curve 2.7 in Figure 2.5 is a simplified version of curve 2.6. It exhibits an inverse temperature dependence of the thermal conductivity of the water-saturated porous rock.

Figure 2.5: Three thermal conductivity functions for shale. The mathematical formulae for the three curves are given in the text. Formula (2.7) is the temperature dependence function used in this study for some sedimentary rock types, (see table 2.2).

THERMAL CONDUCTIVITY OF SHALE

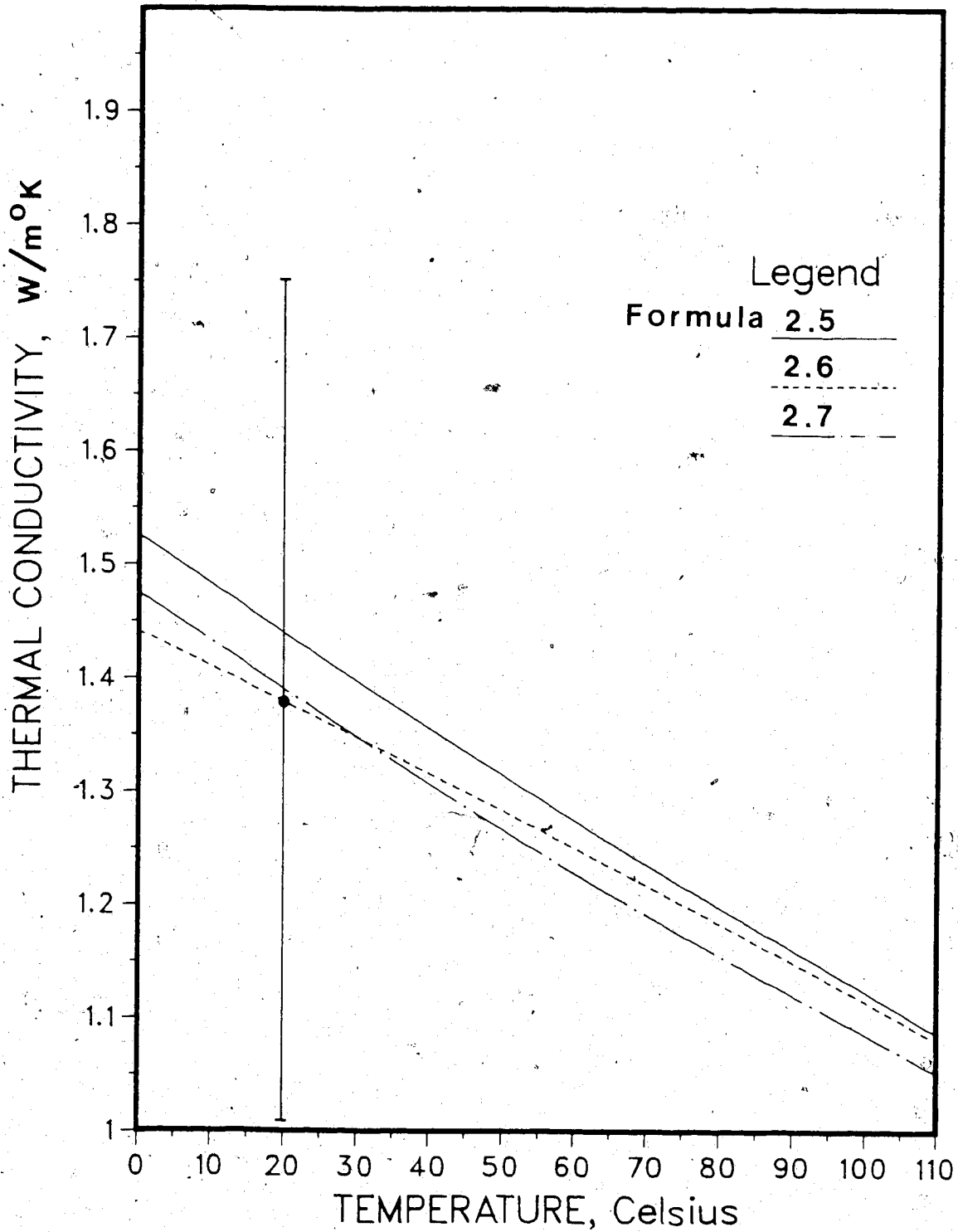
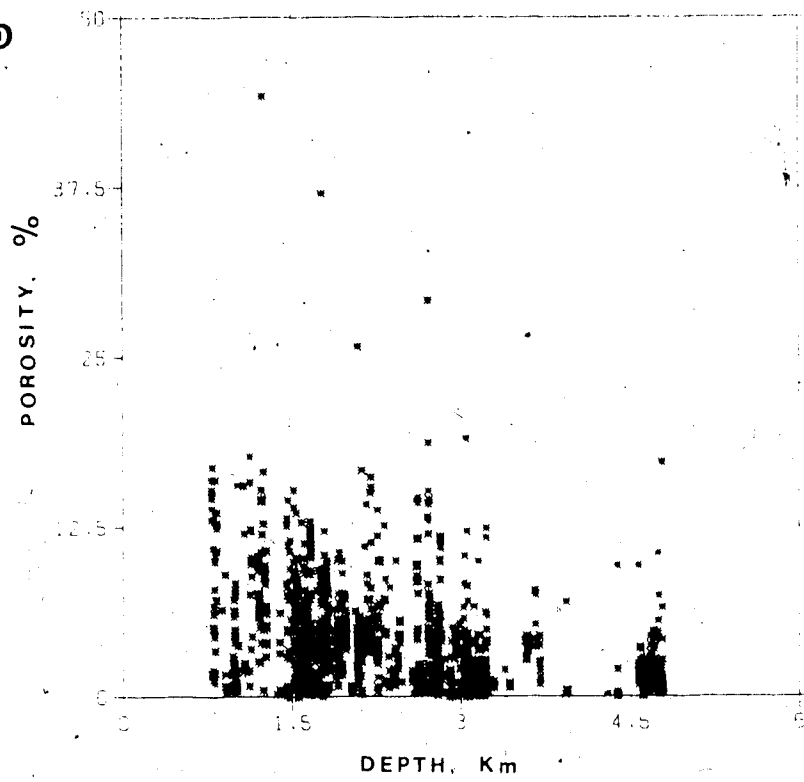


Figure 2.6: a) The 1588 porosity-depth measurements. b) The best fit exponential decay function for the data in a).

9)



10)

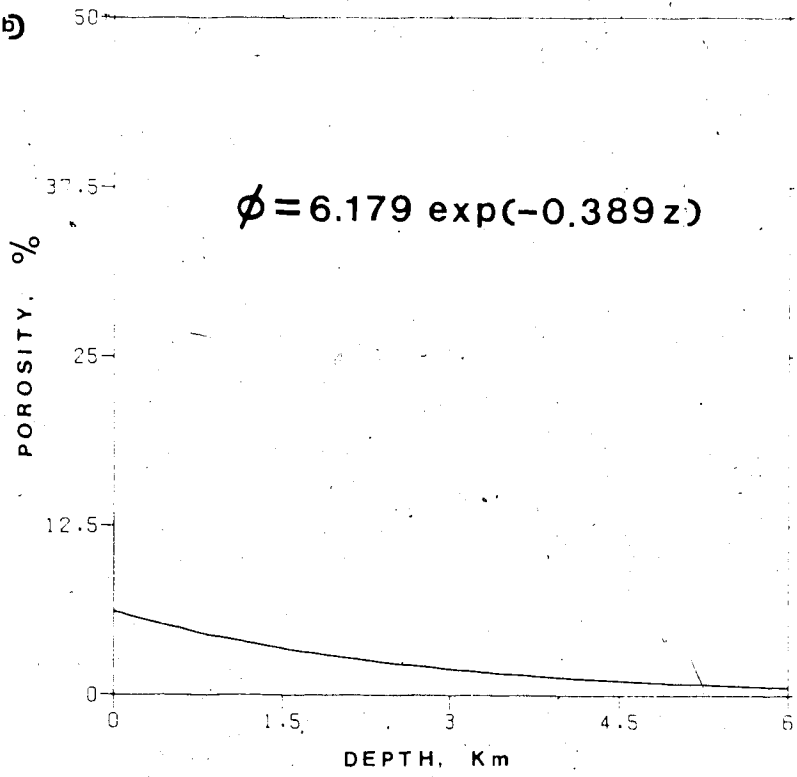


Figure 2.5 shows that over a temperature range of 110°C, corresponding to a depth of about four kilometers, the thermal conductivity of shale decreases by about one error bar. Although the majority of the heat flow calculations are for wells less than 2.5 Km deep, a number lie in the range 3.0-4.0 Km, so the temperature dependence of thermal conductivity is considered here. Considering the large uncertainty in the thermal conductivity, there is effectively no difference between formula 2.6 and formula 2.7 for expressing the temperature dependence. Formula 2.7 is used in this study because it is simpler and in some cases only the thermal conductivity of a rock type is known, while the corresponding porosity is not known. All of the 13 sedimentary rock types are assumed to have a temperature dependence of the form (2.7) except chert, coal, and glacial till, which are assumed to have a constant thermal conductivity over the temperature range pertinent to this study.

Thermal Conductivities of Remaining Rock

Types

For the cases where experimental thermal conductivity data from Alberta samples were not available, published data were used to estimate the thermal conductivities of rock types. The uncertainties in the thermal conductivities of the remaining rock types are reasonable estimates by the author.

Anhydrite and Marlstone. Published values for the thermal conductivities of anhydrite and marlstone at 50°C are given in Table 6.3.3 of Kappelmeyer and Haenel (1974). The temperature dependence formula 2.7 gives thermal conductivities at 22°C to be 5.8 ± 1.1 W/m²K for anhydrite and 3.0 ± 1.1 W/m²K for marlstone.

This value of the thermal conductivity of anhydrite is in agreement with the value of 4.8 ± 0.2 W/m²K calculated from a formula due to Moss and Haseman (1981), who studied the temperature dependence of anhydrite for a nuclear waste repository site near Carlsbad, New Mexico.

Rock Salt. The estimate for the thermal conductivity of rock salt given here is based on the work of Alm and Bäckstrom (1975). From their work, the thermal conductivity of NaCl at 25°C and one atmosphere pressure is 6.0 W/m²K. On this basis the thermal conductivity of rock salt was estimated to be 6.0 ± 1.0 W/m²K. This is the solid rock conductivity.

To arrive at a value for the thermal conductivity of porous rock salt, the porosity-depth curve of Figure 2.6b was integrated between 0 and 4 Km to give a mean porosity of 3.1%. Substituting this porosity into equation 2.1, the thermal conductivity of porous rock salt was calculated to be 5.7 ± 1.0 W/m²K at 22°C.

Chert. The rock type chert consists mostly of silica. Skvarla et al. (1981) investigated the temperature dependence of the thermal conductivity of silica. According to their results, the thermal conductivity of silica at 22°C is 1.4 W/m°K. Also, the thermal conductivity of silica is nearly constant over the temperature range 0-120°C. As in the case of rock salt, the thermal conductivity of porous chert was calculated assuming a porosity of 3.1%. The result is 1.4 ± 0.5 W/m°K for the thermal conductivity of porous chert.

Coal. The thermal conductivity of coal is taken to be 0.2 ± 0.2 W/m°K. This estimate is based on the work of Tye et al. (1981) who examined the thermal conductivity of Pittsburgh seam coal over the temperature range 0-900°C. Of course, their measurements are more precise than the uncertainty here suggests; but this is an estimate of the thermal conductivity of any coal sample found in Alberta. The thermal conductivity of coal will also be taken as a constant over the temperature range 0-120°C.

Glacial Till. The thermal conductivity of glacial till is taken to be 1.5 ± 0.5 W/m°K (Andersland and Anderson 1978, pp.114-120). It is assumed that the glacial till is not frozen. The thermal conductivity of glacial till is assumed to be a constant with temperature variation.

Conglomerate. The thermal conductivity of conglomerate posed a problem because its composition is highly variable. It was decided that the thermal conductivity of conglomerate would be estimated by calculating the arithmetic mean of all the conductivities, excluding the skipped interval. The result for the thermal conductivity of conglomerate at 22°C is 3.2 ± 1.8 W/m°K. The uncertainty here is estimated from the spread in thermal conductivity values of conglomerate given in Figure 1 of Kappelmeyer (1979). In any case, the thermal conductivity of conglomerate is not important because it only constitutes 0.08% of the total number of kilometers of rock for all the wells.

Skipped Interval. The thermal conductivity of a skipped interval was taken to be the weighted average of the conductivities of all the rock types. The result is 2.3 ± 2.0 W/m°K.

Summary of Thermal Conductivity Results

Table 2.2 gives the thermal conductivity results of this chapter.

TABLE 2-2: Summary of Thermal Conductivity Results for Sedimentary Rock Types

No.	Rock Type	no of samples	k (W/m ² K)	Mean Porosity (%)	Temp (°C)	k ± (295/273+T) ²	k/k (per cent)
1	Limestone	679	2.42 ± 0.88	3.2	22	yes	yes
2	Dolomite	254	3.1 ± 1.4	2.2	22	yes	yes
3	Anhydrite	7	5.8 ± 1.1		22	yes	yes
4	Shale	72	1.38 ± 0.42	4.5	22	yes	yes
5	Sandstone	225	3.1 ± 1.3	7.3	22	yes	yes
6	Siltstone	165	3.2 ± 1.3	4.0	22	yes	yes
7	Marlstone	3	3.0 ± 1.1		22	yes	
8	Chert	--	1.4 ± 0.5	3.1	22	constant	
9	Coal		0.2 ± 0.2		50	constant	yes
10	Conglomerate	--	3.2 ± 1.8		22	yes	
11	Rock Salt	--	5.7 ± 1.0	3.1	22	yes	yes
12	Glacial Till	--	1.5 ± 0.2	10	not frozen	constant	
13	Skipped Interval		2.3 ± 2.0		22	yes	

Effective Conductivity of Sediments

As mentioned in Chapter 1, the effective conductivity of a stratigraphic sequence is defined by:

$$k_{\text{eff}} = \frac{\sum_{i=1}^n \Delta z_i}{\sum_{i=1}^n \left(\frac{\Delta z_i}{k_i} \right)} \quad (1.3)$$

where k_i is the thermal conductivity of the layer of thickness Δz_i . In this study, the sediments are treated as effectively one layer, or two layers if there is a split depth (see Chapter 3). For a given sedimentary layer, k_{eff} was calculated according to formula (1.3), with Δz_i taken as one depth interval in the net rock analysis for the well, and k_i taken as the thermal conductivity of the depth interval. Temperature dependence was taken into account in the effective conductivity calculation in accordance with the results of Table 2.2. The average conductivity for a given depth interval was calculated at the temperature of the midpoint of the interval, assuming a temperature gradient of 30 °C/Km and a mean surface temperature of zero degrees Celsius.

Uncertainty in Effective Conductivity

Formula (1.3) could not be used to calculate the uncertainty in the effective conductivity of a layer because the thermal conductivities of the depth intervals Δz_i are not independent; they are all weighted averages of the

thermal conductivities of the thirteen basic rock types. The following formula was used to calculate the uncertainty in the effective conductivity of a sedimentary layer:

$$k_{\text{eff}} = \frac{\sum \Delta z_{ti}}{\sum \left(\frac{\Delta z_{ti}}{k_{ti}} \right)} \quad (2.8)$$

This is the same as formula (1.3), except the symbols have different meanings. In formula 2.8, Δz_{ti} is the total thickness of rock type i in the layer, and k_{ti} is the thermal conductivity of rock type i at 22 °C. The number of terms in the sums in formula (2.8) is now fixed and equal to thirteen; and the thermal conductivities appearing in the formula are all independent. Taking the thermal conductivity of rock type i to be $k_{ti} \pm \delta_{ti}$ (see Table 2.2), a standard error analysis of formula (2.8) gives the following expression for the uncertainty in the effective conductivity of a layer:

$$\delta k_{\text{eff}} = \frac{\left(\sum \Delta z_{ti} \right) \sqrt{\sum \left(\frac{\Delta z_{ti} k_{ti}}{k_{ti}^2} \right)^2}}{\left(\sum \frac{\Delta z_{ti}}{k_{ti}} \right)^2} \quad (2.9)$$

Table 2.3 below gives the effective thermal conductivities of the top and bottom layers of each well. In some cases the effective thermal conductivity of the bottom layer is not given because there is no split depth. Note that the uncertainties in the effective conductivities are very

nearly the same for all layers, and equal to $0.4 \text{ W m}^{-2}\text{K}^{-1}$.

Table 2.3: Sedimentary Thicknesses and Effective Conductivities of Sedimentary Layers

Well Index	Sedimentary Thickness (Km)	Split Depth (Km)	k_{eff} (W m ⁻¹ K) Top Layer	k_{eff} (W m ⁻¹ K) Bottom Layer
1	2.5381	1.17	1.80 ± 0.39	2.36 ± 0.42
2	1.6621	0.58	1.74 ± 0.44	2.58 ± 0.39
3	1.8209	0.64	1.81 ± 0.37	2.30 ± 0.41
4	2.4658	1.24	1.96 ± 0.38	2.05 ± 0.39
5	2.8990	1.86	2.04 ± 0.38	1.91 ± 0.41
6	2.6228	1.19	1.81 ± 0.39	1.93 ± 0.40
7	1.8980	0.69	1.85 ± 0.40	2.72 ± 0.41
8	1.7020	0.64	1.76 ± 0.38	2.99 ± 0.41
9	2.0656	0.80	1.84 ± 0.39	2.34 ± 0.44
10	2.7289		1.81 ± 0.37	
11	3.0962		1.90 ± 0.37	
12	3.2309	1.70	1.80 ± 0.39	2.19 ± 0.42
13	3.8262		1.92 ± 0.38	
14	3.6314		2.01 ± 0.38	
15	2.7968		1.96 ± 0.37	
16	1.9885		2.00 ± 0.39	
17	1.7608	0.64	1.89 ± 0.37	2.70 ± 0.45
18	2.1610	1.09	2.18 ± 0.40	2.20 ± 0.42
19	2.4140		2.17 ± 0.37	
20	3.0687	1.33	1.87 ± 0.40	1.84 ± 0.41
21	2.6408	0.60	1.73 ± 0.41	2.16 ± 0.40
22	2.2759	0.60	1.65 ± 0.41	2.03 ± 0.41
23	1.8885	0.56	1.94 ± 0.36	2.22 ± 0.42
24	1.8870		2.09 ± 0.38	

CHAPTER 3

Temperature Gradients

As stated in the introduction, in order to calculate the vertical heat flow in a sedimentary strata the average temperature gradient and the effective conductivity must be known. Various methods were used here to calculate the best temperature gradient possible with the temperature data available. The effect of perturbations in the surface temperature will also be considered.

Bottom-hole temperature data were available for the area considered, and are the same data as used by Majorowicz et al. (1985a). For each of the wells, local gradients were calculated using all of the bottom-hole temperature (BHT) measurements in the 3 X 3 township-range area centered about the well location. Initially, corrected temperatures were calculated for each well using the Horner extrapolation technique (see Fertl and Wichmann, 1977). Corrected temperature gradients were then calculated for each well using a fixed mean surface temperature. The mean surface temperatures at the well locations were estimated from a map by McKay (1950). In some cases there were not enough

The temperatures used in this study are the mean surface temperatures of the air above the ground. In Alberta, the mean annual ground temperature is about 2°C higher than the mean annual surface temperature (Judge, 1973).

corrected temperature data points to calculate a reasonable corrected temperature gradient, so regional corrections were applied to the uncorrected local gradients to obtain corrected local gradients. Regional corrections will be discussed in more detail later on in this chapter.

The uncertainties in the individual BHT measurements are not known, so the spread in the data must be used to estimate the uncertainties in the temperature gradients.

It was found that there were five cases to be considered when calculating the most accurate temperature gradients possible at the twenty-four well locations. Each of these cases will be described below.

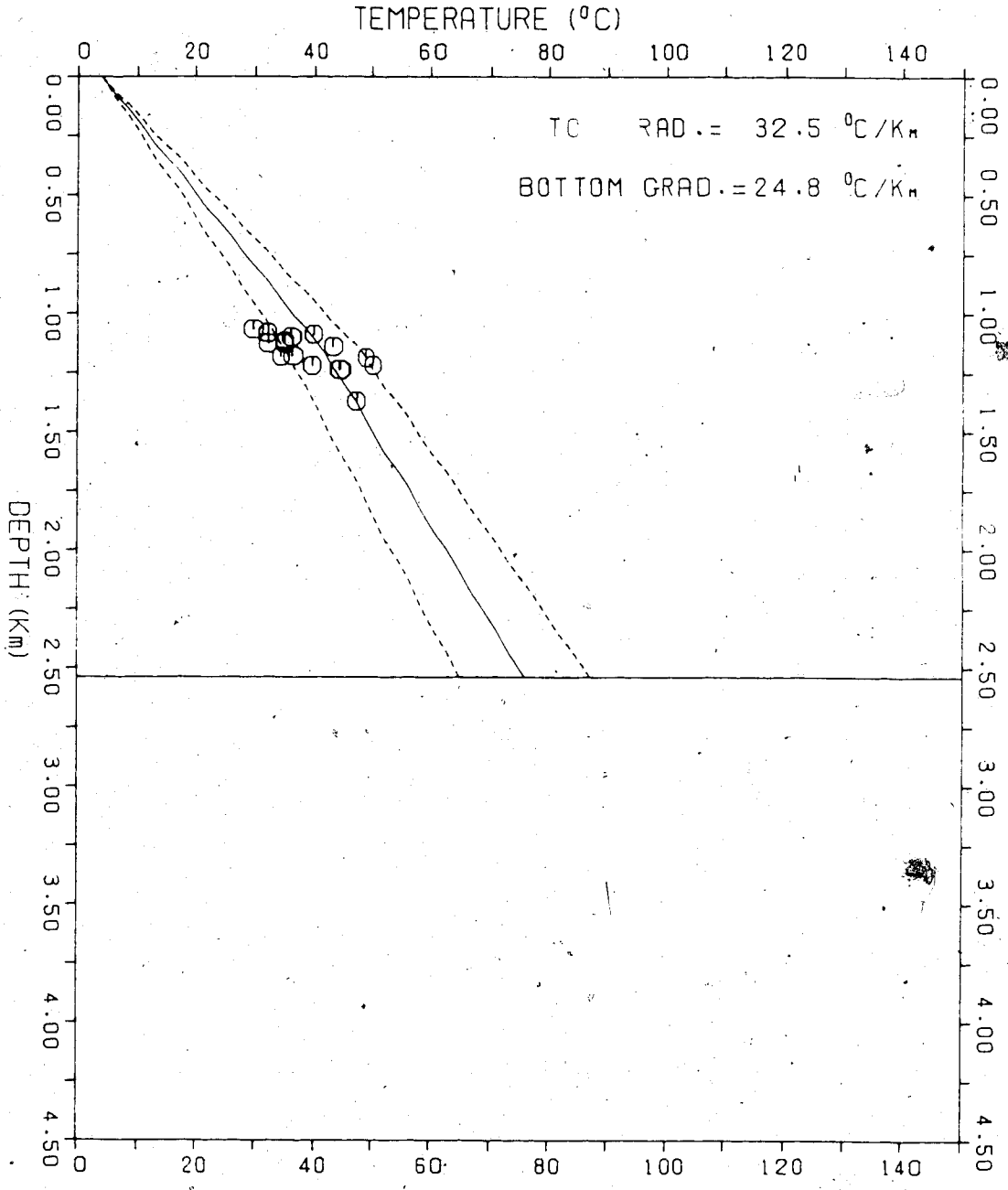
Cases 1, 2, and 3

Case 1. In this case, the bulk of the corrected temperature data is centered about some intermediate depth which is not close to the base of the sediments. An example of this case is well number 1, shown in Figure 3.1. In this case a least squares straight line gradient is calculated with a fixed mean surface temperature. The average depth of the temperature data is also calculated, and is referred to as the 'split depth'. It is assumed that this least squares temperature gradient is a reasonable approximation to the average gradient down to the split depth:

$$\langle VT \rangle = \frac{\sum \Delta z_i VT_i}{h} \quad (3.1)$$

Figure 3.1: An example of case 1: temperature as a function of depth for well index 1. The dashed lines represent the probable uncertainty in the temperature. The solid horizontal line represents the base of the sediments. The calculation of the heat flow and temperature at the base of the sediments will be described in Chapter 4.

WELL INDEX: 1.
HEAT FLOW: 59. ± 16. MW PER SQ. METER
TEMPERATURE AT
BASE OF SEDIMENTS: 76. ± 11. °C



where h is the split depth. The calculation of the gradient for the lower interval shown in Figure 3.1 will be discussed in Chapter 4. The dashed lines shown in Figure 3.1 represent the probable uncertainty in the temperature as a function of depth.

The uncertainty in the mean surface temperature is taken to be negligible. The uncertainty in the temperature at the split depth is the probable uncertainty, based on the spread in the temperature data. In some cases the uncertainty in the temperature at the split depth could be estimated by plotting the information density on the temperature axis and calculating the standard deviation.

Case 2. In the second case, there are enough corrected temperature data so that the temperature distribution is known from the surface to the base of the sediments. Again, the gradient is calculated with a fixed mean surface temperature. An example is well number 19, shown in Figure 3.2. Some of the BHT measurements appear to be below the base of the sediments is because the sedimentary rocks dip in this 3 X 3 township-range area.

Case 3. In this case there is a split depth, and the corrected gradient for the lower interval is calculated by a straight line least squares fit without a fixed mean surface temperature. An example is well number 9, shown in Figure 3.3. The gradient in the upper interval as shown in the

Figure 3.2: An example of case 2: temperature as a function of depth for well index 19. The explanation of this figure is the same as for Figure 3.1.

WELL INDEX: 19.
HEAT FLOW: 72. ± 14. MW PER SQ. METER
TEMPERATURE AT
BASE OF SEDIMENTS: 82. ± 7. °C

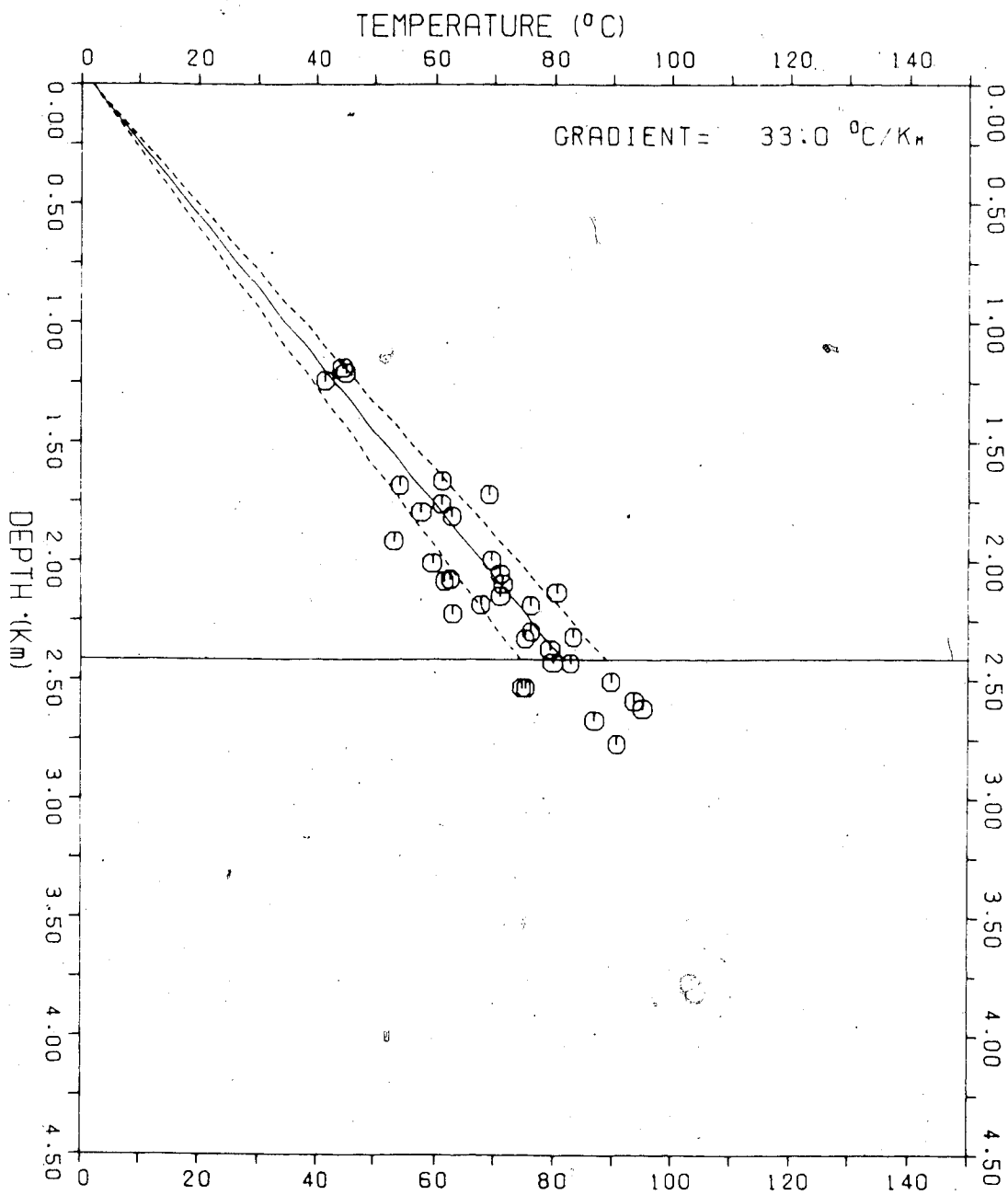


Figure 3.3: An example of case 3: temperature as a function of depth for well index 9. The explanation of this figure is the same as for Figure 3.1.

WELL INDEX: 9.
HEAT FLOW: 55. ± 19. MW PER SQ. METER
TEMPERATURE AT
BASE OF SEDIMENTS: 64. ± 8. °C

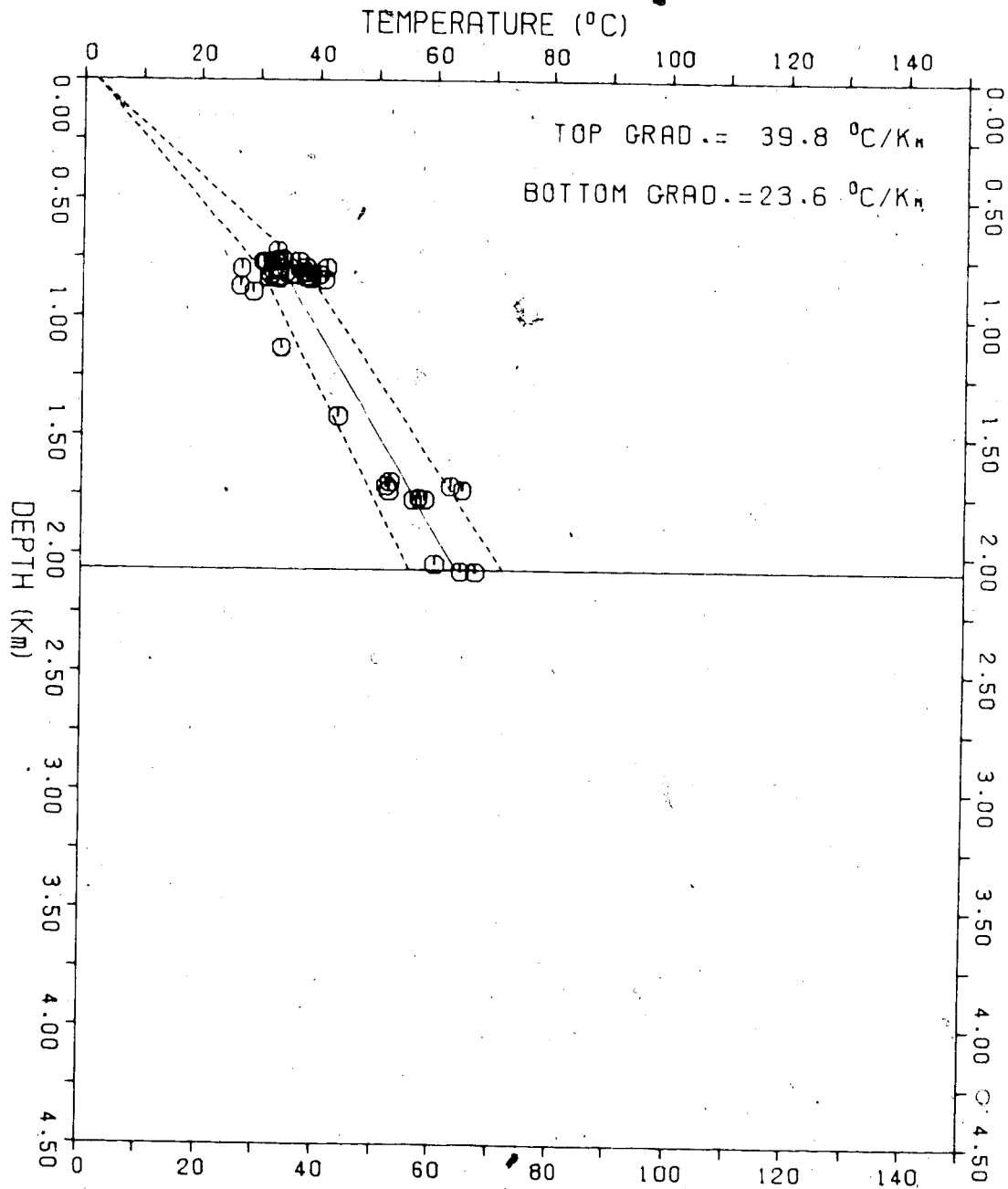


figure is simply a straight line between the mean surface temperature and the temperature at the split depth.

Cases 4 and 5: Regional Corrections

For these two cases, there were insufficient corrected temperature values in the local 3 X 3 township-range areas to calculate a reasonable temperature gradient. This was the case for well numbers 10, 15, 21 and 24. For these locations corrected gradients were calculated by applying regional corrections to the local uncorrected gradients.

Three regions were selected in the $\Delta Q=0$ zone. These regions are labeled I, II, and III on the map in Figure 1.3. For each region, corrected and uncorrected temperature gradients were calculated without fixed mean surface temperatures. They are shown in Appendix II.

The corrected regional gradients are greater than the uncorrected gradients because the effect of drilling and circulation is to reduce the temperature gradient (Kappelmeyer and Haenel, 1974, pp. 183-188). The percentage increases that must be applied to the uncorrected regional gradients so that they equal the corrected regional gradients are listed in the table below for the three regions.

Table 3.1: Regional Percentage Corrections to Temperature Gradients

Region	Uncorrected Gradient (°C/Km)	Corrected Gradient (°C/Km)	Percentage Correction
I	26.5	29.4	10.9
II	23.1	25.4	10.0
III	28.0	31.1	11.1

The percentage corrections in Table 3.1 are applied to the local uncorrected gradients to obtain corrected local gradients. It should be pointed out that the percentage correction is nearly constant for the three regions, and equal to about 11%. Cases 4 and 5 will now be described.

Case 4. In this case the uncorrected temperature gradient is plotted with a fixed mean surface temperature, and the regional percentage correction is applied to obtain the corrected gradient. Also, in this case, the gradient is known from the surface to the base of the sediments. An example is well number 10, and the local uncorrected temperature gradient is shown in Figure 3.4. The dashed lines in the figure are the 95% confidence limits. The uncertainty in the corrected local temperature gradient is assumed to be the same as for the uncorrected local gradient.

Figure 3.4: An example of case 4: the uncorrected local temperature gradient for well index 10. The least squares gradient is calculated with a fixed mean surface temperature. The dashed lines represent the 95% confidence limits.

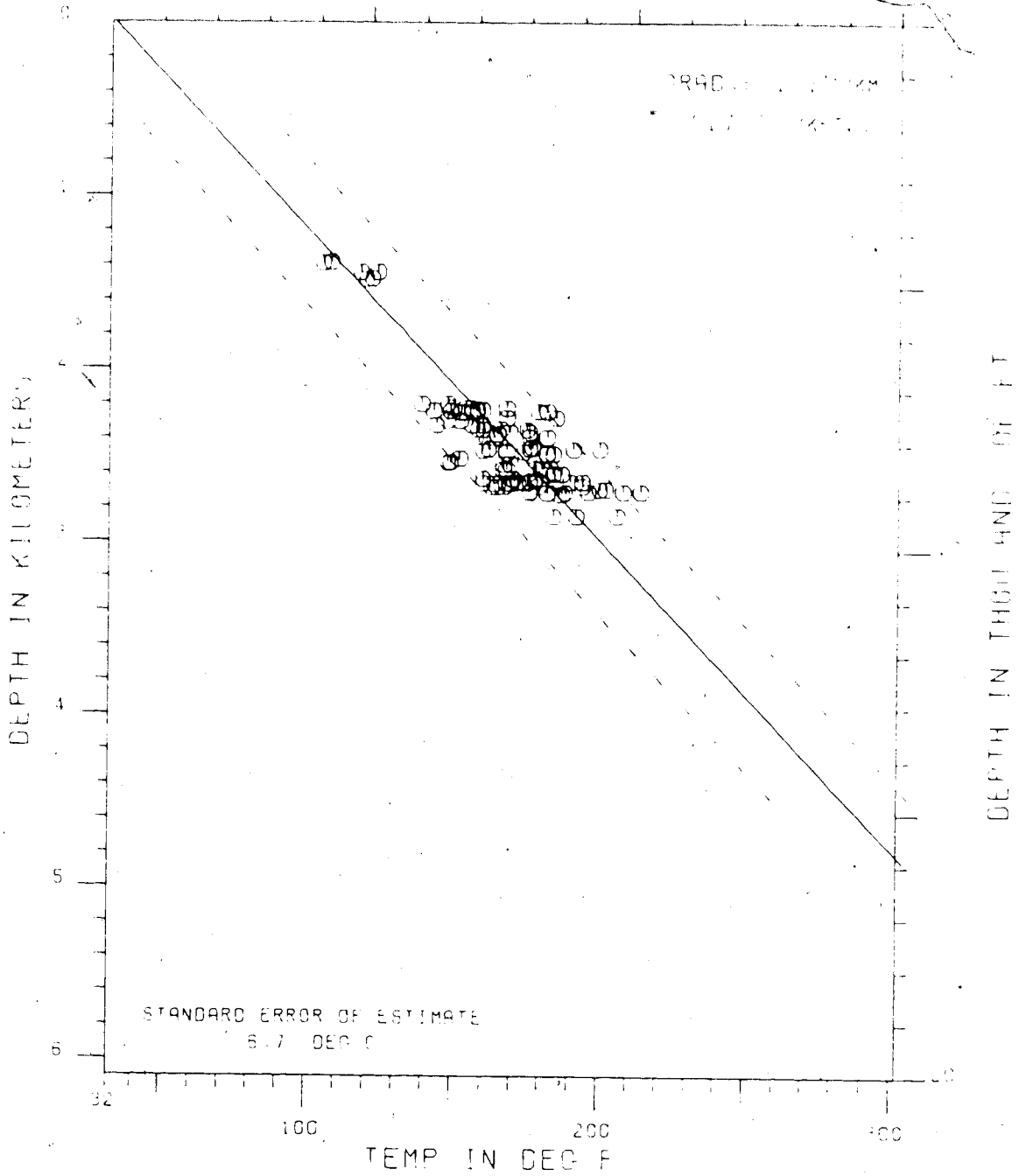
WELL INDEX: 10
UNCORRECTED LOCAL GRADIENT

W51BHTW TWP. 07 88 89 RDE. 10 11 12 13 14 15 16 17 18 19 20 21 22 23 24 25 26 27 28 29 30 31 32 33 34 35 36 37 38 39 40 41 42 43 44 45 46 47 48 49 50 51 52 53 54 55 56 57 58 59 60 61 62 63 64 65 66 67 68 69 70 71 72 73 74 75 76 77 78 79 80 81 82 83 84 85 86 87 88 89 90 91 92 93 94 95 96 97 98 99 100

TEMP IN DEG C

50

100



Case 5. In this case the uncorrected gradient is plotted without a fixed mean surface temperature. An example is well number 21, and its uncorrected temperature gradient is shown in Figure 3.5. Case 5 is similar to case 3, except that the percentage regional correction must be applied to determine the corrected gradient for the lower interval. The gradient in the upper interval is calculated from the straight line between the mean surface temperature and the corrected temperature at the split depth. As in case 4, the uncertainty in the uncorrected gradient is carried over to the corrected gradient.

Table 3.2 below lists the local uncorrected gradients and the local corrected gradients after the percentage corrections have been applied, for the case 4 and case 5 wells. The local uncorrected gradients for the case 4 and case 5 wells are given in Appendix III.

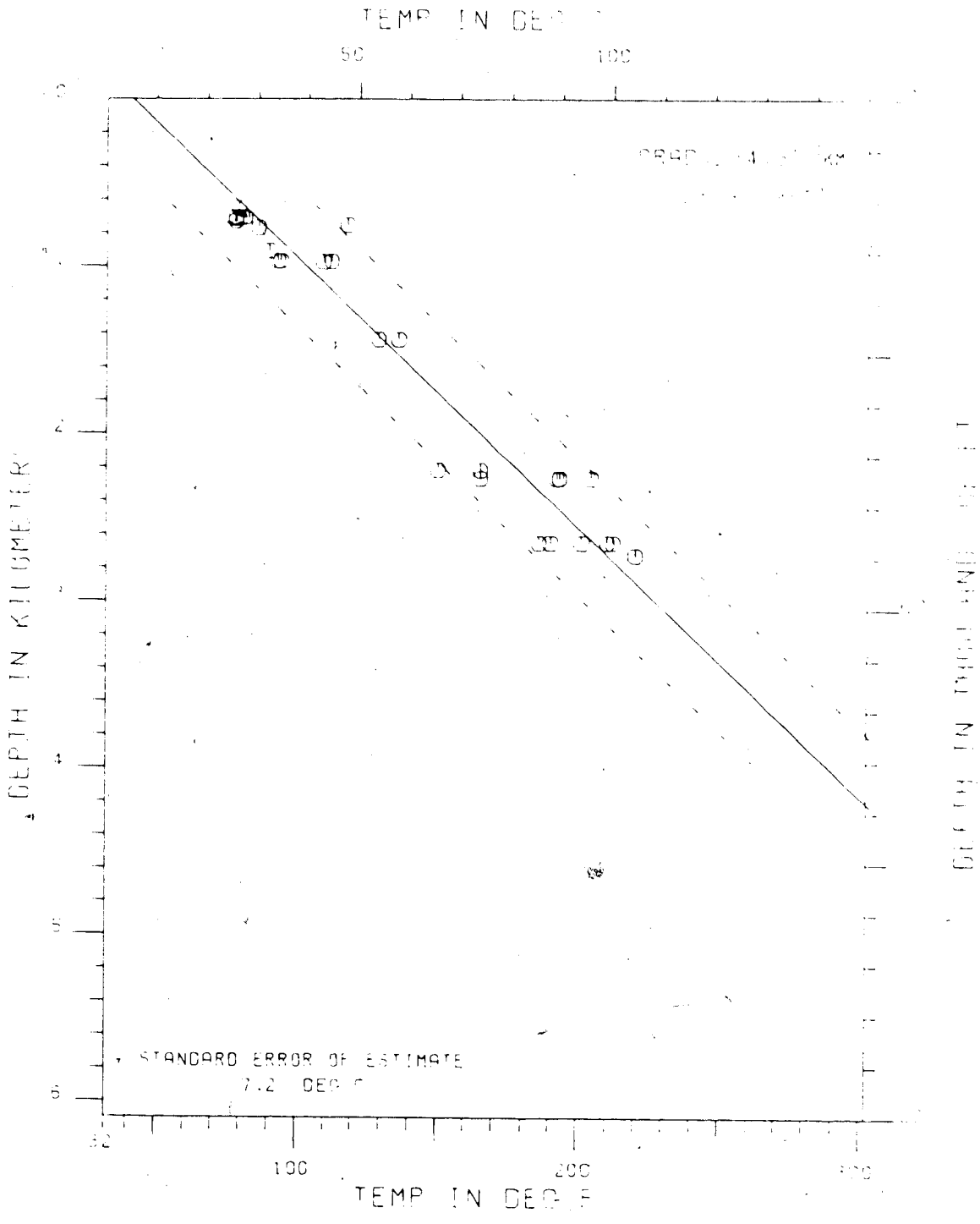
Table 3.2: Regional Corrections to Local Gradients

Well Index	Case	Uncorrected Gradient (°C/Km)	Percentage Correction	Corrected Gradient (°C/Km)
10	4	31.1	10.9	34.5
15	4	24.9	10.0	27.4
21	5	34.5	11.1	38.3
24	4	32.9	11.1	36.6

Figure 3.5: An example of case 5: the uncorrected local temperature gradient for well index 21. The least squares gradient is calculated without a fixed mean surface temperature. The dashed lines represent the 95% confidence limits.

WELL INDEX: 21
 UNCORRECTED LOCAL GRADIENT

WS(BHT) TWP. 24-33-103 R. 2E. 101 N.



Periodic Perturbations of the Surface
Temperature

As mentioned in Chapter 1, this study assumes a steady state temperature gradient. Strictly speaking, however, this is not correct because there are daily and seasonal variations of the surface temperature, as well as longer period variations in the surface temperature due to the advance and retreat of glaciers in geologic time. As might be expected, the depth of penetration of periodic disturbances of the surface temperature is greatest for long period perturbations.

Seasonal variations in the mean surface temperature have a period of one year and a depth of penetration of about 20 meters (Judge, 1973). Most of the temperature measurements in this work are at a depth greater than one kilometer, so the effect of this perturbation on the calculated temperature gradients is negligible.

Long period perturbations in the surface temperature are due to the advance and retreat of glaciers. The amplitude of the perturbation in this case is about four degrees celsius, and the depth of penetration is perhaps two kilometers. The maximum perturbation at a depth of one kilometer would only be about two degrees celsius and the uncertainty in the temperature at this depth is greater than two degrees celsius, so a glacial correction is not applicable to this work. A discussion of the glacial correction to temperature data is found in Kappelmeyer and

Haenel (1974), Jessop (1971), and Cermak and Jessop (1971).

CHAPTER 4

Heat Flow, Temperature at the Base of the Sediments, and Heat Generation

Heat Flow and Temperature at the Base of the Sediments

Recall from the Introduction that for a sedimentary sequence with effective conductivity k_{eff} and average gradient $\langle \nabla T \rangle$ the vertical heat flow is given by

$$q = k_{eff} \cdot \nabla T \quad (1.2)$$

The effective conductivities used in the heat flow calculations were given in Table 2.3. The calculation of the average gradients was discussed in Chapter 3. The calculation of the heat flows and temperatures at the base of the sediments will now be discussed for each of the cases described in Chapter 3.

Case 1. In this case the average corrected gradient is known down to some intermediate split depth. The heat flow is calculated from formula (1.2) for the top layer and assumed to be the same in the bottom layer. Under this assumption the temperature at the base of the sediments is given by the following formula:

$$T_B = T_{sp} + \frac{qh}{k_{eff}} \quad (4.1)$$

where T_B is the temperature at the base of the sediments, T_{sp} is the temperature at the split depth, q is the heat flow calculated for the top layer, h is the thickness of the bottom layer, and k_{eff} is the effective conductivity of the bottom layer from Table 2.3.

A standard uncertainty analysis applied to formula (4.1) gives the following expression for the uncertainty in the temperature at the base of the sediments:

$$\delta T_B = \left\{ (\delta T_{sp})^2 + \left[\left(\frac{\delta q}{q} \right)^2 + \left(\frac{\delta k_{eff}}{k_{eff}} \right)^2 \right] \cdot \left(\frac{qh}{k_{eff}} \right)^2 \right\}^{1/2} \quad (4.2)$$

An example of this calculation is Figure 3.1 of Chapter 3. The uncertainty δq in formula (4.2) was found by applying a standard uncertainty analysis to equation (1.2):

$$\delta q = \left\{ [k_{eff} \cdot (\delta \langle \nabla T \rangle)]^2 + [\langle \nabla T \rangle \cdot \delta k_{eff}]^2 \right\}^{1/2} \quad (4.3)$$

Cases 2 and 4. In these two cases either the corrected gradient is known down to the base of the sediments (case 2), or it may be calculated by applying a regional correction (case 4). Therefore, the temperature at the base of the sediments is known, and the heat flow calculation is straightforward. An example of case 2 is Figure 3.2 of Chapter 3.

21

Cases 3 and 5. In case 3 and case 5 the corrected bottom gradient is either known (case 3) or can be calculated by applying a regional correction (case 5). In these two cases the true heat flow is taken to be the heat flow in the bottom layer. An example of case 3 is Figure 3.3 of Chapter 3. The top average gradient is the slope of the straight line drawn through the mean surface temperature and the temperature at the split depth. For comparison purposes, the heat flow in the top layer was also calculated for the wells of case 3 and case 5. The results are shown in Table 4.1.

Table 4.1 gives the split depths for wells 9, 21, and 22 as well as the depths to the Paleozoic erosional surface. The split depth is approximately equal to the Paleozoic erosional surface depth in each case. The ΔQ values have also been calculated for the wells. The uncertainties in the ΔQ values are not the square roots of the sums of the squares of the uncertainties in the top and bottom heat flows because these two uncertainties are not independent.

Since the split depth is about equal to the Paleozoic erosional surface depth, the ΔQ values calculated in the table may be compared with the ΔQ values expected from the ΔQ map in Figure 1.1. From Figure 1.1, well number 9 is close to the $\Delta Q=0$ line, so ΔQ would be expected to be zero. The heat flow for well number 9 is 18 ± 20 mW/m² and zero is within the probable uncertainty. Well numbers 21 and 22 are on a $\Delta Q=-20$ mW/m² contour. From the table, the calculated ΔQ

TABLE 4.1 Heat Flow Above and Below the Split Depth for Case 3 and Case 5 wells

Well Index	Case	Split Depth (Km)	Depth of Paleozoic Erosional Surface (Km)	Q(top) (mW/m ²)	Q(bot) (mW/m ²)	Q(top)-Q(bot) (mW/m ²)
9	3	0.8	0.76	73 ± 18	55 ± 19	18 ± 20
21	5	0.6	0.62	89 ± 26	83 ± 19	6 ± 25
22	3	0.6	0.58	85 ± 25	77 ± 27	8 ± 30

values are 6 ± 25 mW/m² and 8 ± 30 mW/m², respectively. The value of -20 mW/m² is within the probable uncertainty in each of these results.

It is interesting to note that all three ΔQ values calculated here are higher than would be expected from the map in Figure 1.1. However, the number of cases are too few to suggest a discrepancy between this work and the work of Majorowicz et al. (1985b). Finally, note that the ΔQ values for each case in Table 4.1 are equal to zero within experimental uncertainty. This gives support to the interpretation that the heat flow values are equal to the heat flux at the surface of the Precambrian basement. It is also a check on the assumption that ΔQ is equal to zero for the calculations of temperatures at the base of the sediments for case 1.

Summary

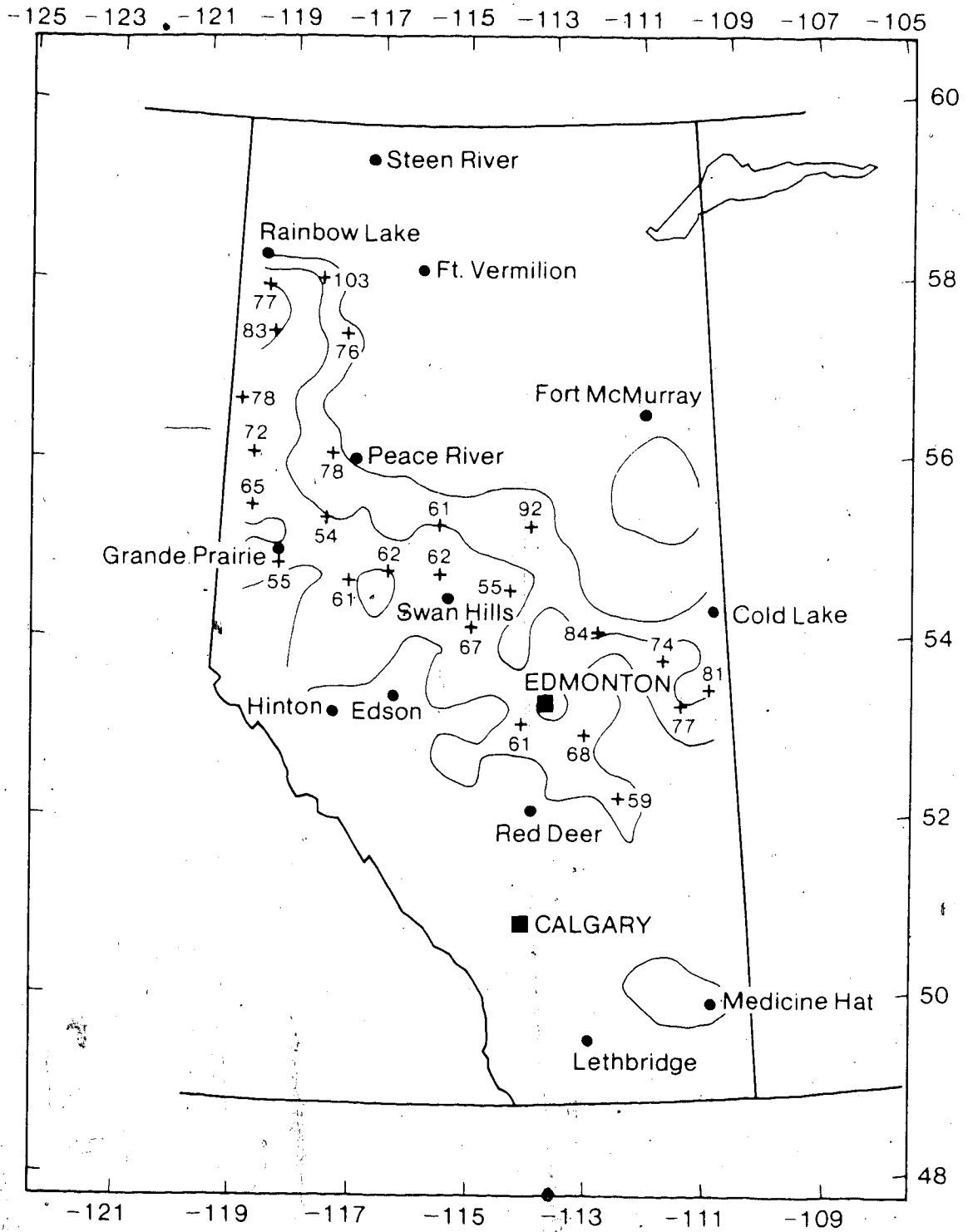
A summary of the calculations of this section for all twenty-four wells is given in Table 4.2 and the map of Figure 4.1. The temperature-depth distribution plots for all the wells are given in Appendix IV. From the table, the average heat flow for all twenty-four wells is 71 mW/m², with a standard deviation of 12 mW/m². This is in good agreement with the work of Majorowicz et al. (1985b), who concluded that the heat flow in the $\Delta Q=0$ region is 60-80 mW/m². From the map in Figure 4.2, the heat flow values calculated for well numbers 4 and 5 in the vicinity of

TABLE 4.2. Heat Flows and Temperatures at the Base of the Sediments

Well Index	Case	Mean Surface Temp ($^{\circ}\text{C}$)	Top Gradient ($^{\circ}\text{C}/\text{Km}$)	Bottom Gradient ($^{\circ}\text{C}/\text{Km}$)	Heat Flow (mW/m^2)	Temp at Base ($^{\circ}\text{C}$)
1	1	4.0	32.5	24.8	59 ± 16	76 ± 11
2	1	1.0	46.5	31.4	81 ± 27	62 ± 13
3	1	2.0	42.7	33.6	77 ± 19	69 ± 12
4	1	4.0	34.9	33.4	68 ± 18	88 ± 13
5	1	4.0	30.0	32.0	61 ± 15	93 ± 11
6	1	2.0	36.9	34.6	67 ± 17	95 ± 16
7	1	1.0	45.5	30.9	84 ± 22	70 ± 11
8	1	1.0	42.1	24.8	74 ± 18	54 ± 7
9	3	2.0	39.8	23.6	55 ± 19	64 ± 8
10	4	1.0	34.5		62 ± 14	95 ± 9
11	2	1.0	32.4		62 ± 13	101 ± 10
12	1	1.0	33.8	27.8	61 ± 16	101 ± 14
13	2	2.0	28.8		55 ± 12	112 ± 11
14	2	0.0	32.1		65 ± 13	117 ± 10
15	4	2.0	27.4		54 ± 11	79 ± 5
16	2	2.0	30.6		61 ± 14	63 ± 8
17	1	1.0	48.6	34.0	92 ± 22	68 ± 11
18	1	2.0	36.0	35.7	78 ± 18	79 ± 11
19	2	2.0	33.0		72 ± 14	82 ± 7
20	1	2.0	41.9	42.6	78 ± 20	128 ± 25
21	5	3.0	51.6	38.3	83 ± 19	106 ± 10
22	3	3.0	54.2	37.9	77 ± 27	91 ± 17
23	1	3.0	53.2	46.5	103 ± 23	89 ± 18
24	4	2.0	36.6		74 ± 15	67 ± 6

Figure 4.1: Heat flows at the twenty-four well locations of this study. The contour lines are the +20, -20, and 0 mW/m^2 contours which define the $\Delta Q=0$ region (see Figure 1.1).

Heat Flow (mW/m^2)



Edmonton are 68 ± 18 mW/m² and 61 ± 15 mW/m². These heat flow values are in good agreement with the measured results of Garland and Lennox (1962). They found the heat flow in the Leduc area 32 Km southwest of Edmonton to be 67 mW/m², and the heat flow in the Redwater area 56 Km Northeast of Edmonton to be 61 mW/m².

Heat Generation in Sediments

Heat is generated in sedimentary rocks due to the decay of radioactive isotopes. The most important radioactive isotopes for heat generation are ²³⁸U, ²³⁵U, ²³²Th, and ⁴⁰K. In general, heat generation in sedimentary rocks is less than the heat generation in igneous and metamorphic rocks (Rybach, 1981).

The effect of heat generation in the sediments is to change heat flow with depth. If only the heat generation term in the general one dimensional heat flow equation (1.4) is considered, we have:

$$\frac{\partial q}{\partial z} = -A(z) \quad (4.4)$$

If A is taken to be constant with depth, heat flow increases linearly toward the surface:

$$q(z) = q_0 - Az \quad (4.5)$$

where q_0 is the heat flow at the base of the sediments. If there are several rock types present, each with its own heat generation value A_i , the change in heat flow at the surface

will be:

$$\Delta q = \sum_i \sum_j A_j \Delta z_i \quad (4.6)$$

where the sum is taken over the depth intervals Δz_i . Formula (4.6) was applied to the sedimentary sequence of each well in this study to estimate the increase in heat flow from the base of the sediments to the surface due to heat generation in the sediments.

The heat generation values used in the calculations were from Table 1.4 of Rybach (1981). This table is reproduced below.

Table 4.3: Heat Production of Sedimentary Rocks

Rock Type	A ($\mu\text{W}/\text{m}^3$)	ρ † (Kg/m^3)	Δq (mW/m^2)
Carbonates		2600	
Limestone	0.62		0.6
Dolomite	0.36		0.4
Sandstones		2400	
Quartzite	0.33		0.3
Arkose	0.85		0.8
Graywacke	1.0		1.0
Shales	1.8	2400	1.8

† Broad average since ρ depends strongly on porosity.

In the last column of the table, the Δq values are the contributions to the surface heat flow per kilometer of rock. The heat generations in limestone, dolomite, shale, and sandstone were taken into account in the calculations. In the case of sandstone, the average heat generation value of quartzite, arkose, and graywacke ($0.7 \mu\text{W}/\text{m}^3$) was used.

Note that shale has the largest heat generation value (1.8 $\mu\text{W}/\text{m}^3$), which is more than twice as large as the other rock types listed in the table. The results of the heat generation calculations are given in Table 4.4.

From Table 4.4, the ΔQ values for a given well range from 1.4 to 3.7 mW/m^2 , with a mean of 2.5 mW/m^2 . This is small compared to the uncertainties in the heat flow values given in Table 4.2, where the mean uncertainty is 18 mW/m^2 . It should be emphasized that the results in Table 4.4 are only rough estimates. This is because there are large variations in the uranium and thorium concentrations for a given sedimentary rock type (see Table 6.7.3 of Kappelmeier and Haenel, 1974).

Heat Generation at the Surface of the Precambrian Basement

The heat generations at the surface of the Precambrian basement were calculated for 182 samples in Western Canada following the work of Burwash and Cumming (1976), who determined the uranium and thorium concentrations of the samples. The results of the heat generation calculations are listed in the table in Appendix V. The following formula was used for the calculations (Rybach, 1976):

$$A(\mu\text{W}/\text{m}^3) = \rho \cdot 10^{-5} (9.52c_U + 2.56c_T + 3.48c_K) \quad (4.7)$$

where c_U and c_T are the concentrations of natural uranium and thorium in the core sample in weight ppm, c_K is the percentage weight of natural potassium, and ρ is the density

Table 4.4: Contribution of Heat Generation in Sediments to Surface Heat Flow

Well Index	ΔQ (mW m ⁻²)
1	2.46
2	1.41
3	1.90
4	2.59
5	3.16
6	3.04
7	1.70
8	1.49
9	2.10
10	3.27
11	3.38
12	3.39
13	4.00
14	3.74
15	2.81
16	2.15
17	1.59
18	1.99
19	2.29
20	3.50
21	2.67
22	2.47
23	1.92
24	1.84

of the rock in Kg/m^3 . The potassium concentrations were from Burwash (1984). In formula 4.7, ρ is assumed to be 2700 Kg/m^3 .

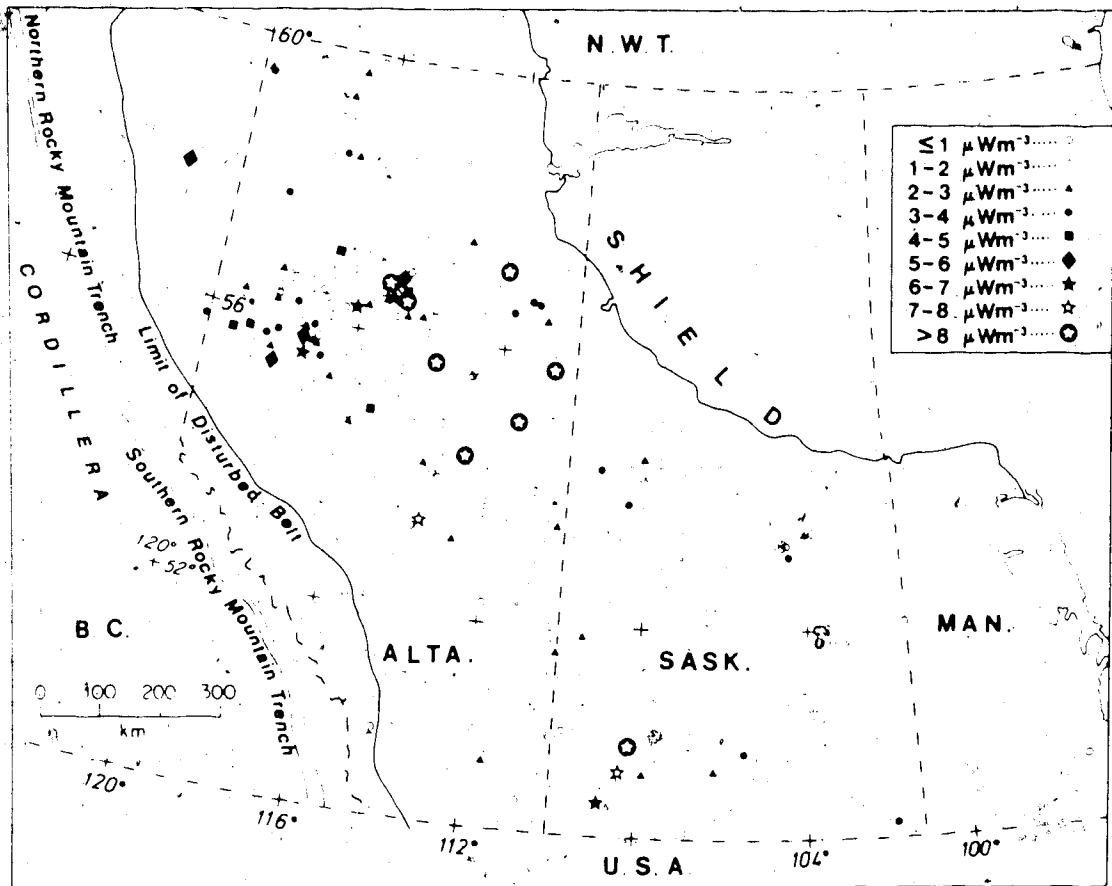
Heat Flow vs. Heat Generation

If heat generation in the Precambrian basement contributes significantly to heat flow through the sediments, then there should be a relationship between these two quantities. In this section it will be assumed that heat flow from the mantle is uniform in the $\Delta Q=0$ region, and that a function exists describing the variation of heat generation with depth from the surface of the Precambrian basement to the base of the crust of the earth. The aim of this section is to examine a possible relationship between heat flow through the sediments in the $\Delta Q=0$ region of Alberta and heat generation at the surface of the Precambrian basement.

Majorowicz and Jessop (1981) calculated the heat generation at the surface of the Precambrian basement and their result is the map shown in Figure 4.2. From the map, it is evident that the amount of heat generation can vary abruptly over short lateral distances. Nevertheless, Burwash and Cumming (1976) found that a regional variation in the concentration of Uranium and Thorium exists at the surface of the Precambrian basement.

The following method was used to arrive at heat generation values at the locations of the net rock analysis

Figure 4.2: Heat generation at the surface of the Precambrian basement as calculated by Majorowicz and Jessop (1981).

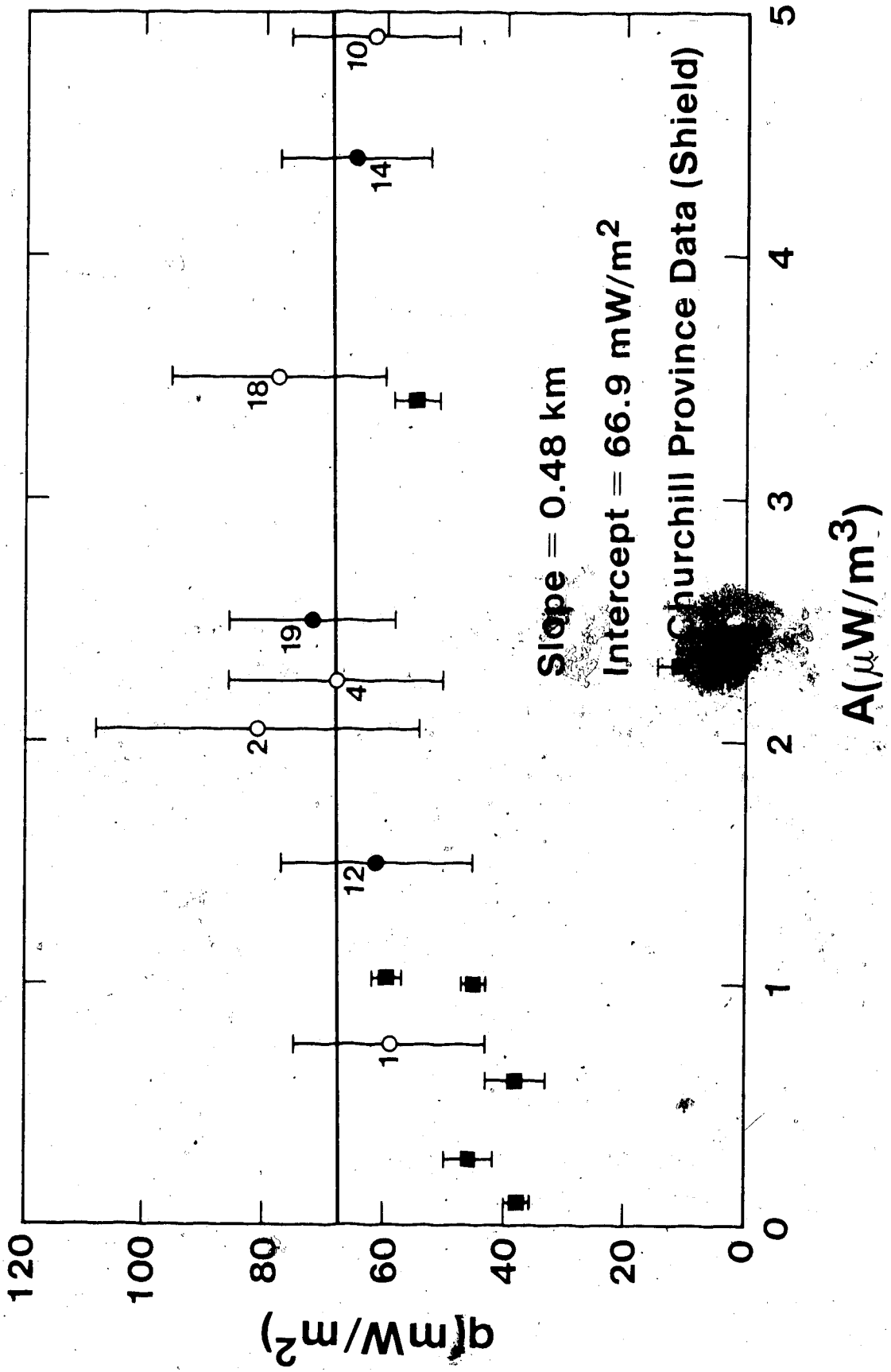


wells. The data file in Appendix V was searched for all the heat generation results in the 3 X 3 township-range neighborhoods of the twenty-four wells considered in this study. It was found that at most one heat generation result exists in the file for each township-range area. Heat flow was then plotted versus heat generation and the result is the graph shown in Figure 4.3. The uncertainty in heat generation is negligible compared to the uncertainties in heat flow. The open circles represent cases where the heat generation value is from the same well as the net rock analysis. The least-squares straight line was calculated from the circles only, and not the square data points.

The square data points in Figure 4.3 are Churchill province data from Drury (1985), who claimed there is a linear relationship between heat flow and heat generation for the Churchill province. The heat generation data point greater than $3 \mu\text{W}/\text{m}^3$ was rejected on the basis that it occurs, apparently, in an area of anomalously high radioactivity.

There are two interpretations of the data shown in Figure 4.3. One interpretation is the straight line graph shown in the figure. It does not show a notable increase in heat flow with an increase in heat generation. Physically, this means that heat flow is independent of heat generation and consequently heat generation in the Precambrian basement does not contribute significantly to heat flow through the sediments.

Figure 4.3: Heat flow vs. heat generation in the $\Delta Q=0$ region of Alberta. The circles are the heat flow results from this study. The numbers beside the data points are the well index numbers as given in Figure 1.2. The open circles represent the cases where the heat generation measurement is from the same well as the net rock analysis. The squares are values from the Churchill Province from Drury (1985).



Another interpretation exists which leads to a very different result. If the data in Figure 4.3 corresponding to heat generation values greater than $3\mu\text{W}/\text{m}^3$ are regarded as anomalously high and not representative of the 3×3 township-range area around the net rock analysis well location, then the remaining five data points combined with the Drury data less than $3\mu\text{W}/\text{m}^3$ does suggest an increase in heat flow with an increase in heat generation. The slope of a least-squares straight line through these data is 15.3 Km, and the intercept is $37.8 \text{ mW}/\text{m}^2$. Physically, this second straight line means that heat generation in the Precambrian basement contributes significantly to heat flow through the sediments.

To estimate this contribution, consider the exponential model (Lachenbruch and Sass, 1977):

$$A(z) = A_0 \exp(-z/z_0) \quad (4.8)$$

Substituting this relation into equation (4.4) yields a linear relationship between heat flow at the surface and heat flow at depth z :

$$q(z) = C + z_0 A(z) \quad (4.9)$$

where

$$C = q(0) - A_0 z_0 \quad (4.10)$$

If different heat generation values are thought to be the result of erosion then equation (4.9) may be interpreted as

a lateral relationship between heat flow and heat generation:

$$q(x,y) = Q + z_0 A(x,y) \quad (4.11)$$

Taking A_0 to be $2.5 \mu\text{W}/\text{m}^3$ and z_0 to be 15.3 Km and integrating the function (4.8) over a 35 Km basement thickness gives the contribution of heat generation in the basement to surface heat flow to be $34 \text{ mW}/\text{m}^2$, almost half the average heat flow through the sediments in the $\Delta Q=0$ region.

These two interpretations of the data in Figure 4.3 lead to quite different conclusions. The author believes that to make a reasonable estimate of the contribution of heat generation in the Precambrian basement to heat flow through the sediments, heat generation values must be used which are more certainly representative of the region surrounding the well.

Groundwater Motion

As explained in the introduction, the twenty-four wells chosen for this study are located in the $\Delta Q=0$ region. Here the regional groundwater motion is generally lateral, and it may be assumed that there is negligible vertical water motion. In other words, it is reasonable to assume that any vertical components of water motion are negligible. Of course, this is only an assumption, and it is interesting to calculate the vertical component of water motion required to

account for, say, a ΔQ value of 20 mW/m². This would be on the boundary of the $\Delta Q=0$ region.

If only the water motion term in the general one-dimensional heat flow equation (1.4) is considered, we have the following differential equation:

$$\frac{\partial q}{\partial z} = \frac{-q}{s}$$

where

$$s = \frac{k}{Cv}$$

Here k is the thermal conductivity of the porous rock, C is the heat capacity of water per unit volume, and v is the upward volume flux of vertical water motion. Integration of equation (4.8) gives the following expression for the ratio of the heat flow at depth z to the heat flow at the surface:

$$\frac{q(z)}{q(0)} = e^{-z/s}$$

which is given in Lachenbruch and Sass (1977). Taking the thermal conductivity to be 2.0 W/m²K, and the heat capacity of water to be 4.2 x 10⁶ J/°Km³, the vertical component of water motion required to account for a change in heat flow from 60 mW/m² at the surface to 80 mW/m² at a depth of three kilometers is only 1 mm per year, which is very low. Of course, this calculation is oversimplified, and in general, the groundwater motion profile is quite complicated (see Hitchon, 1984).

Figure 1.3 of Chapter 1 illustrates the effects of local topography on groundwater motion at the top of the sediments. In general, local topographic highs are local recharge areas, and local topographic lows are local discharge areas. On a larger scale, the regional groundwater movement is influenced by regional topography. Figure 1.3 shows a regional flow from the foothills area of high elevation to the region of lower elevation in northeastern Alberta.

Conclusions

The numerical results in table 4.2 constitute the chief result of this thesis. In summary, the average of the heat flows calculated for the twenty-four wells in the $\Delta Q=0$ region of Alberta is 71 mW/m^2 , with a standard deviation of 12 mW/m^2 . The contribution of heat generation in the sediments to surface heat flow was found to be about 2.5 mW/m^2 .

No definite relationship was found between heat flow and heat generation at the surface of the Precambrian basement. Heat generation values which are more representative of the region surrounding the well were required for a reasonable estimate of the contribution of heat generation in the basement to heat flow through the sediments. One approach to this problem would be to use the existing data-set and calculate a radius-weighted average heat generation for the closest data points to each well,

omitting the individual result from the graph if the heat generation values were not within some specified radius of the well.

References

- Alm, O. and G. Bäckström (1975). Thermal Conductivity of NaCl up to 40 kbar and 240-400 °K. High Temperatures-High Pressures, 7, 235-239.
- Andersland, O. and D. Anderson (1978). Geotechnical Engineering for Cold Regions. New York: McGraw-Hill, 114-120.
- Birch, F. and H. Clark (1940). The Thermal Conductivity of Rocks and its Dependence on Temperature and Composition. American Journal of Science. Part I: 238, no. 8, 529-558. Part II: 238, no. 9, 613-635.
- Blackwell, D. D., J. L. Steele, and D. W. Steeples (1981). Heat Flow Determinations in Kansas and Their Implications For Midcontinent Heat Flow Patterns. EOS Transactions, American Geophysical Union, 62, no. 17, April 28, Abstract T82.
- Burwash, R. A. (1984). Private communication to Robert Beach.
- Burwash, R. A. and G. L. Cumming (1976). Uranium and Thorium in the Precambrian Basement of Western Canada. I. Abundance and Distribution. Canadian Journal of Earth Sciences, 13, no. 2, 284-293.
- Cermak, V. and A. M. Jessop (1971). Heat Flow, Heat Generation and Crustal Temperature in the Kapuskasing Area of the Canadian Shield. Tectonophysics, 11, 287-303.
- Chapman, D. S., T. H. Keho, M. S. Bauer and M. D. Picard (1984). Heat Flow in the Uinta Basin Determined from Bottom Hole Temperature (BHT) Data. Geophysics, 49, no. 4, 453-466.
- Drury, M. J. (1985). Heat Flow and Heat Generation in the Churchill Province of the Canadian Shield, and Their Palaeotectonic Significance. Submitted to Tectonophysics.
- Fertl, W. H. and P. A. Wichmann (1977). How to Determine Static BHT From Well Log Data. World Oil, 184, 105-106.
- Garland, G. D. and D. H. Lennox (1962). Heat Flow in Western Canada. Geophysical Journal, 6, 245-262.
- Hitchon, B. (1984). Geothermal Gradients, Hydrodynamics, and Hydrocarbon Occurrences, Alberta, Canada. The

American Association of Petroleum Geologists
Bulletin, 68, no. 6, 713-743.

- Jessop, A. M. (1971). The Distribution of Glacial Perturbation of Heat Flow in Canada. Canadian Journal of Earth Sciences, 8, 162-166.
- Jones, F. W., C. Kushigbor, H. L. Lam, J. A. Majorowicz and M. Rahman (1985). Estimates of Terrestrial Thermal Gradients and Heat Flow Variations with Depth in the Hinton-Edson Area of the Alberta Basin Derived from Petroleum Bottom-Hole Temperature Data. Geophysical Prospecting, 32, no. 6, 1111-1130.
- Judge, A. S. (1973). Deep Temperature Observations in the Canadian North. In: Permafrost. The North American Contribution to the Second International Conference. National Academy of Sciences, Washington, D. C., 35-40.
- Kappelmeyer, O. (1979). Implications of Heat Flow Studies for Geothermal Energy Prospects. In: Heat Flow in Western Europe. Editors V. Cermak and L. Rybach, New York: Springer-Verlag, 126-135.
- Kappelmeyer, O. and R. Haenel (1974). Geothermics. Geoexploration Monographs Series 1, no. 4. Editors O. Rosenbach and C. Morel. Berlin: Gebrüder Borntraeger.
- Lachenbruch, A. H. and J. H. Sass (1977). Heat Flow in the United States and the Thermal Regime of the Crust. In: The Earth's Crust. Editor J. G. Heacock. American Geophysical Union Monograph 20, 626-675.
- Majorowicz, J. A., F. W. Jones, H. L. Lam and A. M. Jessop (1985a). Terrestrial Heat Flow and Geothermal Gradients in Relation to Hydrodynamics in the Alberta Basin, Canada. Journal of Geodynamics, in press.
- Majorowicz, J. A., F. W. Jones, H. L. Lam, and A. M. Jessop (1985b). Regional Variations of Heat Flow Differences with Depth in Alberta, Canada. Geophysical Journal Royal Astronomical Society, 81, in press.
- Majorowicz, J. A., and A. M. Jessop (1981). Regional Heat Flow Patterns in the Western Canadian Sedimentary Basin. Tectonophysics, 74, 209-238.
- McKay, G. A. (1950). Climatic Maps of the Prairie Provinces for Agriculture. Climatological Studies number 1. Available from Department of Transport,

Meteorological Branch, Government of Canada.

Moss, M. and G. M. Haseman (1981). Thermal Conductivity of Polyhalite and Anhydrite from the Site of the Proposed Waste Isolation Pilot Plant. N.T.I.S. Report SAND-81-0856. Document no. DE81024046.

Rybach, L. (1981). Geothermal Systems, Conductive Heat Flow, Geothermal Anomalies. In: Geothermal Systems: Principles and Case Histories. Editors L. Rybach and L. J. P. Muffler. New York: John Wiley and Sons, Ltd., 3-36.

Rybach, L. (1976). Radioactive Heat Production: A Physical Property Determined by the Chemistry of Rocks. In: The Physics and Chemistry of Minerals and Rocks. Editor R. G. J. Strens. Toronto: John Wiley and Sons, 309-318.

Skvarla, M. J., J. W. Vandersande, M. L. Linvill, and R. O. Pohl (1981). Thermal Conductivity of Selected Repository Minerals. In: Scientific Basis for Nuclear Waste Management, 3, 43-50.

Tye, R. P., A. O. Desjarlais and J. M. Singer (1981). Thermophysical Properties of Pittsburgh Seam Coal. High Temperatures - High Pressures, 13, 57-68.

Appendix I

Location of the net rock analysis wells in the township-range-meridian system.

Well Index	Lsd.	Sec.	Twp.	Rge.	Mer.
1	1	6	38	15	4
2	14	29	52	2	4
3	11	19	50	6	4
4	16	17	48	20	4
5	15	21	48	27	4
6	10	18	61	6	5
7	8	26	60	16	4
8	16	28	56	8	4
9	12	14	67	2	5
10	8	11	68	10	5
11	10	9	68	17	5
12	1	27	67	22	5
13	10	16	69	5	6
14	7	6	76	9	6
15	6	32	75	25	5
16	4	12	74	10	5
17	4	16	74	24	4
18	16	13	83	24	5
19	11	17	83	9	6
20	10	27	90	11	6
21	6	8	99	7	6
22	15	14	105	8	6
23	10	15	106	1	6
24	6	27	99	22	5

Appendix II

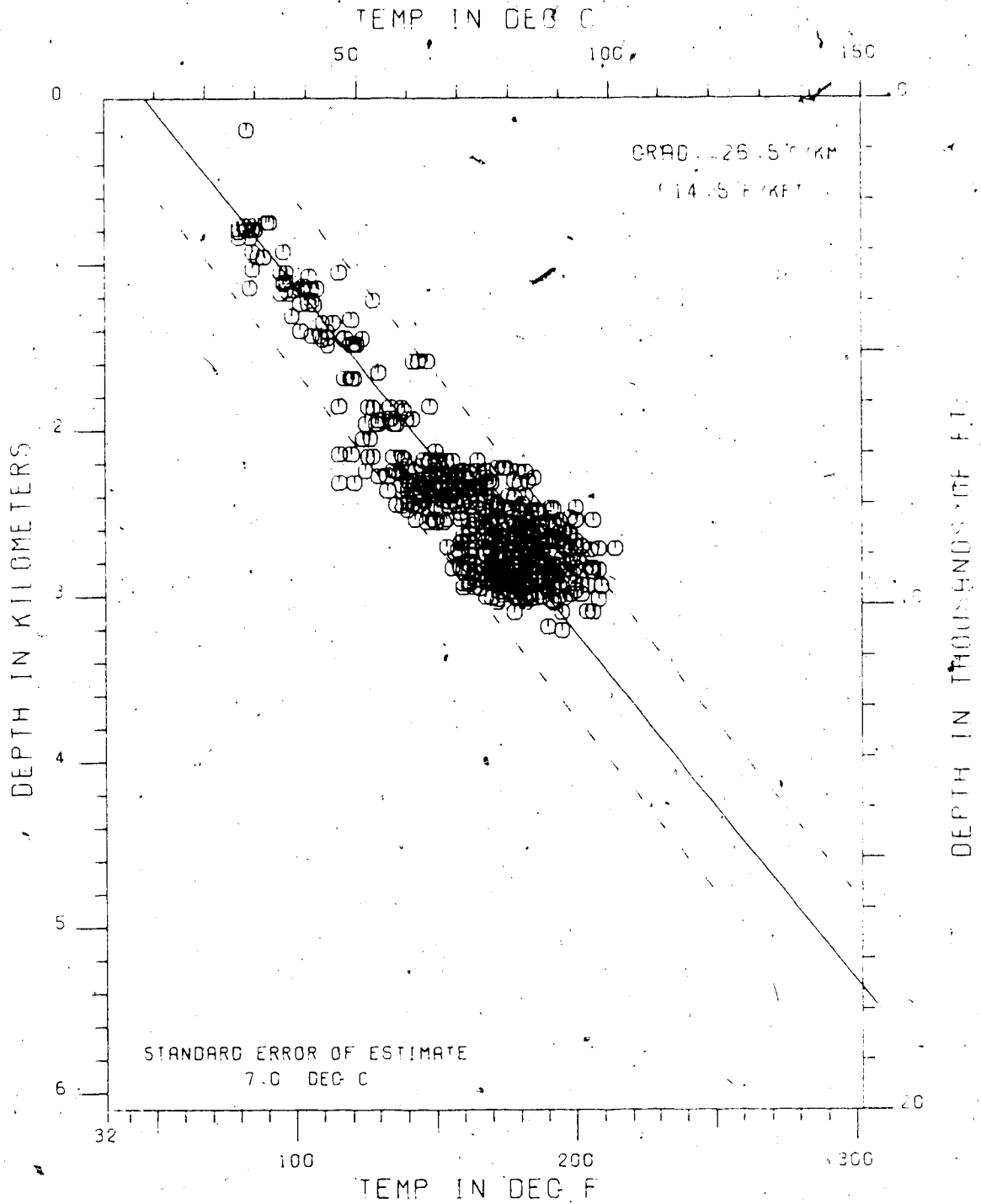
Regional Temperature Gradients

This appendix contains the corrected and uncorrected temperature gradient plots for regions I, II, and III in figure 1.3. Each of the gradients are calculated without a fixed mean surface temperature. The locations of these regions in the township-range-meridian system are as follows:

Region I:	TSP: 64-72	RGE: 10-16	MER: 5
Region II:	TSP: 71-79	RGE: 18-26	MER: 5
Region III:	TSP: 92-99	RGE: 1-7	MER: 6

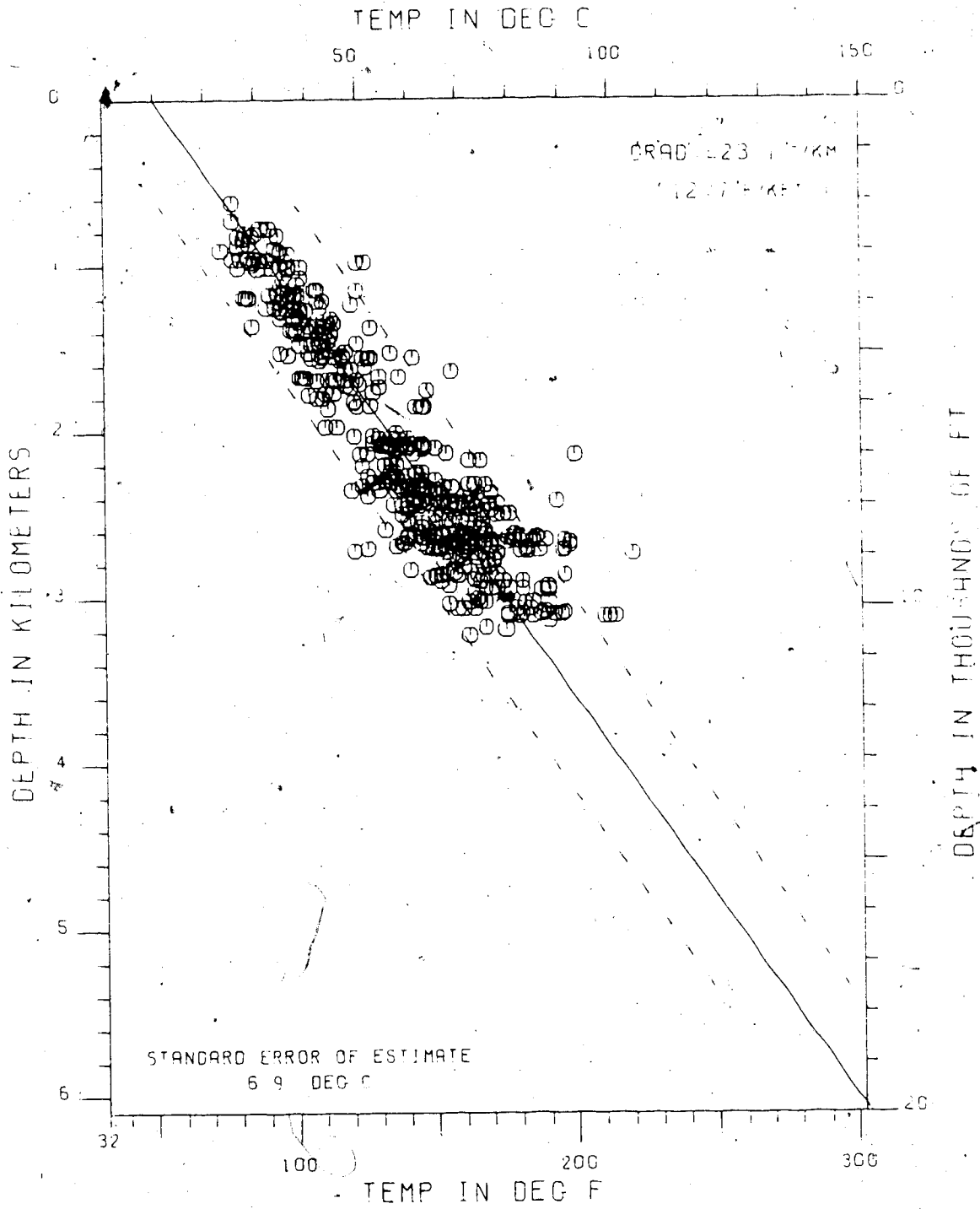
REGION I

UNCORRECTED GRADIENT



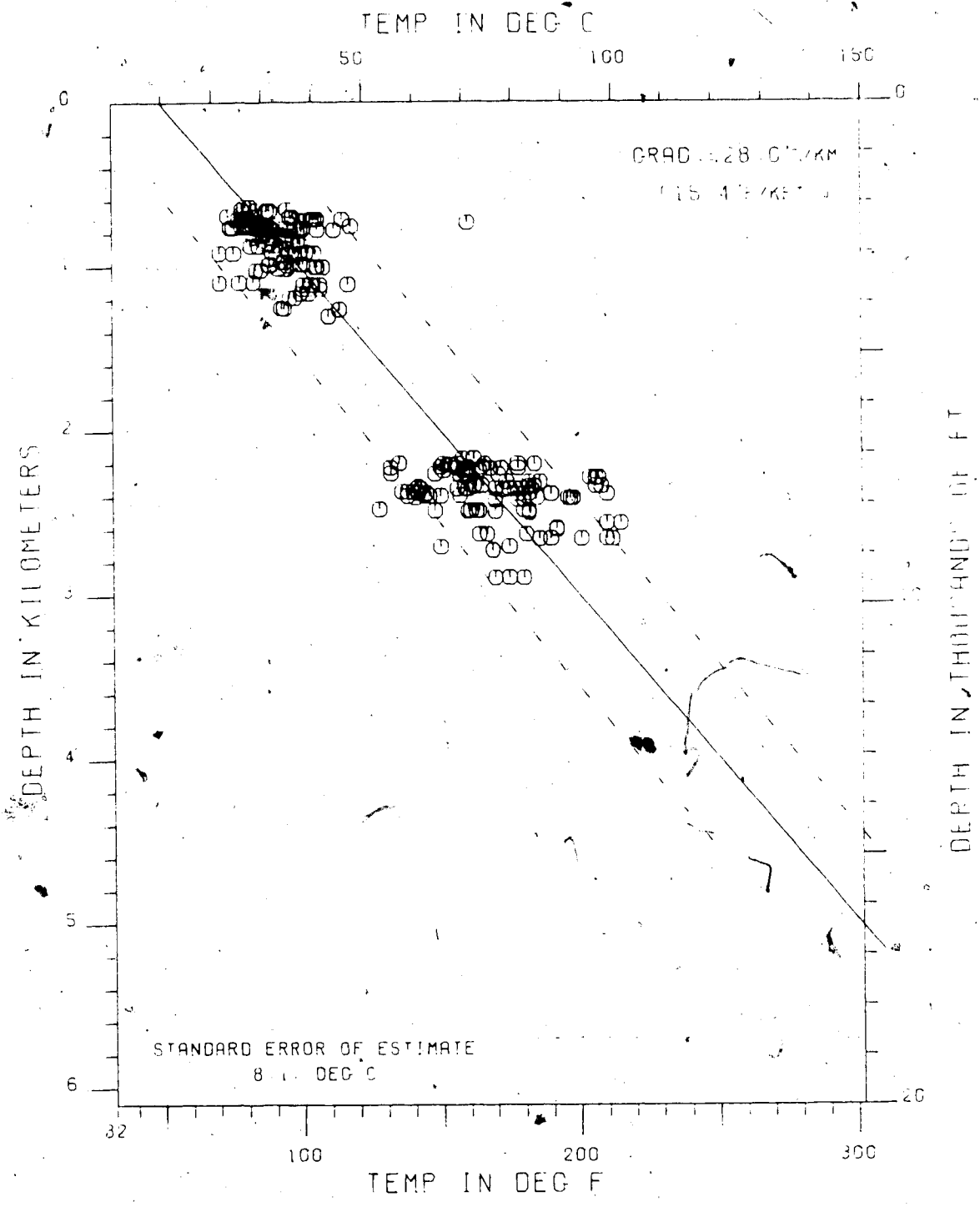
REGION II

UNCORRECTED GRADIENT

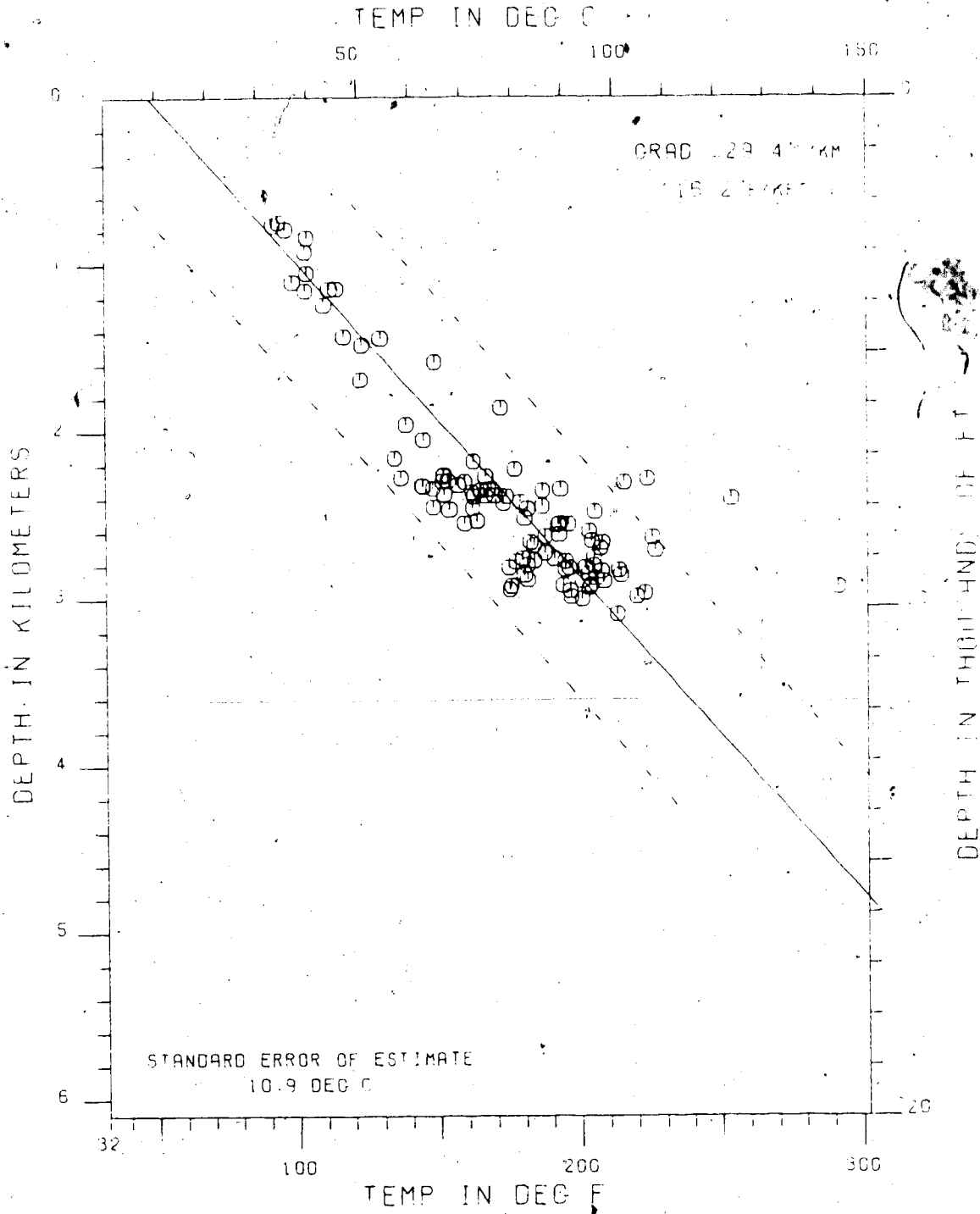


REGION III

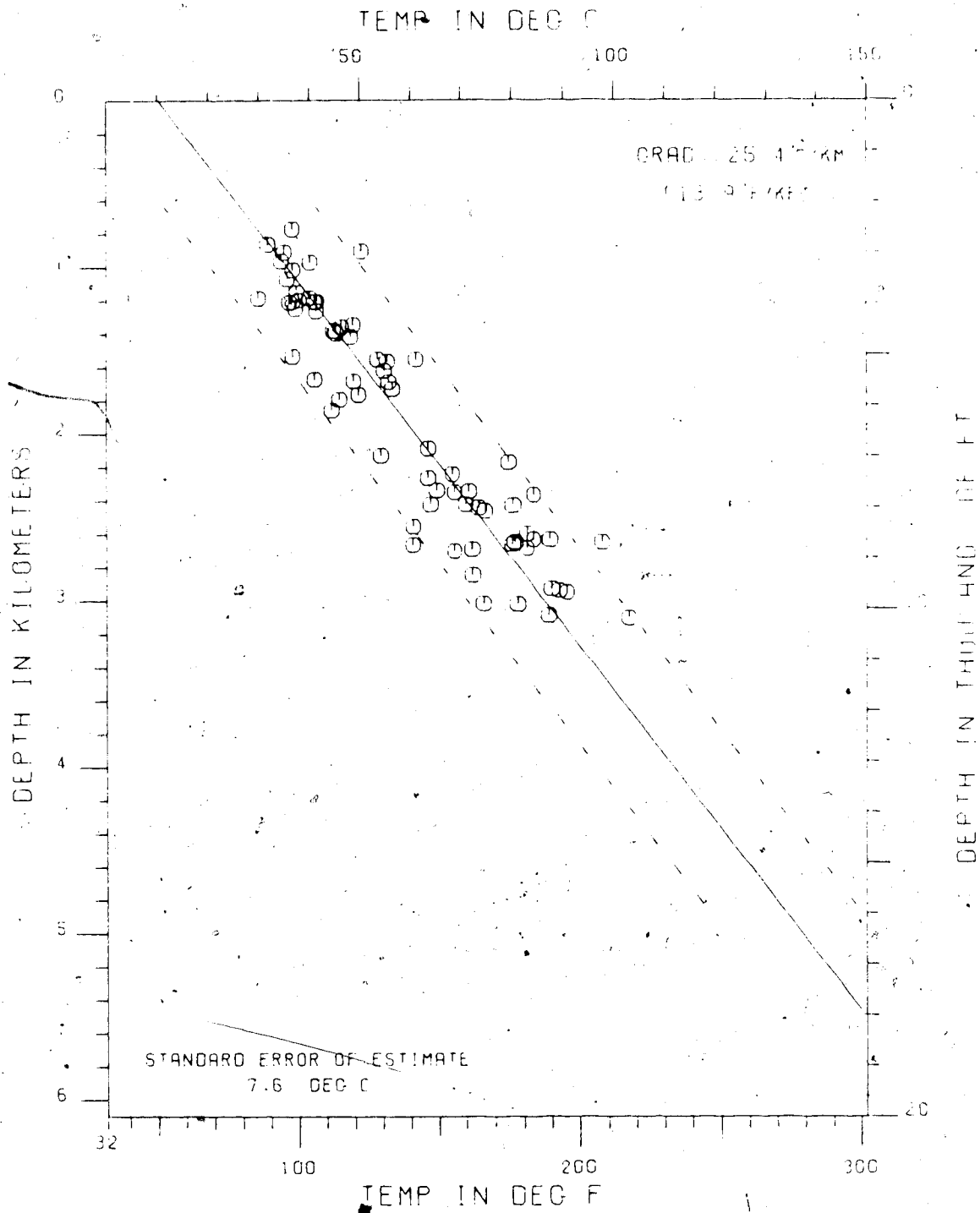
UNCORRECTED GRADIENT



REGION I CORRECTED GRADIENT

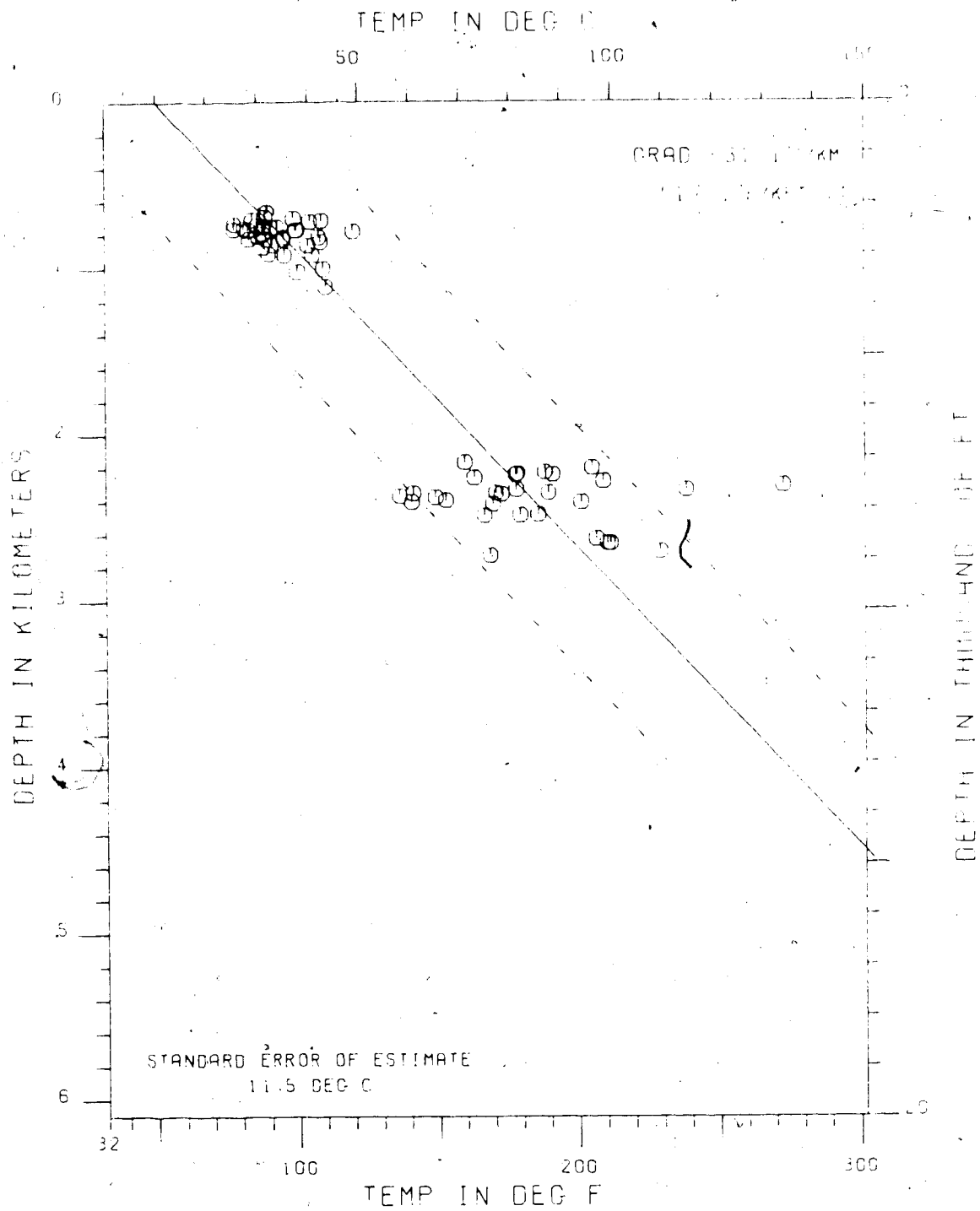


REGION II
CORRECTED GRADIENT



REGION III

CORRECTED GRADIENT



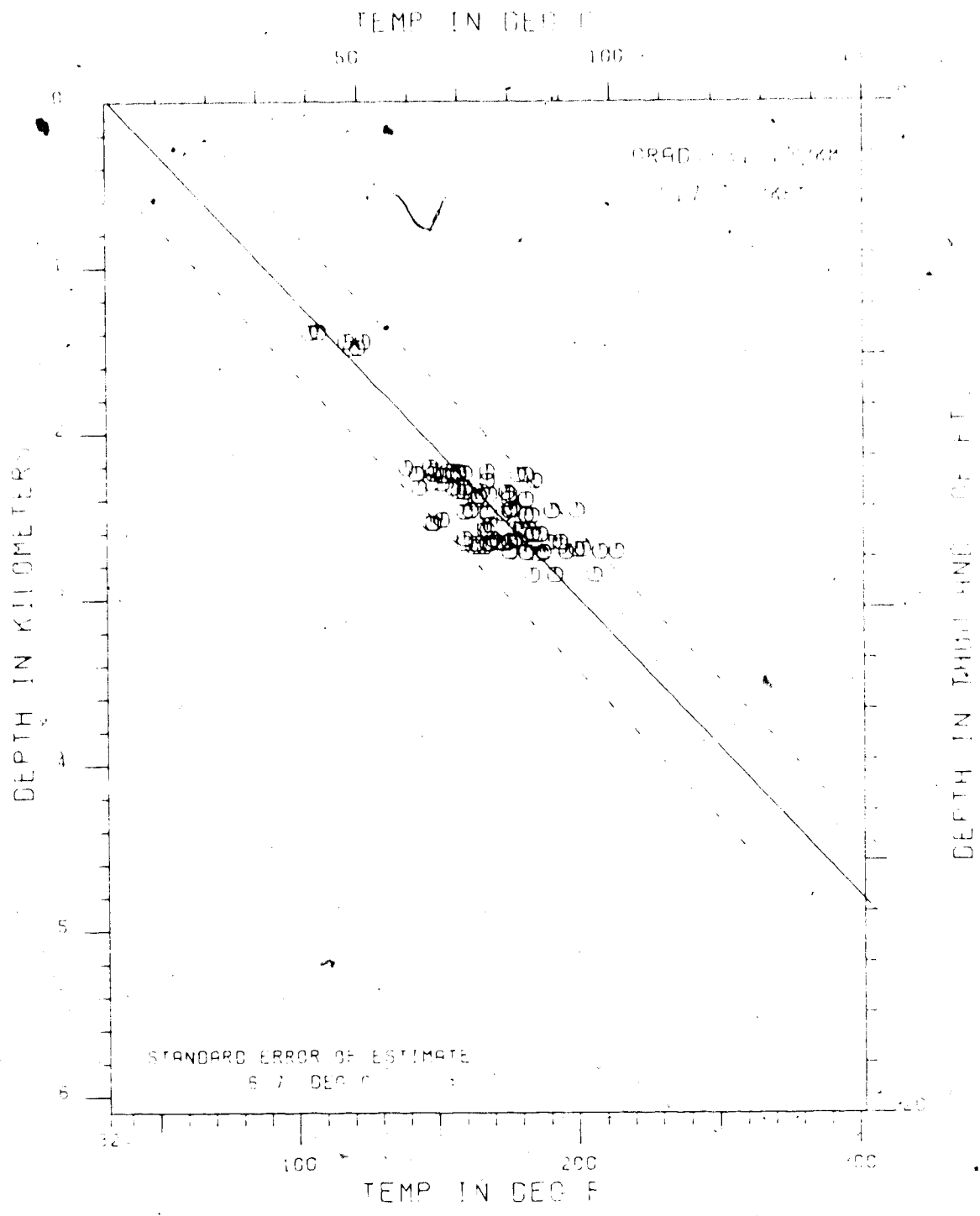
Appendix III

Local Uncorrected Gradients for Case 4 and Case 5 Wells

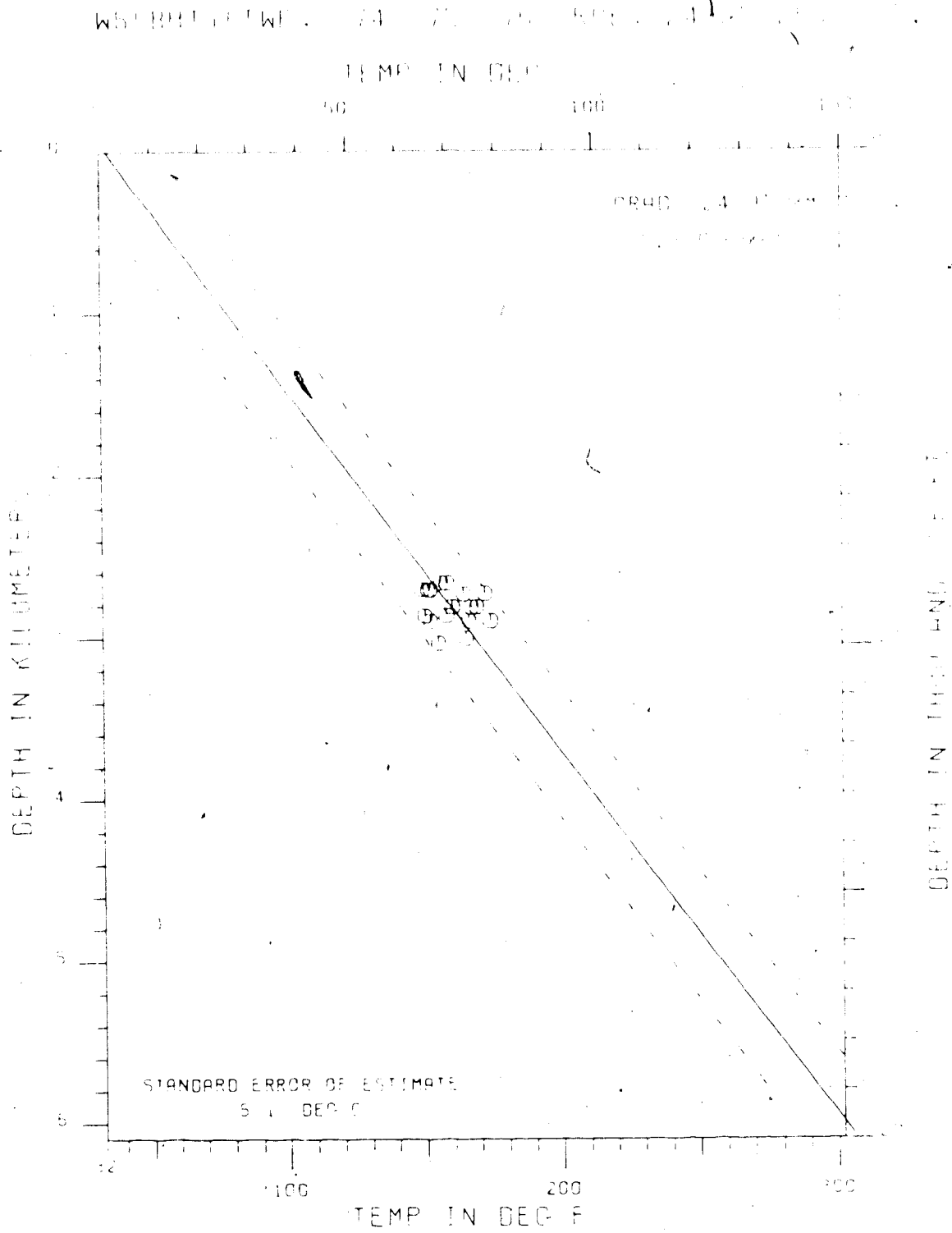
This appendix gives the local uncorrected temperature gradient plots for the case 4 and case 5 wells. The case 4 wells are well numbers 10, 15, and 24. Well number 21 is a case 5 well. The case 4 gradients are least squares gradients with fixed mean surface temperatures. The case 5 gradient is without a fixed mean surface temperature.

WELL INDEX: 10
UNCORRECTED LOCAL GRADIENT

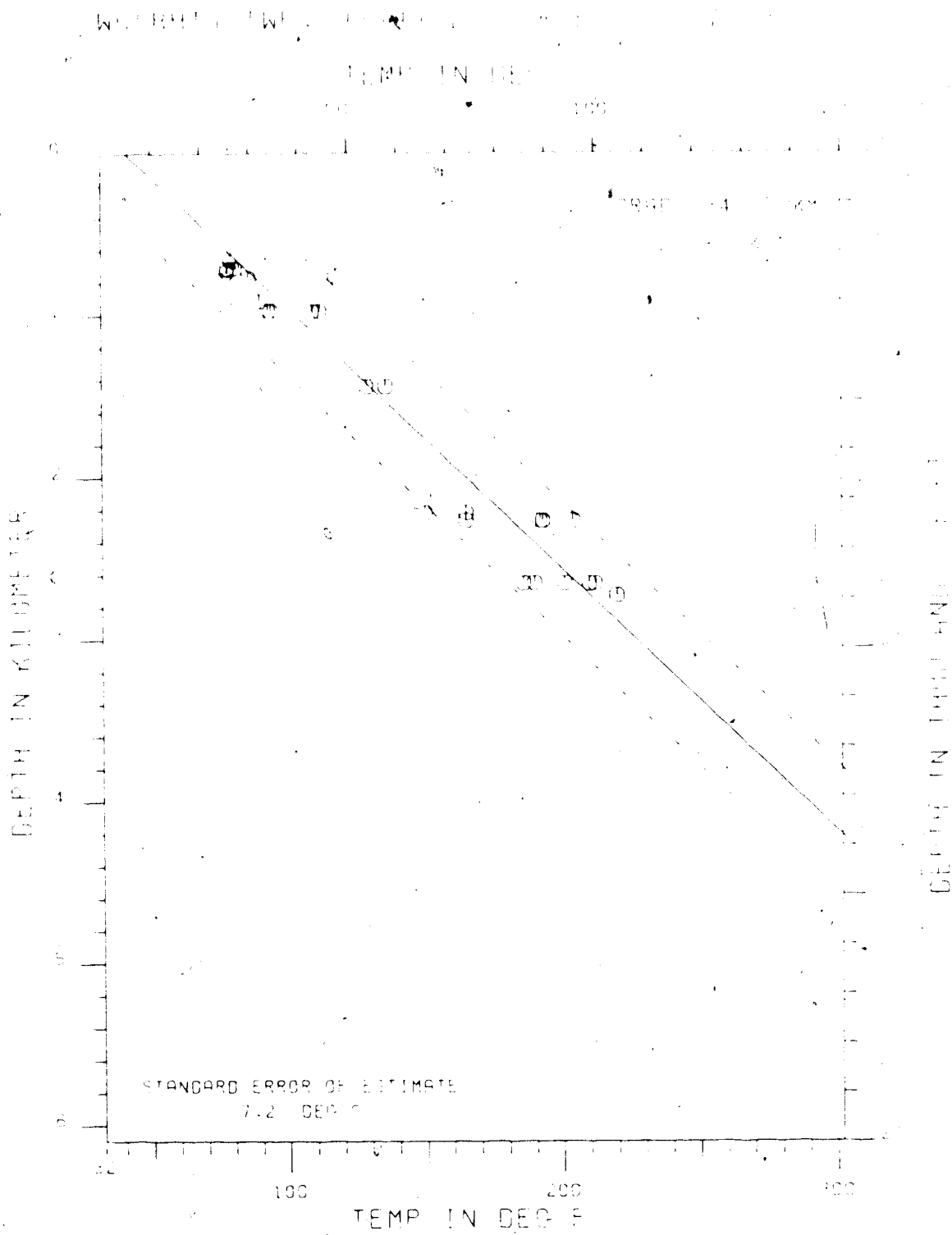
W51R4111WP, 07 98 11 RBL, 1 10 11



WELL INDEX: 15
 UNCORRECTED LOCAL GRADIENT



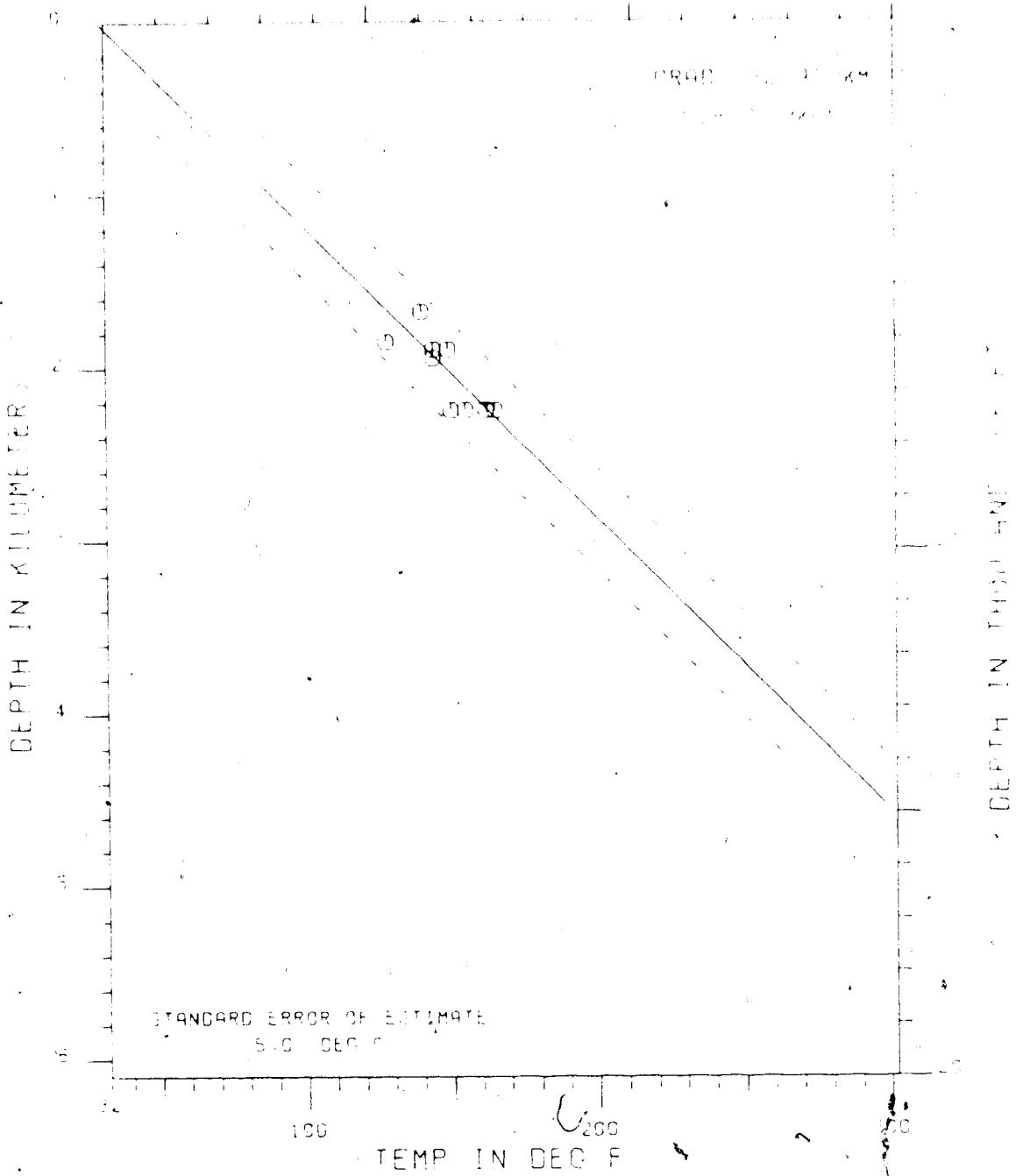
WELL INDEX: 21
UNCORRECTED LOCAL GRADIENT



WELL INDEX: 24
 UNCORRECTED LOCAL GRADIENT

WELL IDENTIFICATION: ...

TEMP IN DEG C

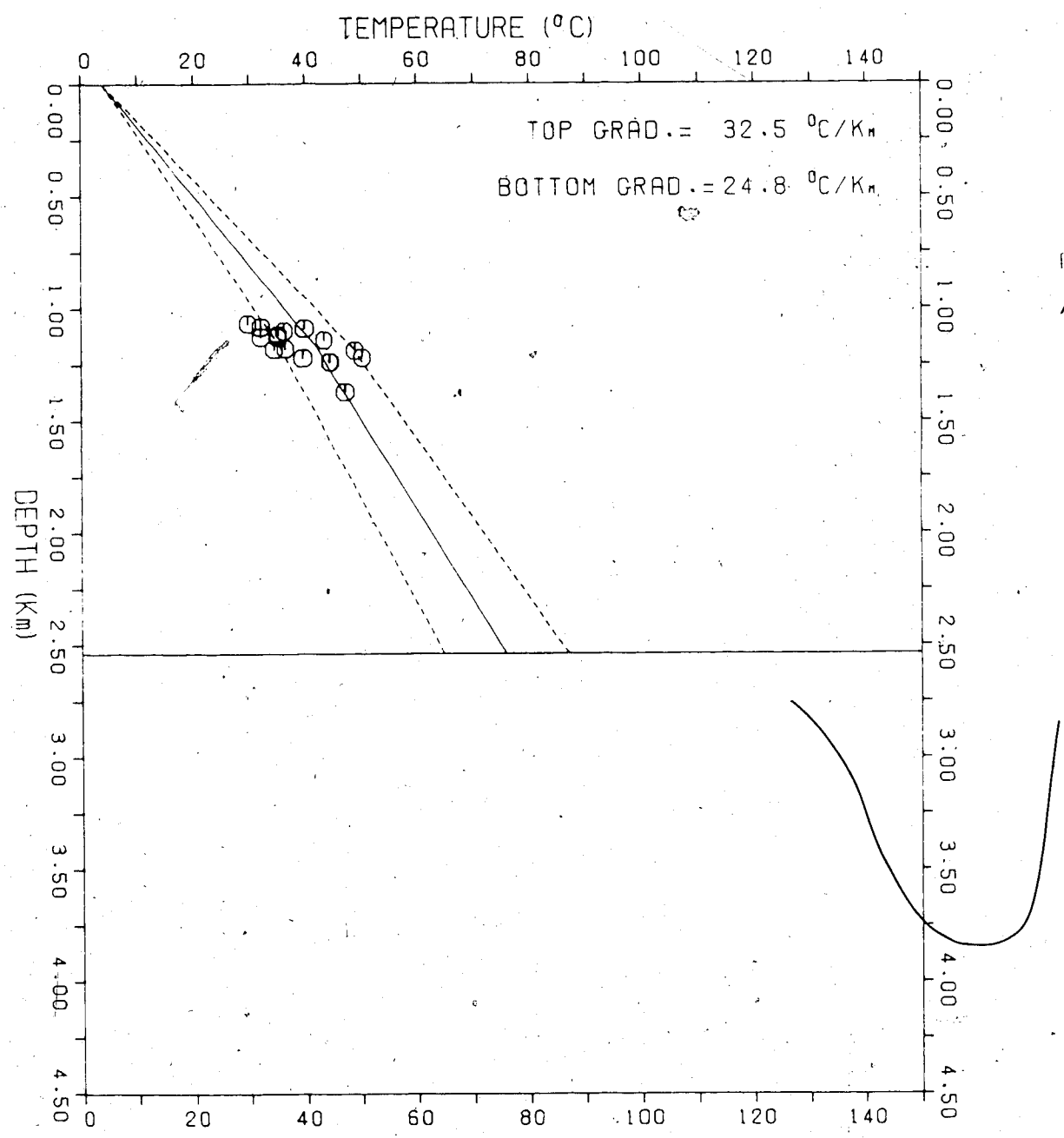


Appendix IV

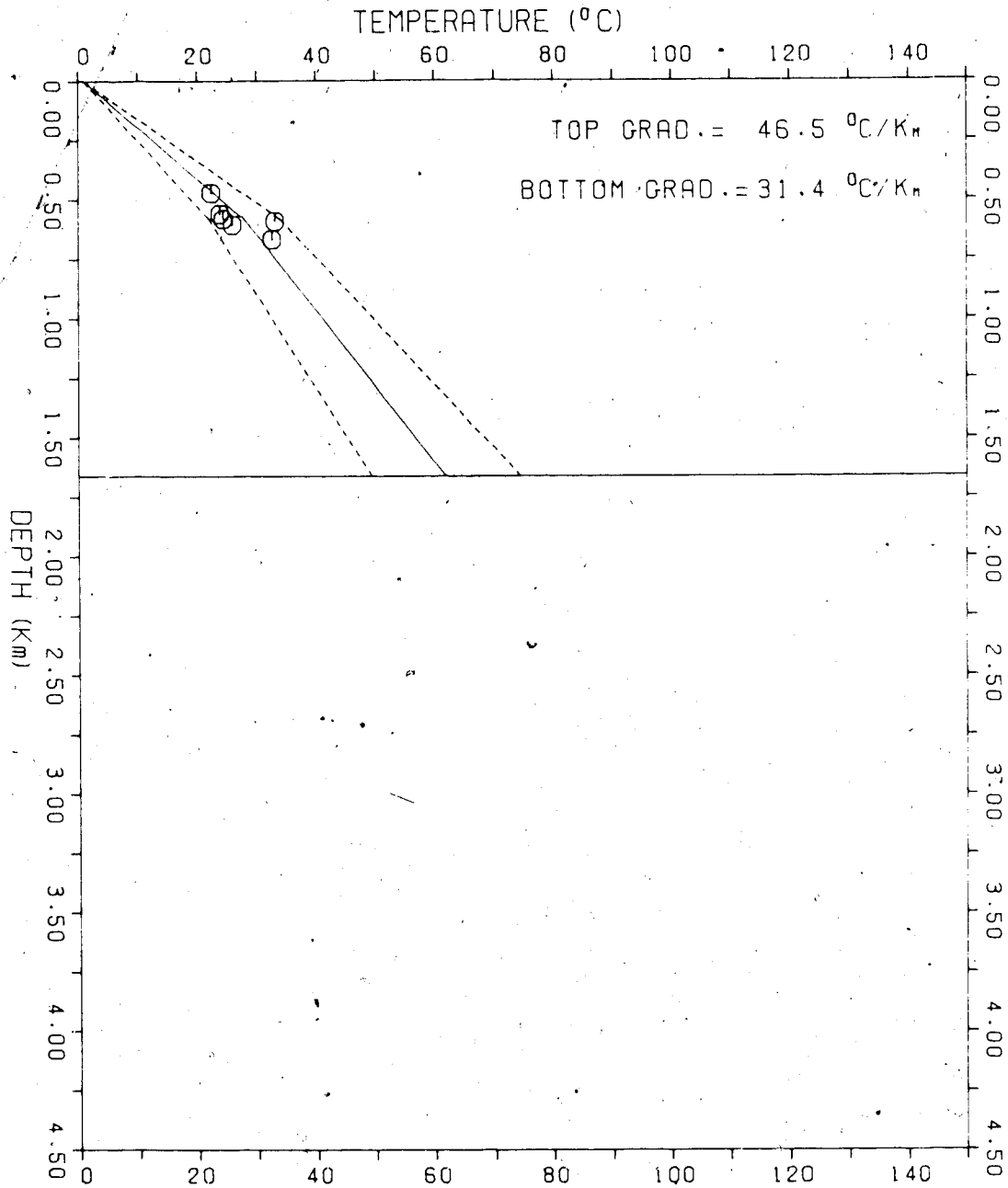
Final Temperature Gradient Plots for Net Rock Analysis Wells

This appendix gives the final temperature gradient plots for the twenty-four net rock analysis wells chosen for this study. The dashed lines represent the probable uncertainty in temperature as a function of depth. The temperature data are also plotted for the case 1, 2, and 3 wells. The temperature data were not plotted for the case 4 and case 5 wells because the final gradients given here are the results of regional percentage corrections being applied to the uncorrected local gradients. The horizontal line in the plots represents the base of the sediments.

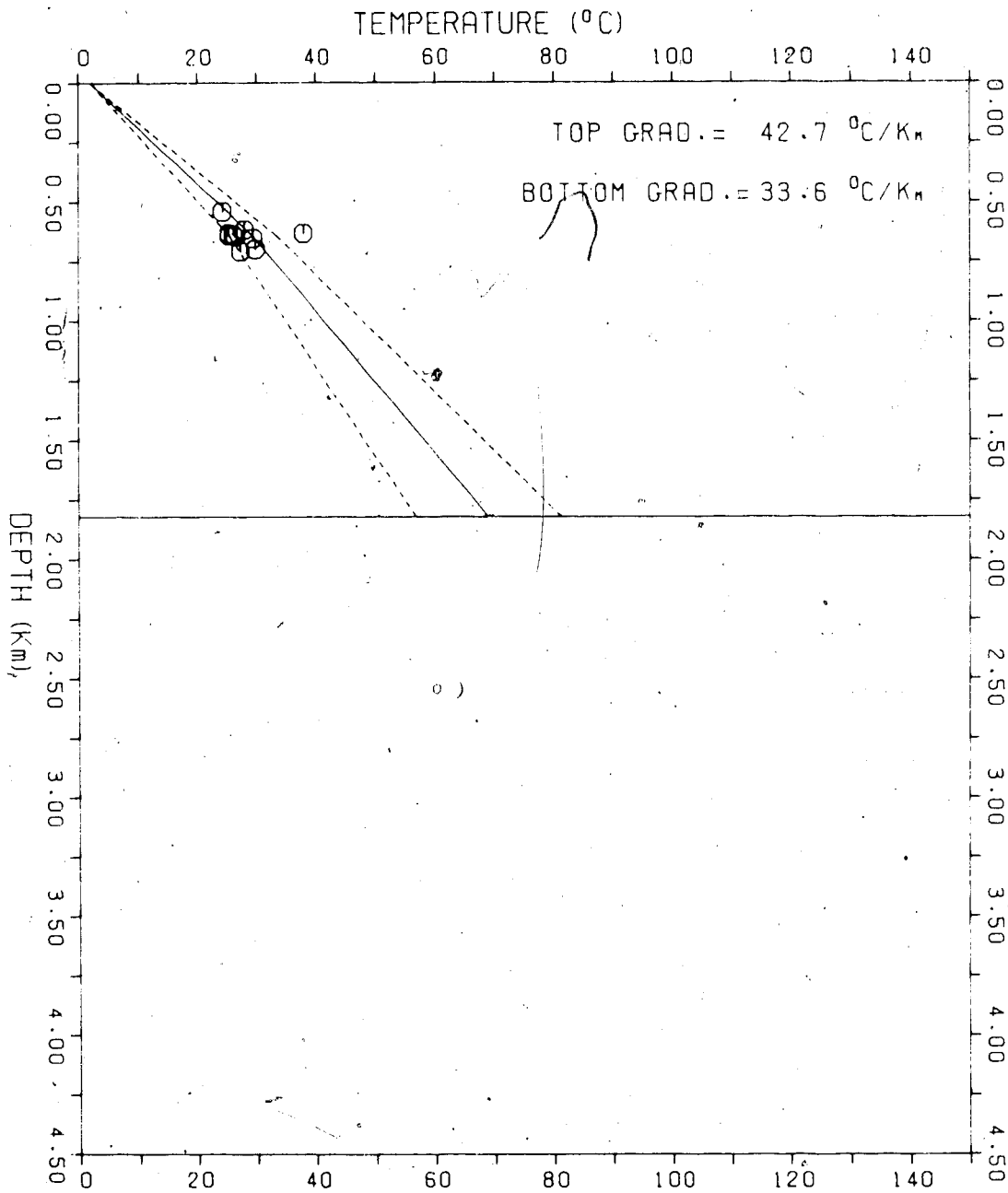
WELL INDEX: 1.
HEAT FLOW: 59. ± 16. MW PER SQ. METER
TEMPERATURE AT
BASE OF SEDIMENTS: 76. ± 11. °C



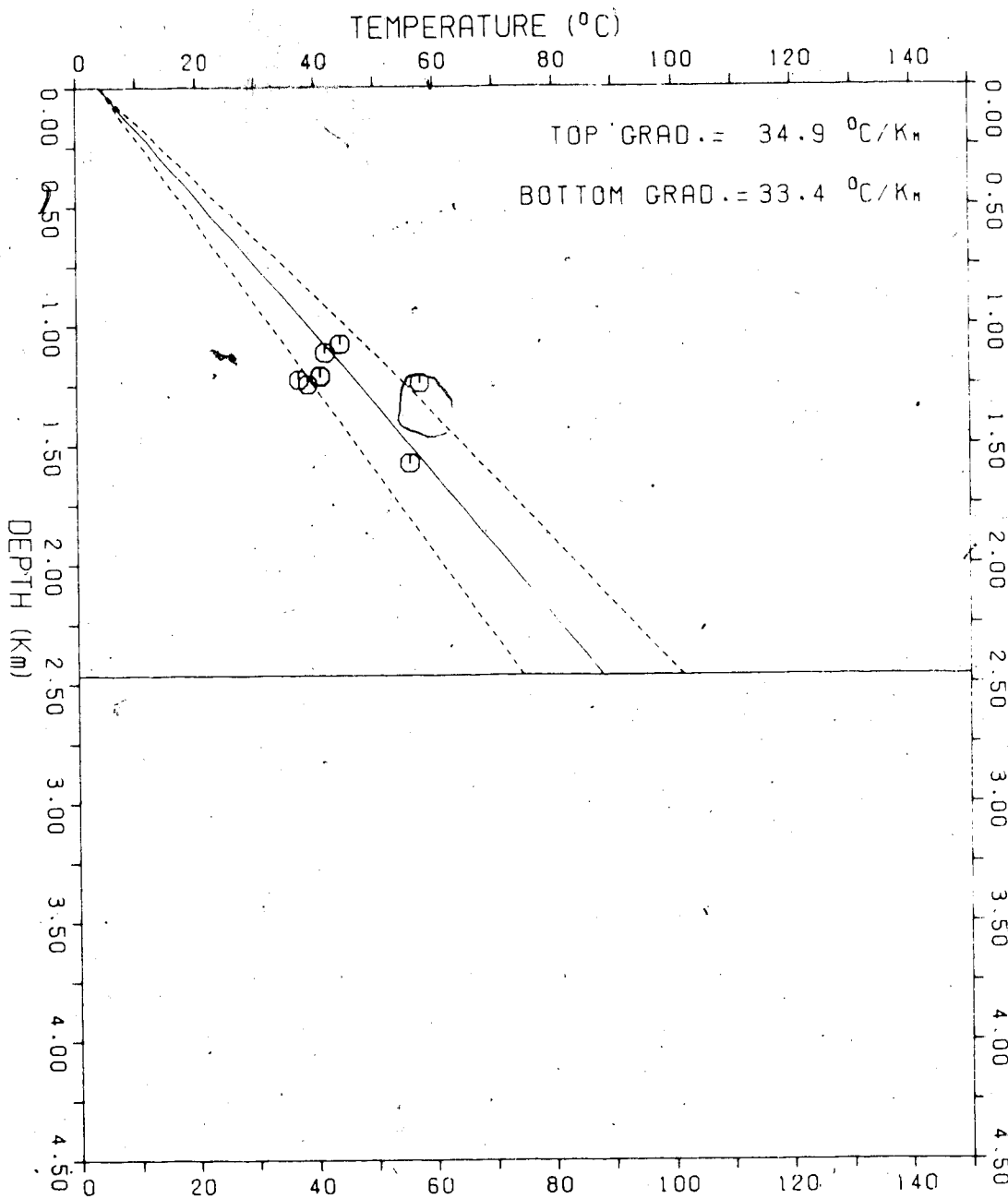
WELL INDEX: 2.
HEAT FLOW: 81. ± 27. mW PER SQ. METER
TEMPERATURE AT
BASE OF SEDIMENTS: 62. ± 13. °C



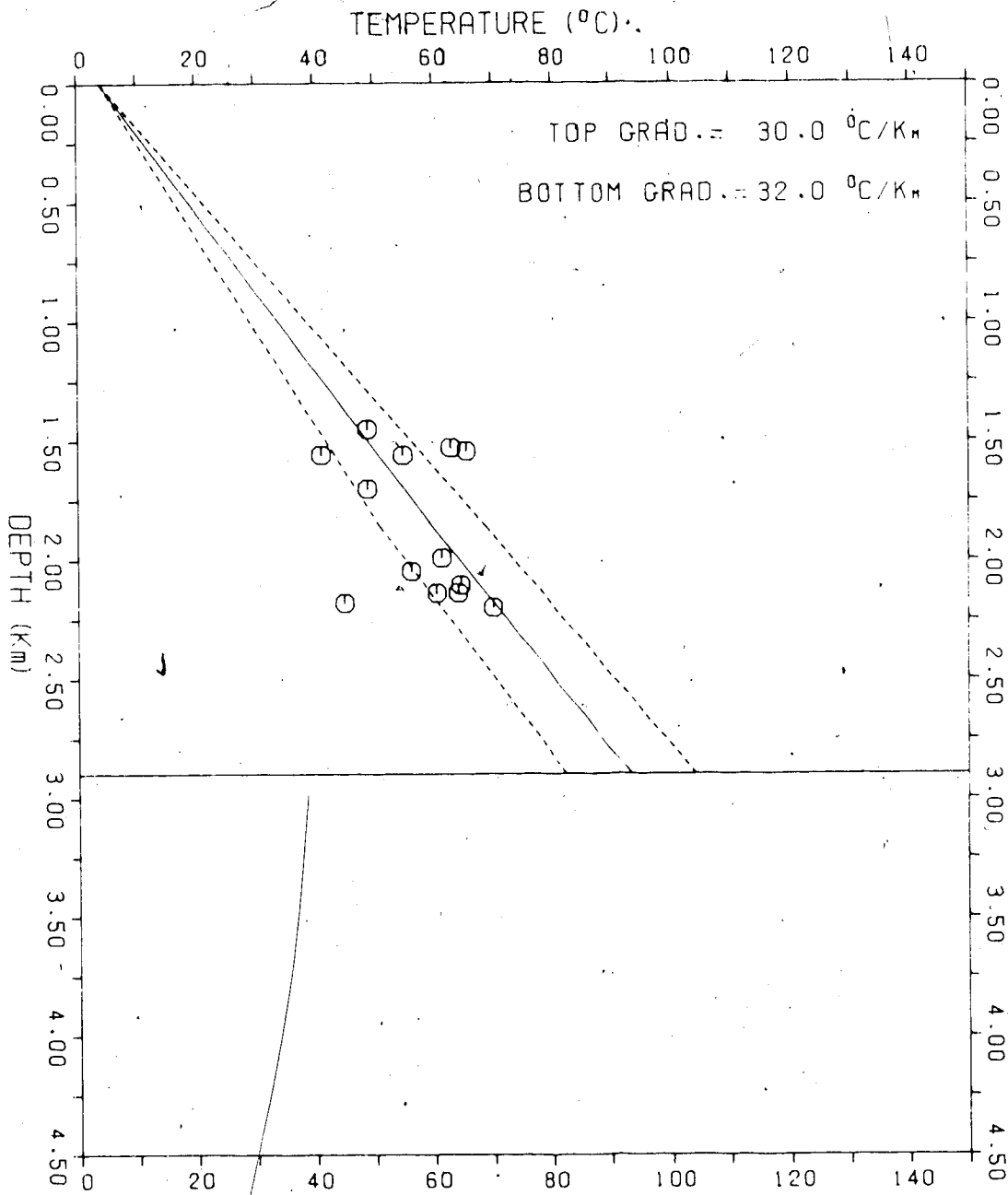
WELL INDEX: 3.
HEAT FLOW: 77. ± 19. MW PER SQ. METER
TEMPERATURE AT
BASE OF SEDIMENTS: 69. ± 12. °C



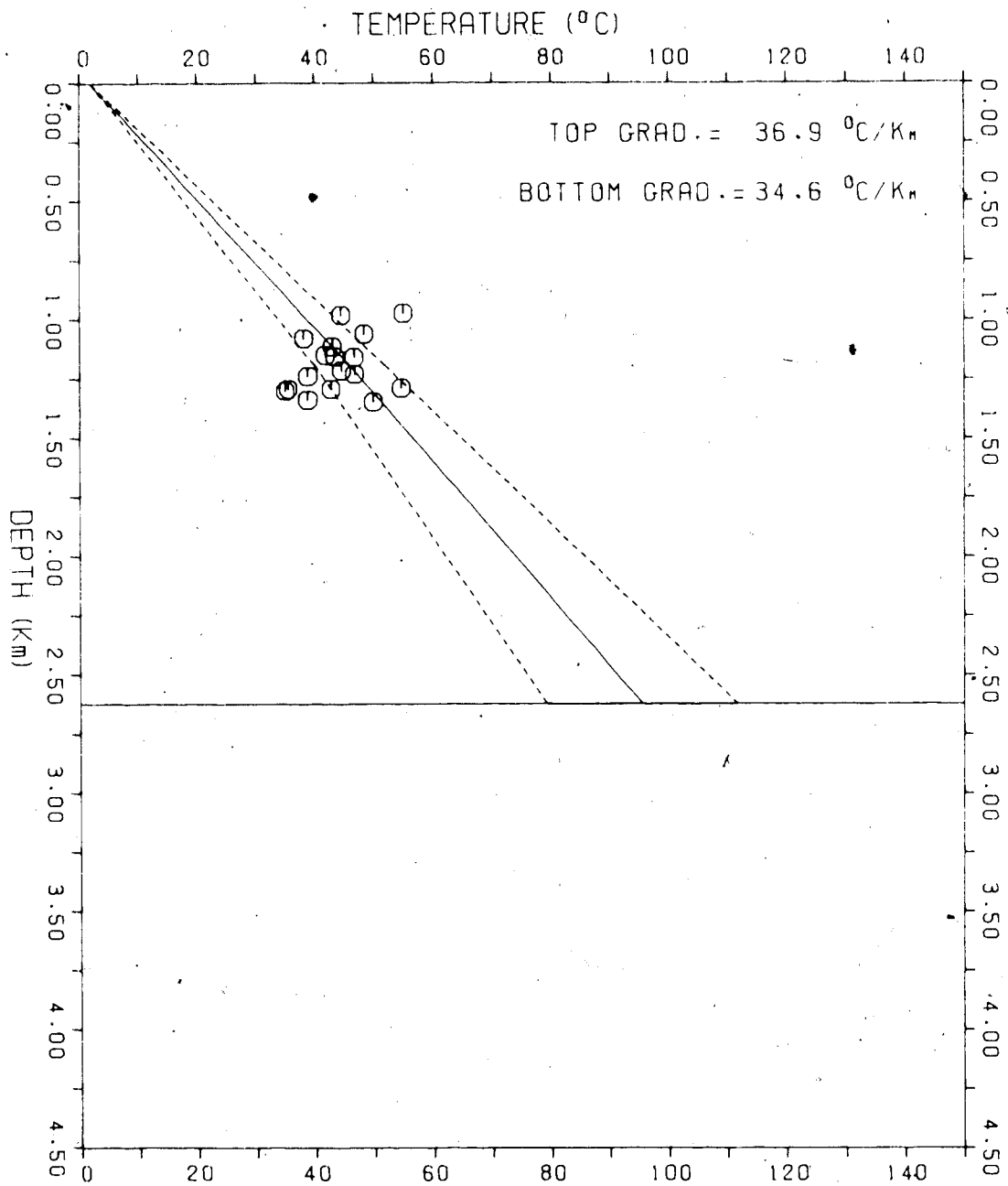
WELL INDEX: 4.
HEAT FLOW: 68. ± 18. MW PER SQ. METER
TEMPERATURE AT
BASE OF SEDIMENTS: 88. ± 13. °C



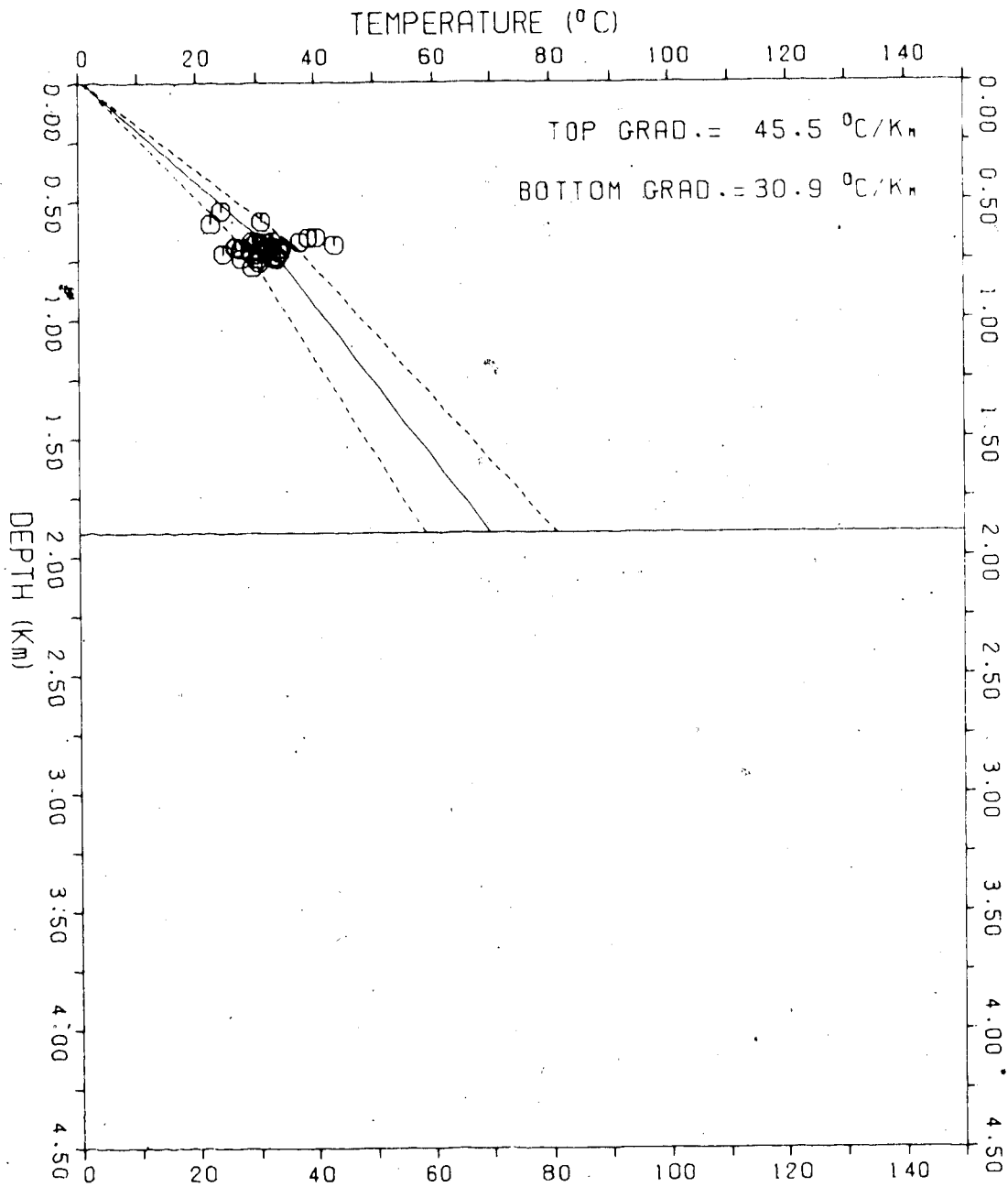
WELL INDEX: 5.
HEAT FLOW: 61. ± 15. MW PER SQ. METER
TEMPERATURE AT
BASE OF SEDIMENTS: 93. ± 11. °C



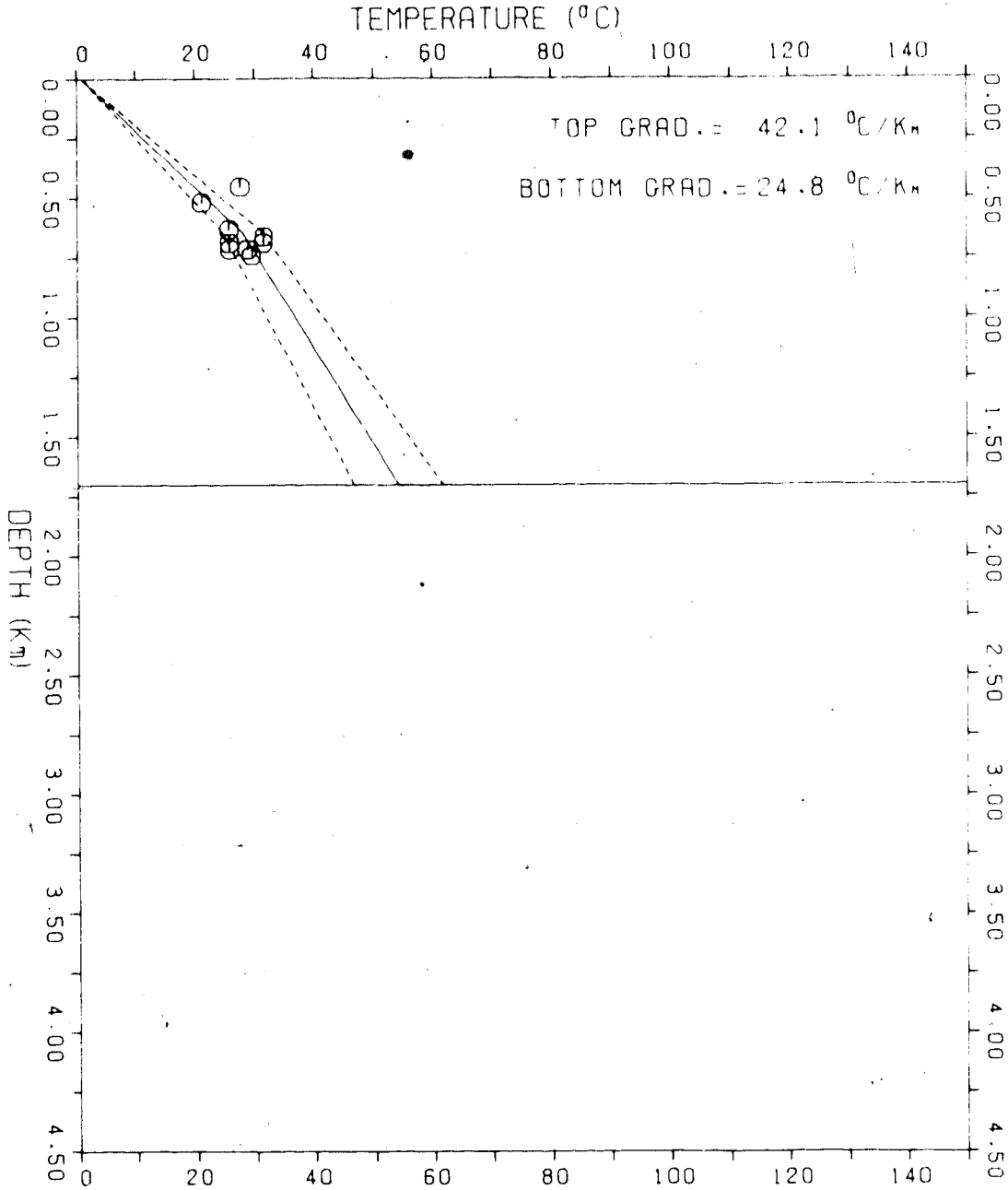
WELL INDEX: 6.
HEAT FLOW: 67. ± 17. mW PER SQ. METER
TEMPERATURE AT
BASE OF SEDIMENTS: 95. ± 16. °C



WELL INDEX: 7.
HEAT FLOW: 84. ± 22. mW PER SQ. METER
TEMPERATURE AT
BASE OF SEDIMENTS: 70. ± 11. °C

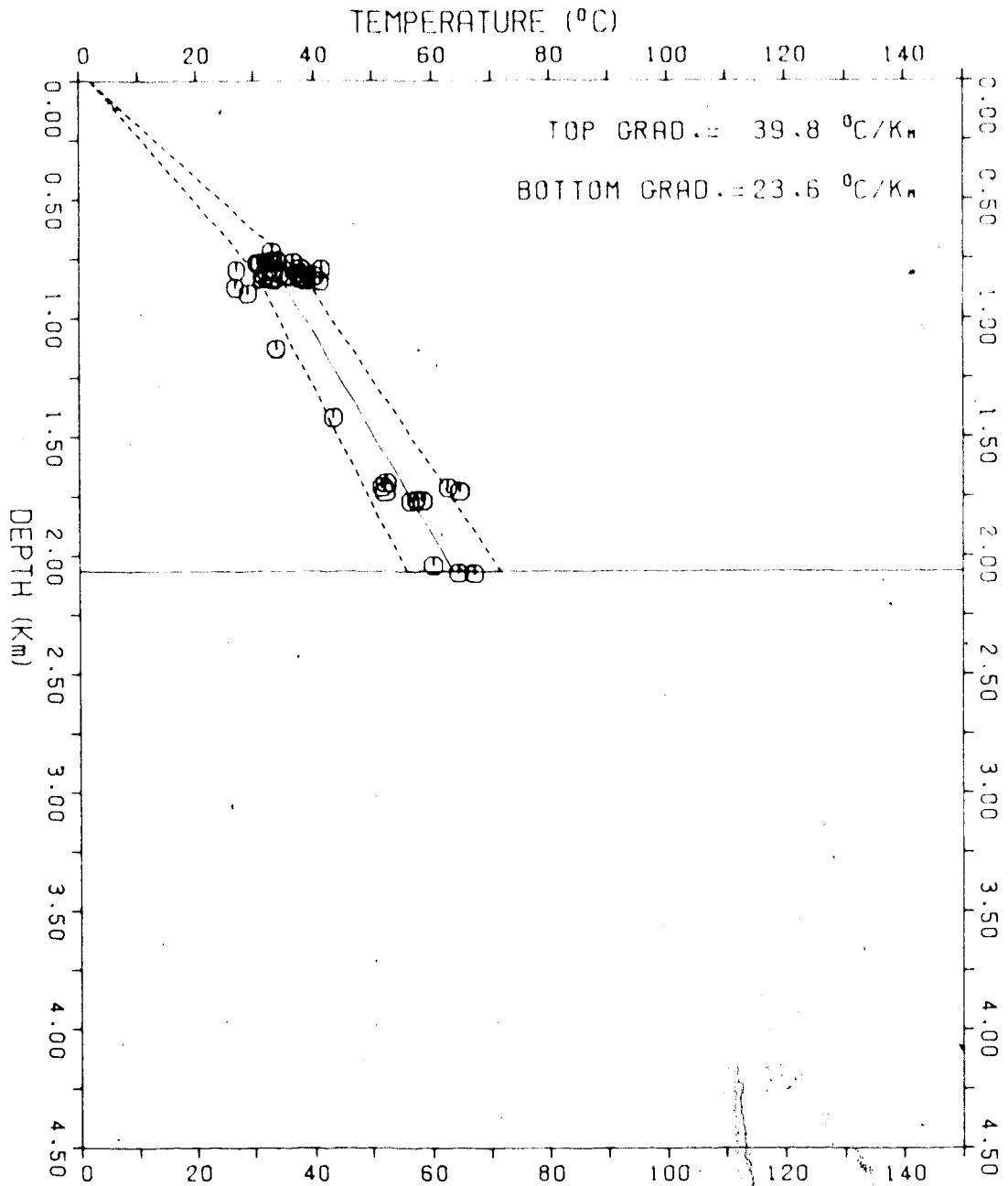


WELL INDEX: 8.
HEAT FLOW: 74. ± 18. MW PER SQ. METER
TEMPERATURE AT
BASE OF SEDIMENTS: 54. ± 7. °C

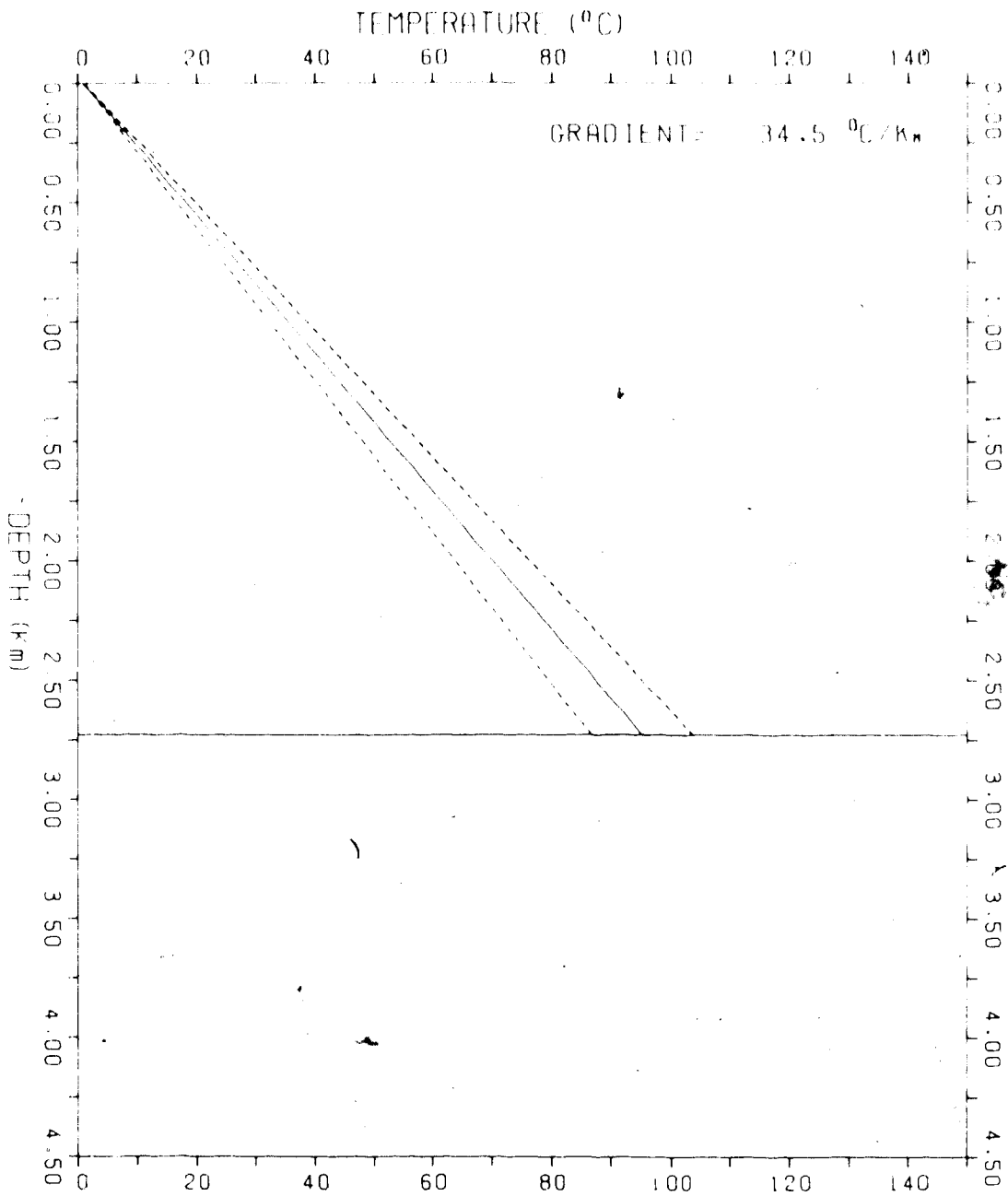


G

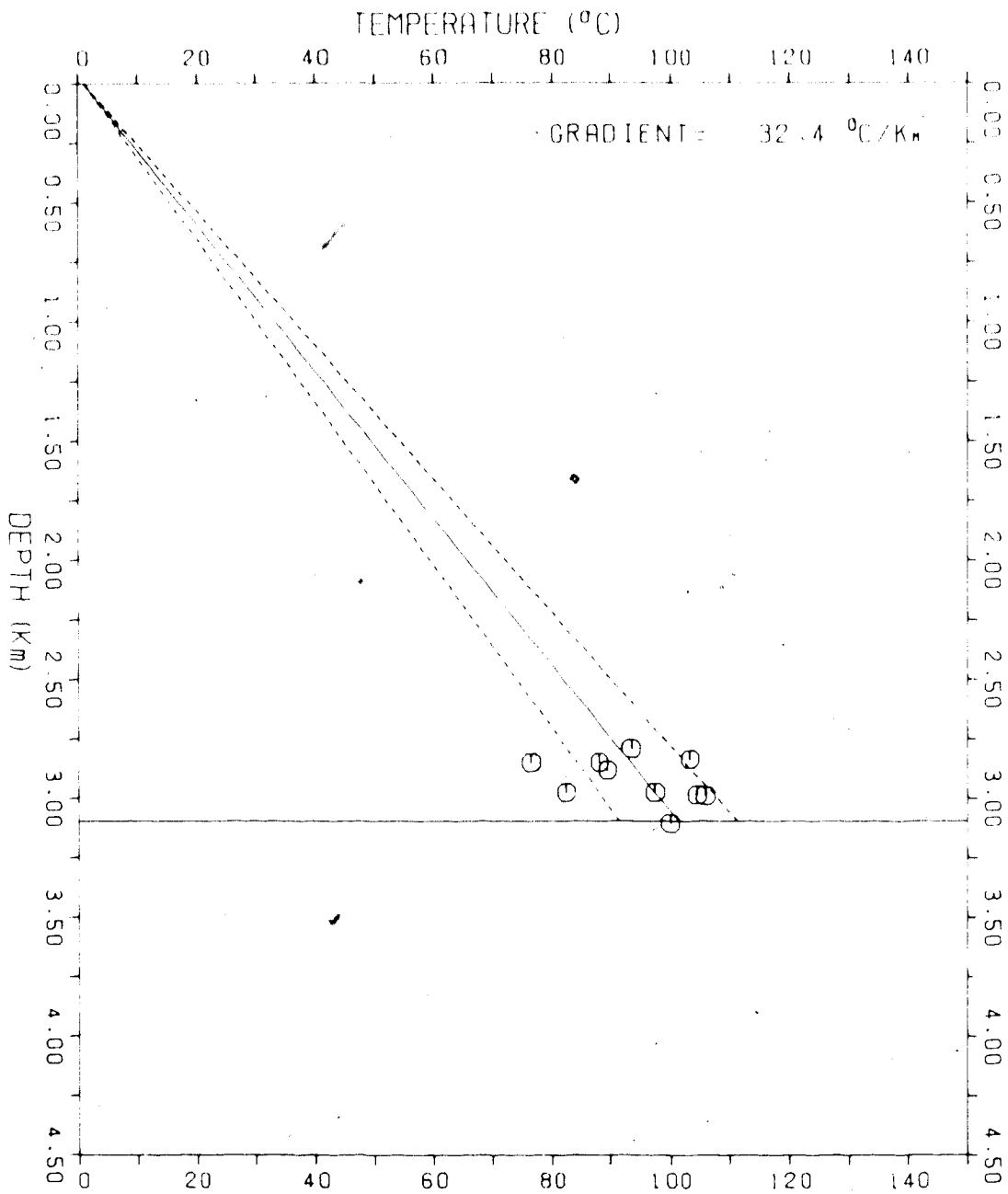
WELL INDEX: 9.
HEAT FLOW: 55. ± 19. MW PER SQ. METER
TEMPERATURE AT
BASE OF SEDIMENTS: 64. ± 8. °C



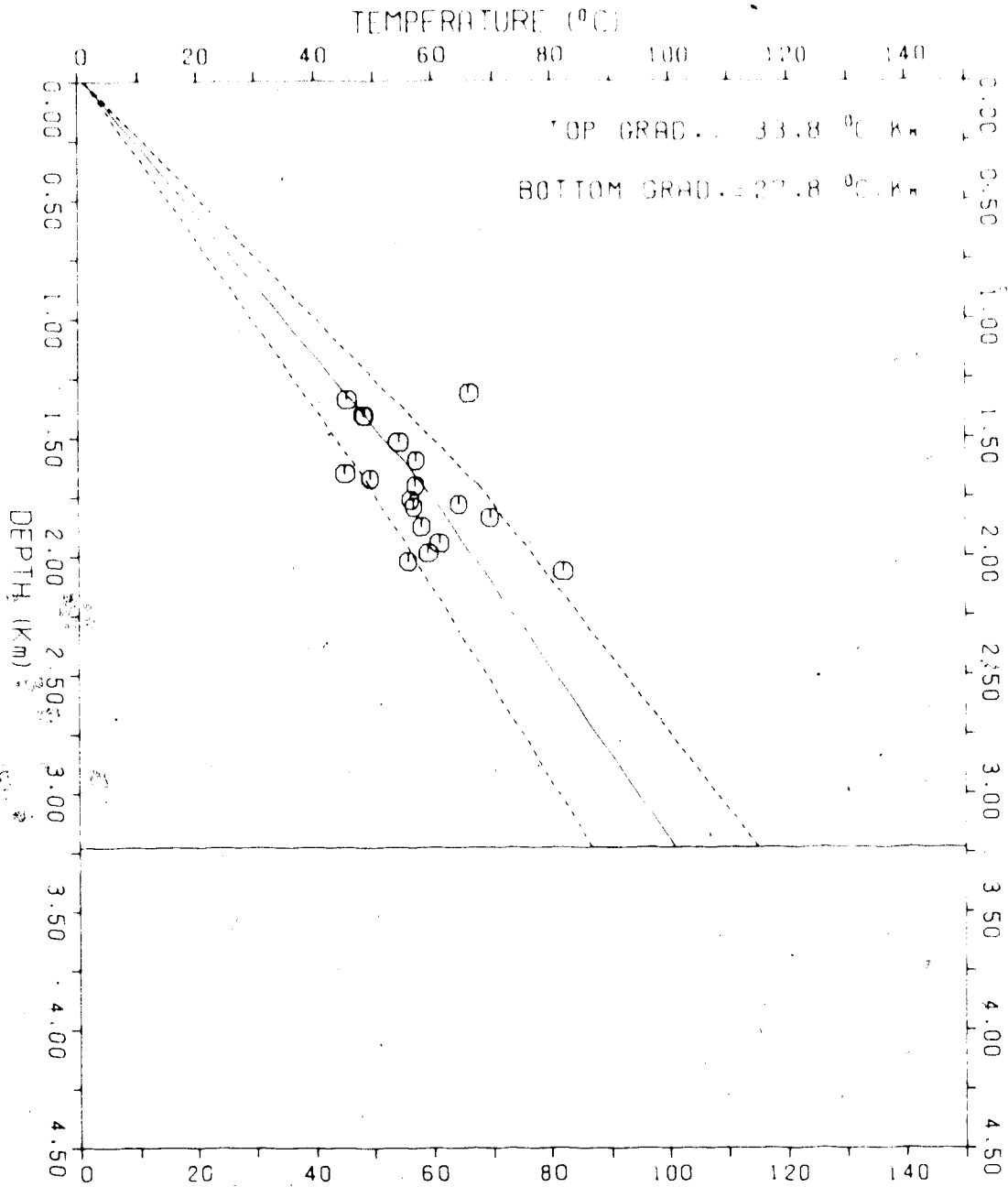
WELL INDEX: 10.
HEAT FLOW: 62. ± 14. mW PER SQ. METER
TEMPERATURE AT
BASE OF SEDIMENTS: 95. ± 9. °C



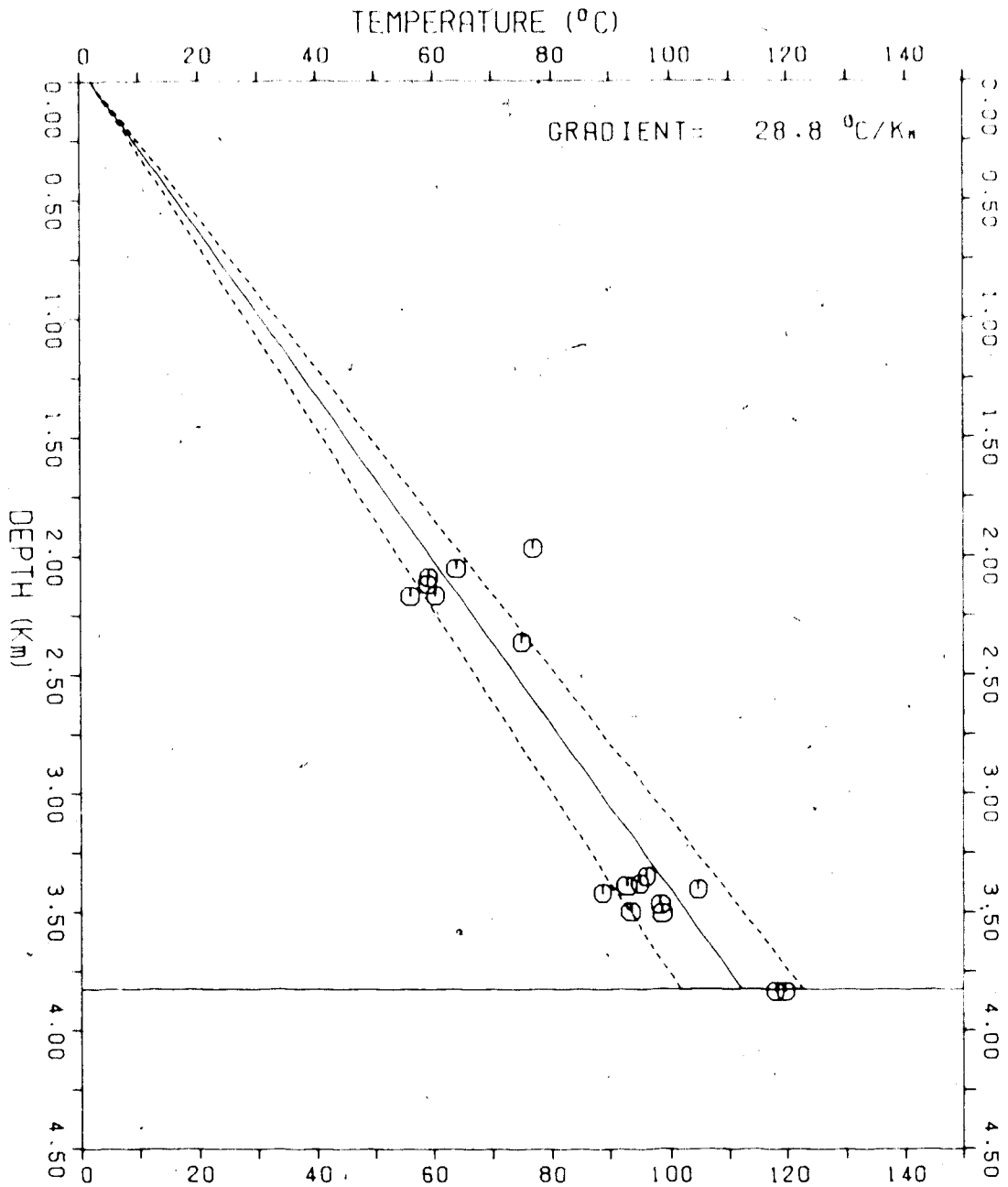
WELL INDEX: 11.
HEAT FLOW: $62. \pm 13.$ mW PER SQ. METER
TEMPERATURE AT
BASE OF SEDIMENTS: $101. \pm 10.$ °C



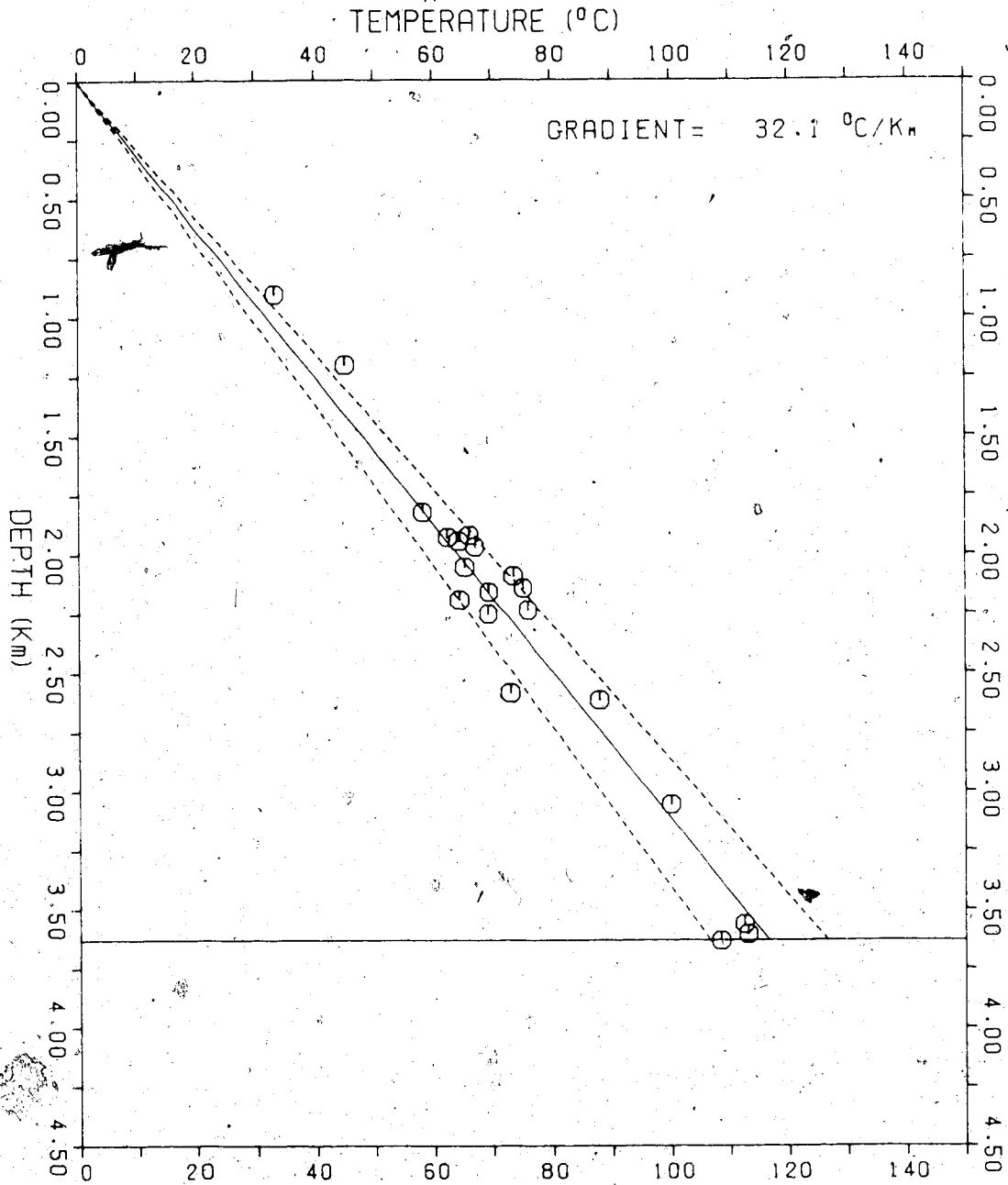
WELL INDEX: 12.
HEAT FLOW: 61. ± 16. MW PER SQ. METER
TEMPERATURE AT
BASE OF SEDIMENTS: 101. ± 14. °C



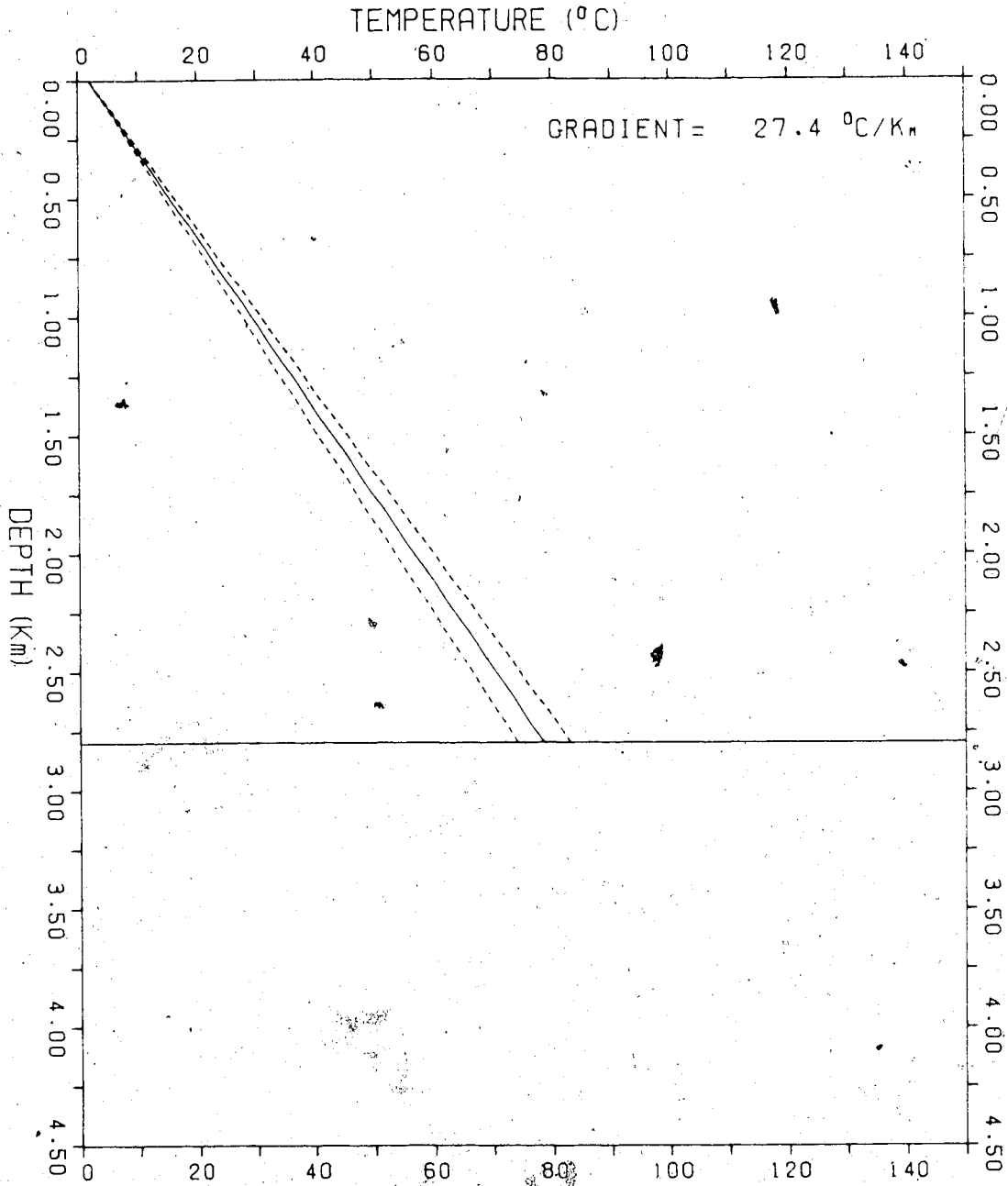
WELL INDEX: 13.
HEAT FLOW: 55. ± 12. MW PER SQ. METER
TEMPERATURE AT
BASE OF SEDIMENTS: 112. ± 11. °C



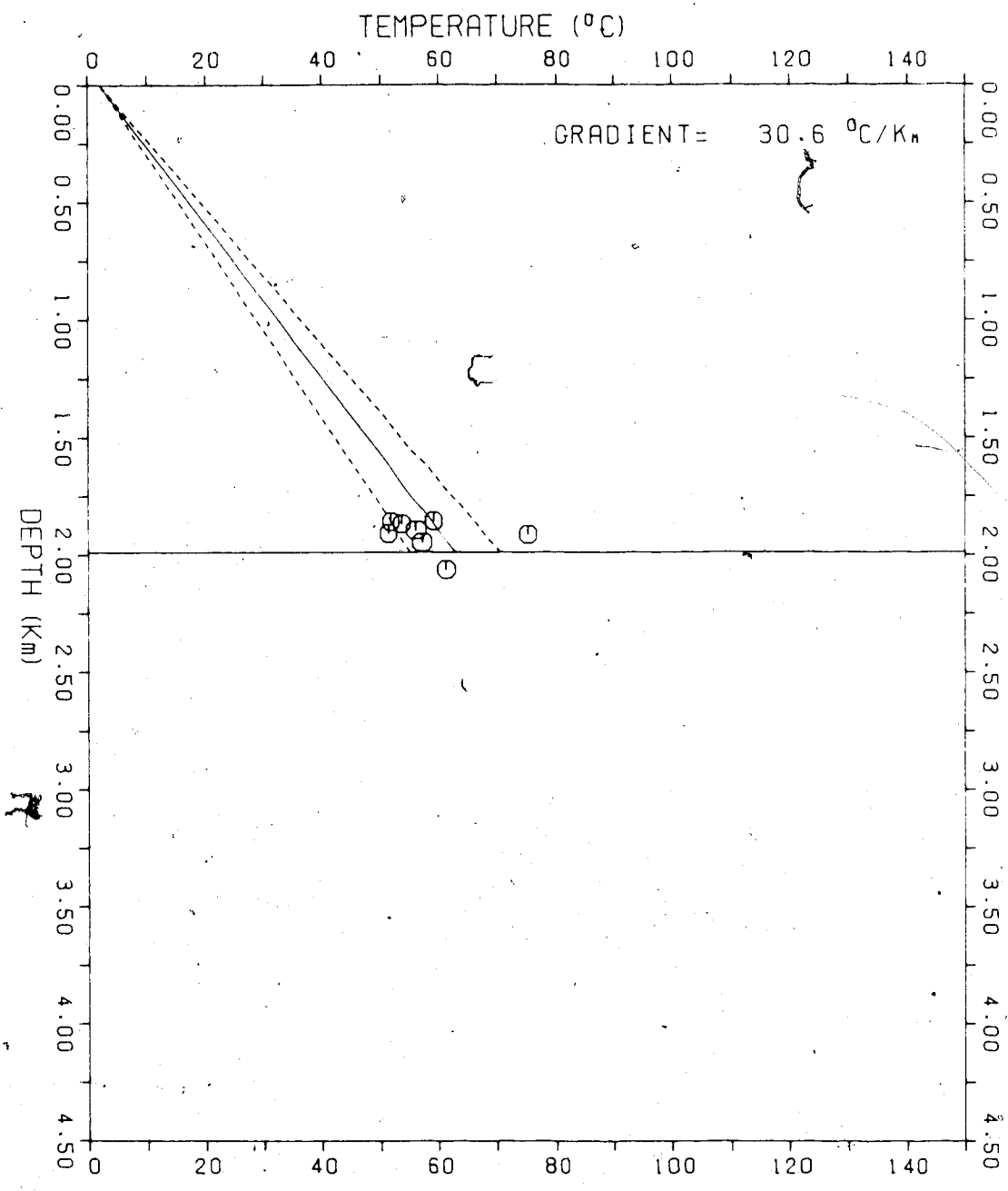
WELL INDEX: 14.
HEAT FLOW: 65. ± 13. MW PER SQ. METER
TEMPERATURE AT
BASE OF SEDIMENTS: 117. ± 10. °C



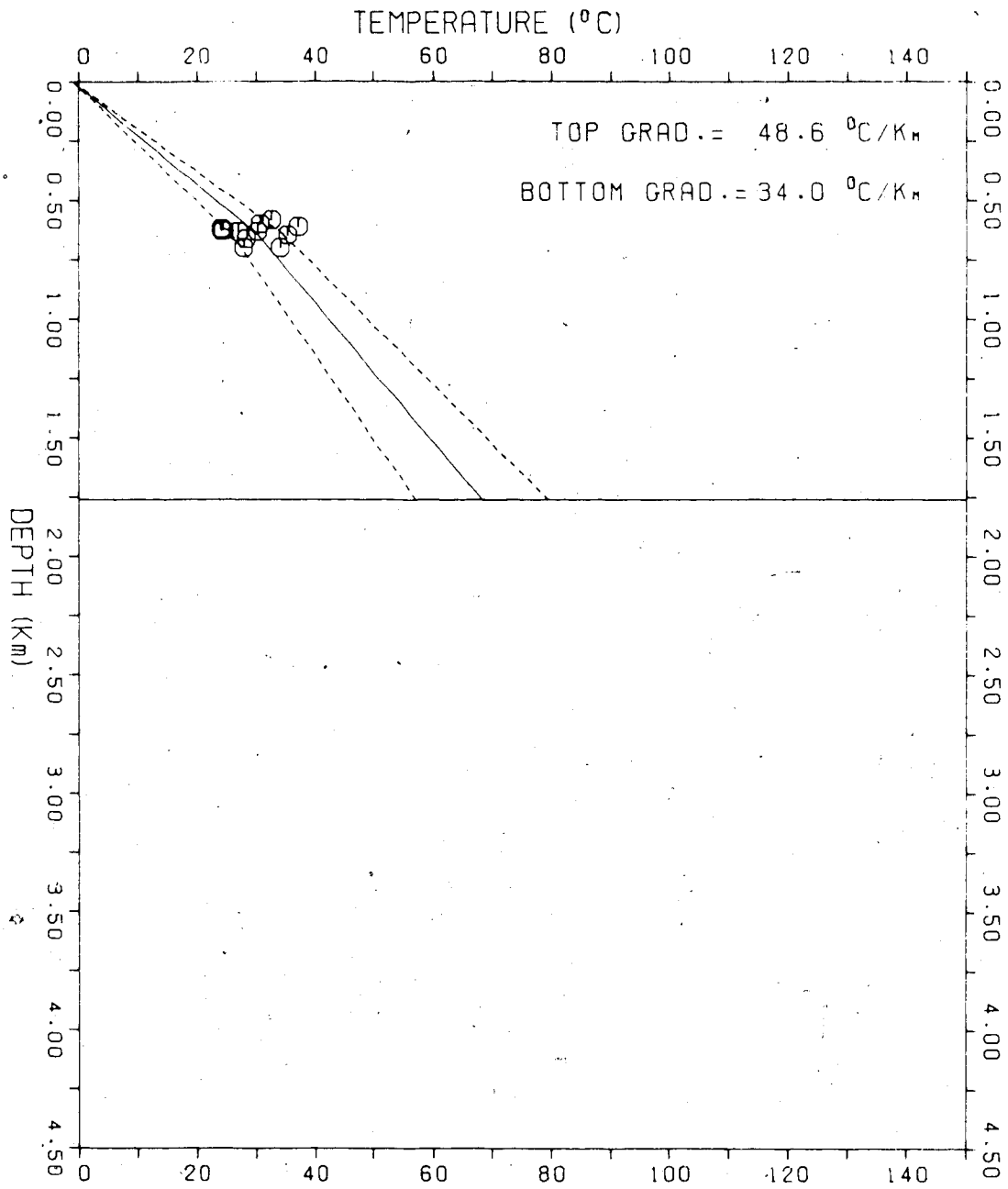
WELL INDEX: 15.
HEAT FLOW: 54. ± 11. mW PER SQ. METER
TEMPERATURE AT
BASE OF SEDIMENTS: 79. ± 5. °C



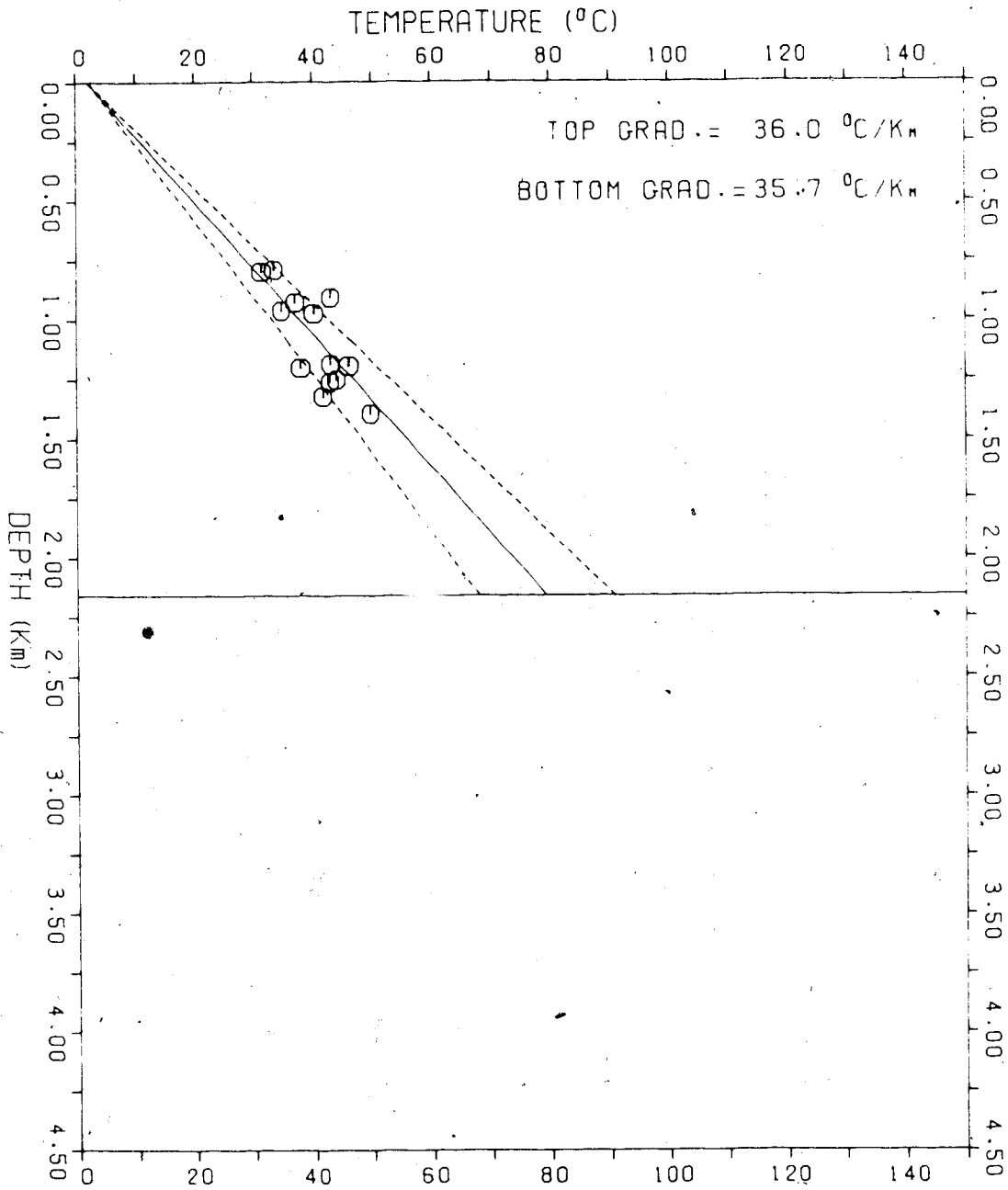
WELL INDEX: 16.
HEAT FLOW: 61. ± 14. mW PER SQ. METER
TEMPERATURE AT
BASE OF SEDIMENTS: 63. ± 8. °C



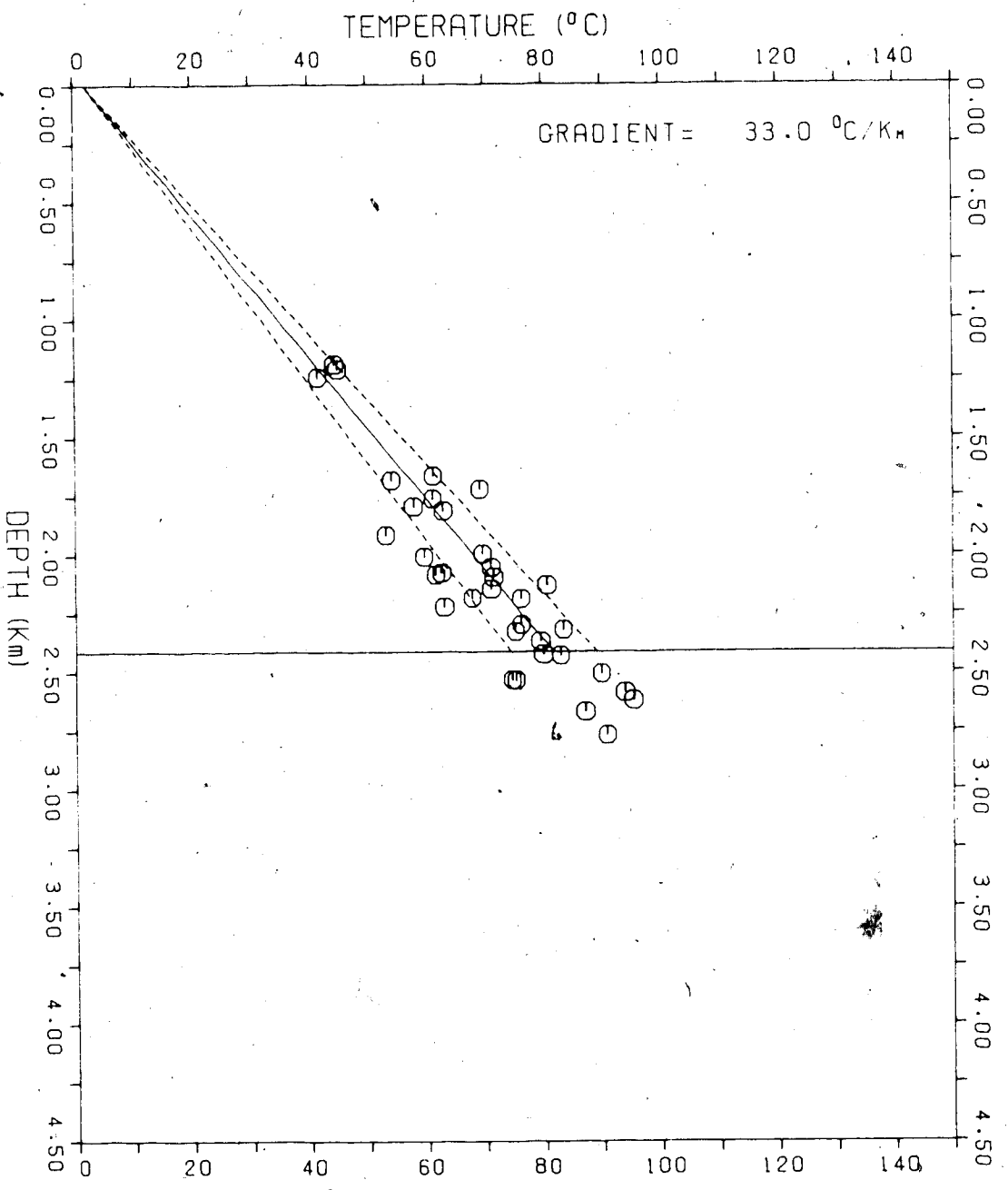
WELL INDEX: 17.
HEAT FLOW: 92. ± 22. MW PER SQ. METER
TEMPERATURE AT
BASE OF SEDIMENTS: 68. ± 11. °C



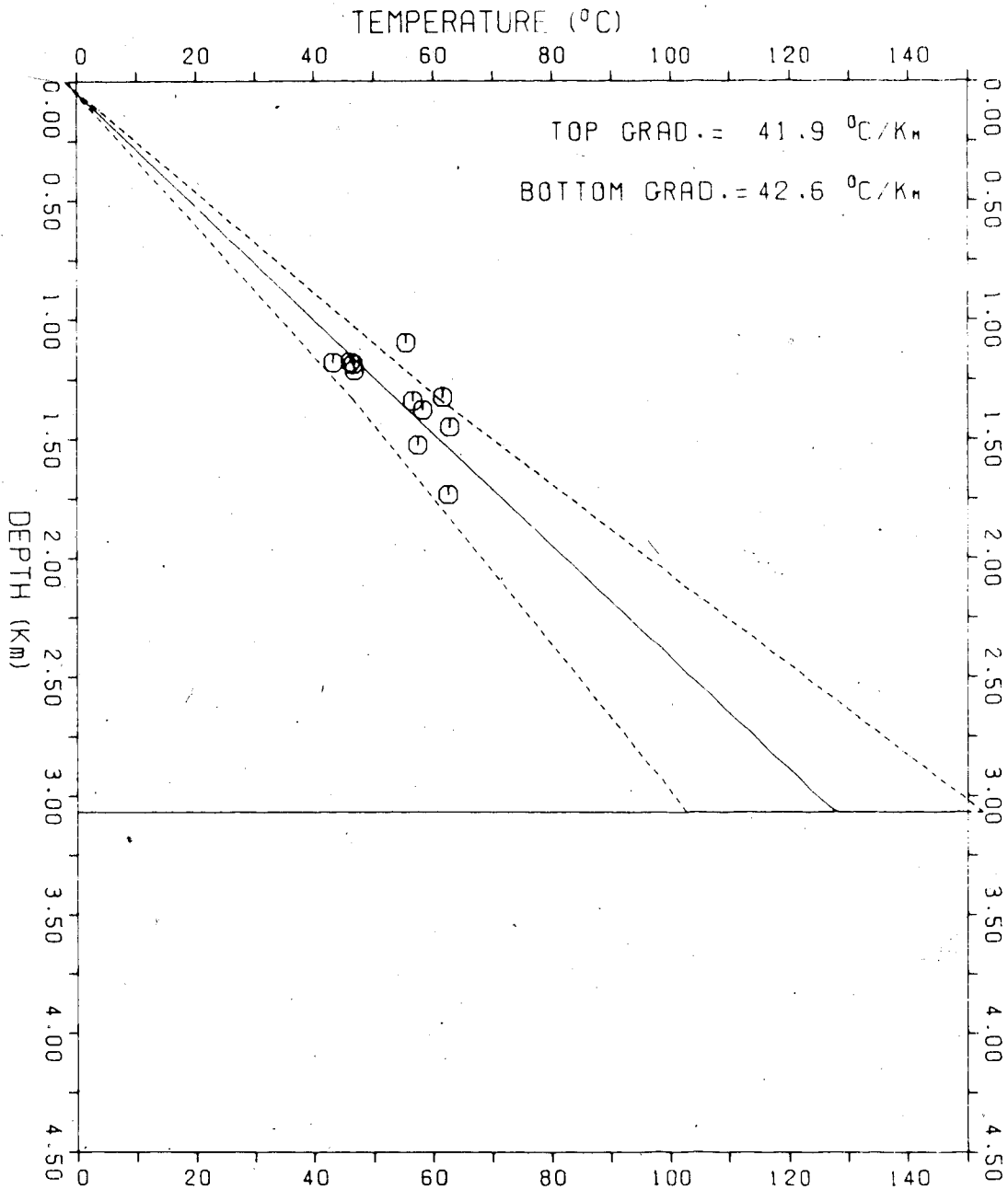
WELL INDEX: 18.
HEAT FLOW: 78. ± 18. mW PER SQ. METER
TEMPERATURE AT
BASE OF SEDIMENTS: 79. ± 11. °C



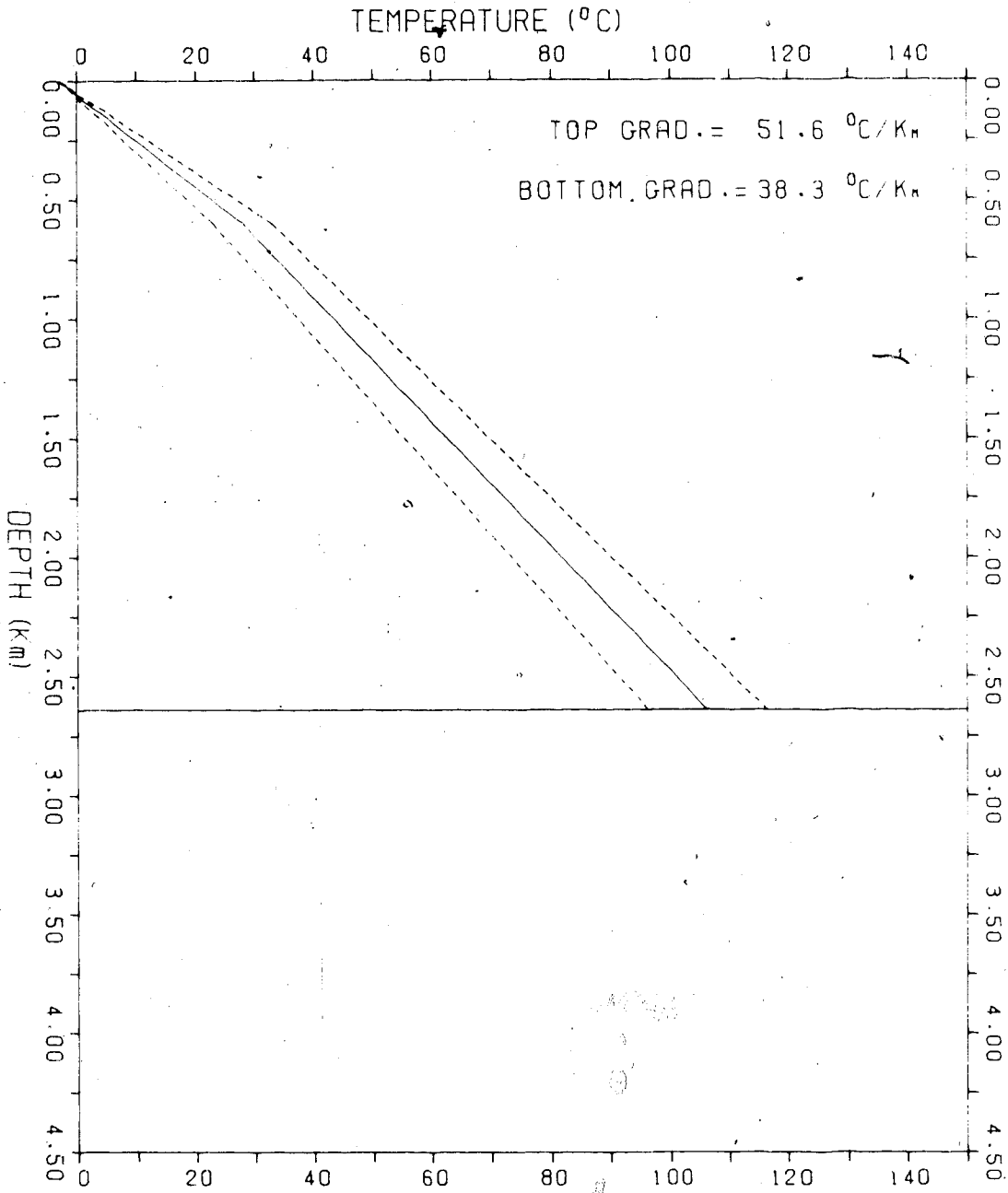
WELL INDEX: 19.
HEAT FLOW: 72. ± 14. mW PER SQ. METER
TEMPERATURE AT
BASE OF SEDIMENTS: 82. ± 7. °C



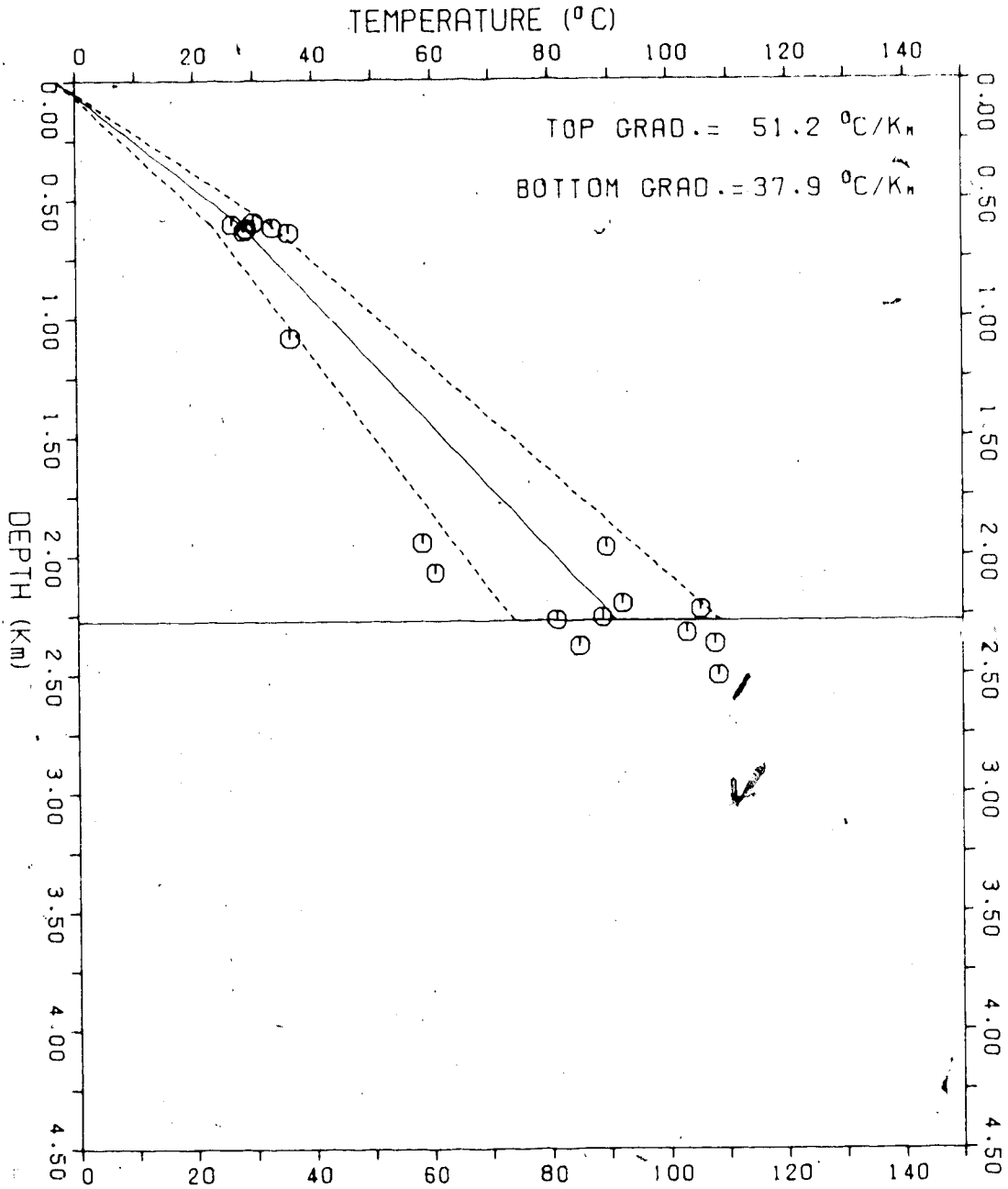
WELL INDEX: 20.
HEAT FLOW: 78. \pm 20. mW PER SQ. METER
TEMPERATURE AT
BASE OF SEDIMENTS: 128. \pm 25. $^{\circ}$ C



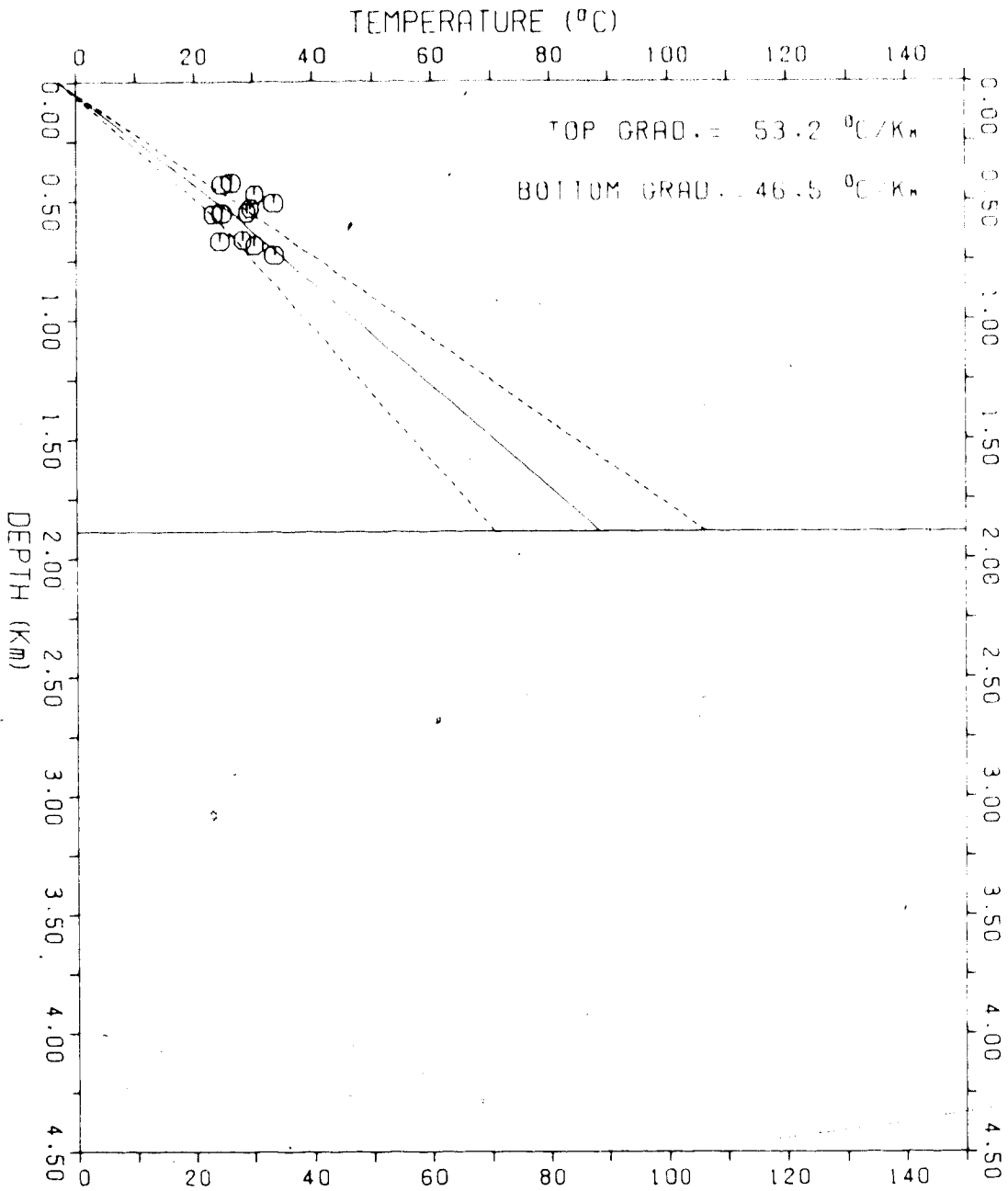
WELL INDEX: 21.
HEAT FLOW: 83. ± 19. mW PER SQ. METER
TEMPERATURE AT
BASE OF SEDIMENTS: 106. ± 10. °C



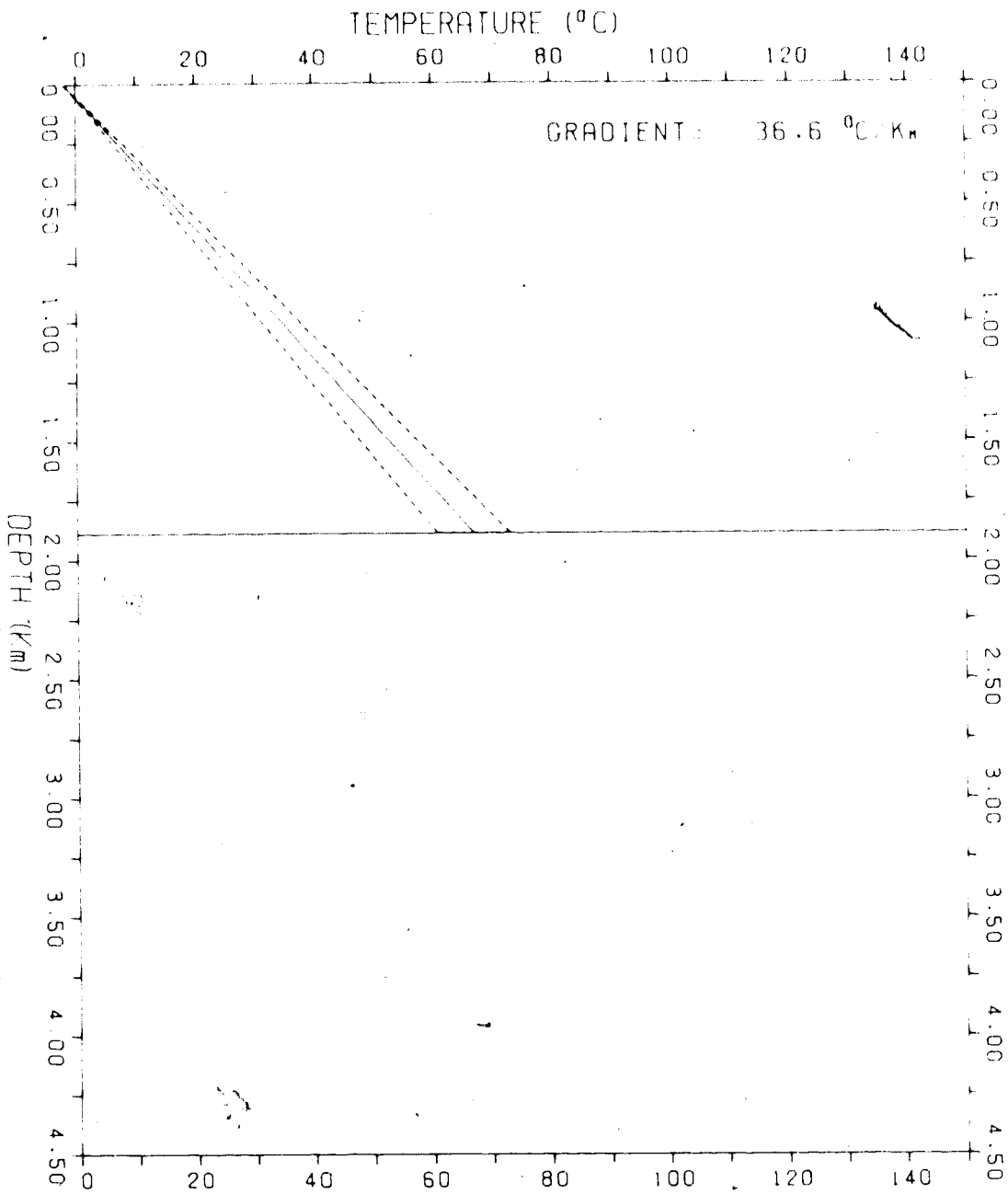
WELL INDEX: 22.
HEAT FLOW: 77. ± 27. mW PER SQ. METER
TEMPERATURE AT
BASE OF SEDIMENTS: 91. ± 17. °C



WELL INDEX: 23.
HEAT FLOW: $103. \pm 23.$ mW PER SQ. METER
TEMPERATURE AT
BASE OF SEDIMENTS: $89. \pm 18.$ °C



WELL INDEX: 24.
HEAT FLOW: 76. ± 15. mW PER SQ. METER
TEMPERATURE AT
BASE OF SEDIMENTS: 67. ± 6. °C



Appendix V

Heat Generation at the Surface of the Precambrian Basement in Western Canada

The following table gives the results of the heat generation calculations described in Chapter 4 (equation 4.7).

No	Location			Twp	Rge	Mer	Precambrian		U (ppm)	D (ppm)	Y	L
	Lsd	Sec	Depth (ft)				Sample Depth (ft)					
1	7	29	12		2	1	708	1009	0.93	1.2	2.28	81
2	3	1	5		2	1	1042	1150	0.75	1.2	2.18	81
3	3	1	8		18	1	3816	3825	0.91	0.8	3.39	81
4	9	1	37		28	1	2035	2045	0.18	0.1	3.24	81
5	16	4	3		32	1	8315	8328	7.97	1.1	3.74	84
6	3	27	8		8	2	8580	8830	0.37	0.1	3.12	84
7	2	11	15		26	2	7682	7738	2.01	1.8	3.22	84
8	1	15	48		17	2	2543	2594	8.81	12.7	5.65	84
9	11	3	50		18	2	3056	3056	0.28	0.1	0.70	84
10	12	9	50		18	2	2170	2170	0.32	0.8	0.32	84
11	12	3	50		18	2	3173	3173	0.29	1.5	4.18	84
12	8	9	50		18	2	2378	2378	1.77	1.4	5.87	84
13	13	18	52		13	2	1586	1615	3.31	1.5	4.13	84
14	12	15	52		14	2	1704	1785	3.19	17.7	2.55	84
15	2	5	61		24	2	1763	1820	1.01	1.5	2.81	84
16	4	31	3		26	3	7240	7335	0.47	2.9	0.16	84
17	9	32	6		22	3	8808	8820	1.76	18.5	4.94	84
18	2	4	10		19	3	8510	8774	3.31	0.8	5.8	84
19	9	20	12		3	3	7779	7785	4.60	23.1	3.83	84
20	2	21	16		17	3	7281	7305	23.16	82.3	1.67	84
21	1	9	17		14	3	6706	6755	1.80	1.1	1.44	84
22	15	13	17		18	3	7246	7260	15.25	10.1	1.35	84
23	1	31	18		28	3	7420	7410	0.12	0.5	1.76	84
24	4	16	37		1	3	5383	5410	1.28	22.3	4.95	84
25	8	15	52		2	3	3250	3200	0.51	1.4	3.94	84
26	7	14	56		17	3	4325	4332	0.33	40.2	1.21	84
27	13	21	61		15	3	2755	2767	0.28	6.1	1.81	84
28	8	11	62		22	3	3452	3460	3.38	11.5	4.72	84
29	1	36	63		5	3	1915	1921	0.11	2.1	3.59	84
30	9	21	63		8	3	2035	2061	1.13	5.2	4.71	84
31	8	8	61		2	3	2003	2009	0.41	1.8	0.89	84
32	8	8	61		2	3	2003	2026	1.17	8.1	3.39	84
33	8	30	61		15	3	2399	2415	1.45	31.7	1.57	84
34	12	14	12		12	1	6930	6935	4.55	2.4	3.14	84
35	4	12	15		27	4	11793	11815	0.50	11.5	2.37	84
36	5	1	17		14	4	7270	7270	1.15	1.4	1.40	84
37	6	9	31		1	4	7168	7174	5.14	3.0	2.73	84
38	13	36	35		2	4	7229	7229	1.34	2.1	3.11	84
39	1	6	38		15	4	8345	8345	1.34	1.1	1.51	84
40	16	17	48		20	4	8105	8105	3.11	11.0	3.64	84
41	8	17	50		26	4	8981	8985	1.75	8.1	1.11	84

42	8	17	50	26	4	8984	8990	5.10	1.1	3.76	1.38
43	14	29	52	2	1	5468	5485	1.52	1.14	6.06	1.38
44	1	11	53	12	1	6435	6437	7.57	1.1	1.88	1.38
45	8	17	53	15	4	7790	7800	3.51	1.1	3.51	1.38
46	14	14	55	15	4	6430	6533	1.03	1.1	2.53	1.38
47	7	14	57	6	4	5207	5210	4.06	1.1	3.48	1.38
48	7	14	57	6	4	5207	5210	0.96	1.1	3.06	1.38
49	6	36	58	23	4	7162	7136	0.85	1.1	3.16	1.38
50	9	29	59	21	4	7340	7527	0.07	1.1	1.47	1.38
51	10	13	60	4	4	4700	4714	0.19	1.1	1.50	1.38
52	1	27	60	26	4	7507	7518	7.52	1.1	3.41	1.38
53	16	19	62	19	4	6590	6604	16.88	1.1	3.31	1.38
54	13	17	67	23	4	6390	6405	2.71	1.1	3.47	1.38
55	4	3	69	10	4	5019	5021	22.52	1.1	4.93	1.38
56	7	24	76	18	4	4628	4633	0.67	1.1	4.48	1.38
57	7	24	76	18	4	4628	4639	0.97	1.1	1.38	1.38
58	6	10	77	25	4	6103	6120	3.15	1.1	4.82	1.38
59	12	27	78	4	4	2557	2567	15.75	1.1	4.44	1.38
60	14	9	86	7	4	1773	1792	1.27	1.1	5.34	1.38
61	7	28	87	12	4	2299	2302	2.47	1.1	5.34	1.38
62	7	11	87	17	4	2850	2860	0.55	1.1	4.83	1.38
63	5	32	88	8	4	789	789	11.20	1.1	4.36	1.38
64	8	36	88	8	4	906	929	0.68	1.1	3.38	1.38
65	8	20	89	9	4	1125	1111	1.75	1.1	3.96	1.38
66	10	14	91	14	4	2408	2414	1.14	1.1	3.4	1.38
67	9	34	94	14	4	1991	2000	2.55	1.1	4.68	1.38
68	12	23	98	21	4	3836	3813	0.85	1.1	4.11	1.38
69	5	29	98	1	5	7505	7575	0.63	1.1	1.88	1.38
70	10	20	62	8	5	9112	9132	1.06	1.1	3.31	1.38
71	5	35	62	18	5	11310	11316	0.23	1.1	3.67	1.38
72	6	36	63	12	5	1668	16709	5.20	1.1	3.7	1.38
73	5	31	65	6	5	8350	8400	0.11	1.1	4.11	1.38
Composite											
74	9	20	65	13	5	10612	10614	4.91	1.1	3.31	1.38
75	9	20	65	13	5	10612	10624	1.34	1.1	3.47	1.38
76	16	12	66	13	5	10507	10511	1.1	1.1	3.12	1.38
77	8	11	66	10	5	8965	8983	1.55	1.1	3.4	1.38
78	3	5	68	22	5	10707	10740	1.1	1.1	3.1	1.38
79	11	18	72	17	5	8502	8502	1.85	1.1	3.1	1.38
80	11	11	73	13	5	7403	7406	2.8	1.1	3.12	1.38
81	6	6	75	5	5	7075	7372	3.18	1.1	3.47	1.38
82	12	16	75	15	5	7180	7141	2.1	1.1	3.12	1.38
83	15	16	75	19	5	7814	7802	1.1	1.1	3.12	1.38
84	14	15	75	22	5	8110	8114	14.33	1.1	3.12	1.38
85	5	1	77	20	5	7837	7837	1.1	1.1	3.12	1.38
86	12	33	77	21	5	7700	7710	0.36	1.1	3.12	1.38

87	15	21	78	20	5	7625	7614	1 93	10 1	2 80	1 16
88	12	11	78	22	5	7818	7820	6 35	18 1	3 69	5 30
89	16	9	79	22	5	7619	7625	1 46	11 1	2 61	2 18
90	1	12	79	22	5	7840	7847	1 52	8 1	3 53	1 28
91	1	16	79	22	5	7420	7421	9 18	12 9	8 24	1 10
92	10	20	79	22	5	7630	7652	2 64	6 2	3 46	1 43
93	2	25	80	17	5	6782	6808	3 13	19 8	5 18	2 66
94	16	25	80	17	5	6754	6769	5 11	29 9	1 38	3 79
95	14	34	80	17	5	6864	6875	6 46	13 0	1 19	5 05
96	8	17	80	21	5	7738	7770	6 34	22 7	2 90	3 47
97	13	18	80	23	5	7580	7598	6 48	0 2	5 97	2 24
98	5	3	81	17	5	6684	6727	7 47	37 9	3 92	4 91
99	10	6	82	1	5	5004	5007	1 12	0 4	4 69	0 71
100	7	5	82	18	5	7271	7290	3 12	11 6	3 19	1 90
101	16	13	83	24	5	7105	7114	10 05	10 9	1 84	3 51
102	13	24	84	2	5	5001	5009	4 87	19 6	4 61	3 04
103	6	11	84	5	5	5340	5348	2 59	20 3	5 12	2 55
104	6	31	84	7	5	5283	5288	0 73	9 9	4 28	1 27
105	2	15	84	16	5	5895	5912	13 59	15 2	1 86	7 07
106	1	22	84	17	5	6090	6095	1 45	1 8	0 72	0 56
107	11	3	85	12	5	5109	5152	1 32	25 7	3 96	2 19
108	16	23	85	19	5	6090	6106	1 35	6 5	3 02	1 08
109	8	22	86	9	5	4980	4981	4 88	12 6	3 53	2 36
110	6	27	86	9	5	4849	4853	0 60	16 7	4 39	1 72
111	12	32	86	9	5	4764	4780	0 85	39 8	5 65	3 50
112	16	25	86	20	5	6010	6076	1 29	5 8	1 93	0 91
113	5	21	86	22	5	6589	6589	0 53	1 0	0 81	0 28
114	2	25	86	26	5	6685	6696	2 34	16 0	0 86	1 79
115	12	30	87	7	5	5023	5028	5 73	70 0	5 58	6 81
116	8	11	87	8	5	4658	4660	2 38	23 4	3 08	2 52
117	16	11	87	8	5	4628	4646	3 37	33 6	5 23	3 68
118	12	14	87	8	5	4993	5050	1 18	19 6	5 77	2 20
119	4	16	87	8	5	4742	4799	5 01	89 8	6 28	8 08
120	12	16	87	8	5	4836	4870	6 10	69 3	6 32	6 95
121	12	17	87	8	5	4778	4797	5 85	66 9	5 81	6 67
122	2	19	87	8	5	4825	4828	11 62	58 7	3 77	7 10
123	11	21	87	8	5	4798	4800	6 27	66 9	1 79	6 69
124	10	3	87	10	5	4749	4751	0 40	2 4	3 01	0 55
125	14	17	88	6	5	5037	5059	3 56	19 2	3 74	4 67
126	4	20	88	7	5	5020	5030	2 17	2 6	5 62	1 34
127	2	4	88	8	5	4814	4817	11 95	39 1	5 95	6 35
128	10	19	88	8	5	4768	4780	2 44	26 5	3 44	2 78
129	2	22	88	8	5	4910	4910	1 52	1 1	7 06	1 15
130	2	23	88	8	5	4860	4866	1 28	11 7	2 06	1 43
131	4	29	88	8	5	4644	4651	32 14	30 2	5 13	10 82
132	2	17	89	7	5	4742	4751	5 13	51 4	5 30	5 65

133	6	20	89	19	5	5890	5905	2 07	11 2	11 2	1 54
134	15	24	90	15	5	5807	5810	2 10	23 7	23 7	2 56
135	15	24	90	15	5	5807	5819	0 49	8 6	8 6	0 90
136	9	35	91	6	5	4686	4703	1 66	16 3	16 3	1 85
137	9	24	93	18	5	5670	5705	1 4 90	14 5	14 5	5 23
138	10	8	99	13	5	5627	5635	0 61	21 6	21 6	1 93
139	15	24	109	17	5	4465	4467	5 28	11 9	11 9	2 59
140	15	32	109	19	5	4868	4871	1 72	25 6	25 6	3 33
141	6	24	111	22	5	6383	6385	1 17	11 5	11 5	1 20
142	7	22	116	22	5	4968	5072	1 01	7 8	7 8	0 91
143	7	10	119	20	5	4525	4528	7 47	8 4	8 4	2 91
144	9	7	124	18	5	3725	3731	5 42	12 5	12 5	2 56
145	16	18	126	14	5	3145	3148	0 54	0 14	0 14	0 55
146	16	25	72	5	6	11695	11700	1 35	8 6	8 6	1 31
147	2	2	73	1	6	10132	10195	5 29	61 4	61 4	5 82
148	13	20	75	2	6	9593	9612	1 00	19 4	19 4	2 89
149	12	20	77	3	6	9337	9347	6 69	20 1	20 1	3 44
150	7	36	77	9	6	11645	11700	7 75	29 6	29 6	4 42
151	4	20	78	1	6	8256	8264	5 88	27 8	27 8	3 82
152	12	20	78	6	6	9775	9818	10 92	22 1	22 1	1 75
153	4	29	81	1	6	7243	7255	4 32	10 1	10 1	2 00
154	2	14	82	2	6	7480	7492	14 63	67 2	67 2	8 75
155	2	5	83	2	6	7930	7977	4 45	11 6	11 6	2 14
156	14	31	84	2	6	7840	8225	0 52	1 1	1 1	0 21
157	16	12	84	8	6	8010	8014	2 99	20 7	20 7	2 53
158	4	27	85	2	6	8750	8750	0 86	9 9	9 9	1 18
159	14	10	88	2	6	6958	6962	4 38	20 1	20 1	2 88
160	8	16	88	2	6	6882	6910	4 33	27 4	27 4	3 40
161	6	11	101	4	6	7300	7320	6 49	20 0	20 0	3 45
162	11	17	102	2	6	6920	6957	4 70	11 2	11 2	2 12
163	2	16	107	6	6	6835	6838	3 14	24 1	24 1	3 27
164	16	18	107	6	6	7315	7360	3 42	11 9	11 9	1 95
165	10	27	109	9	6	7308	7329	3 04	11 2	11 2	1 73
166	15	22	115	10	6	6362	6470	2 50	11 2	11 2	1 59
167	9	26	120	11	6	6980	7005	6 37	11 1	11 1	3 23
168	9	26	120	11	6	6980	7005	4 21	11 1	11 1	3 56
169	2	7	124	2	6	6115	6121	1 53	3 2	3 2	0 99
170	12	30	125	2	6	5965	5992	2 30	14 7	14 7	2 92
171	12	31	78	14	6	11892	12038	5 13	22 2	22 2	3 50
172	6	29	81	15	6	11614	11618	2 34	11 2	11 2	1 61
173	1	26	85	16	6	10906	10909	0 15	0 8	0 8	0 25
174	57° 47' N		120 14' W			9800	10029	10 33	12 8	12 8	5 81
175	58° 5' N		121 54' W			9925	9925	3 17	10 8	10 8	1 75
176	58° 16' N		120 51' W			8439	8437	0 68	6 4	6 4	4 61
177	60° 9' N		121 8' W			8220	8230	6 06	116 6	116 6	10 06
178	60° 51' N		114 24' W			1171	1173	0 83	5 8	5 8	0 89

179	60° 55' N	118° 50' W	2898	2900	0 55	3 5	0 51	0 43
180	61° 19' N	118° 40' W	2192	2230	11 30	21 0	3 24	4 66
181	61° 20' N	122° 30' W	1310	2085	0 97	3 1	2 93	0 76
182	62° 20' N	119° 0' W	3147	3225	1 53	2 2	1 69	0 70